Microscopic Basis for IBM: Study of Vibrational and Rotational Nuclei

by

Subrata Sarangi

Ph.D. Thesis

September 1992

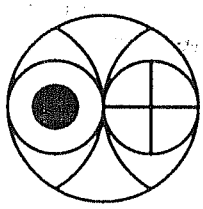

Physical Research Laboratory

Ahmedabad – 380 009

India.

Microscopic Basis for IBM: Study of Vibrational and Rotational Nuclei

Subrata Sarangi

Physical Research Laboratory

Ahmedabad – 380 009

India.

A Thesis Submitted to

Gujarat University

for the Degree of

Doctor of Philosophy

in

Physics

September 1992

Dedicated to

My Parents

and

My Teachers

Declaration

I hereby declare that the contents of this thesis represent original work and that they have not formed the basis for award of any degree or diploma by any University or Institution.

Author

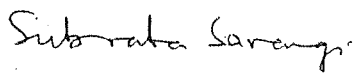

Subrata Sarangi
Theory Group
Physical Research Laboratory
Ahmedabad – 380 009, India

Certified by:

Thesis Supervisor

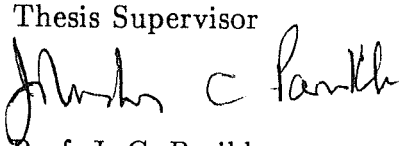

Prof. J. C. Parikh
Theory Group
Physical Research Laboratory
Ahmedabad – 380 009, India.

Contents

List of Figures

List of Tables

Acknowledgement

Honestly, all through a year or thereabout, I looked forward to the time – at long last – when I would sit down to write these lines. But now, as I am about it, I am at a loss. An association with my guide and thesis supervisor Prof. Jitendra C. Parikh is completing a phase. Our relationship despite initial hiccups has grown and matured through these years principally for his patient and understanding disposition. From him, I not only learnt a lot of Nuclear Physics, but I also got ample personal freedom which I overused at times... His remarkable sensitivity gave me a lot of encouragement and support through these tough final days. My sincere apologies, thanks and gratitude to him.

Some people have a knack for putting across ideas (with masked insight which freshers realise later) as if it is easier than breathing. Prof. S. P. Pandya and Prof. Parikh are of this cast. Needless to say, I owe the existence of my thesis to them. My sincere thanks with reverence and gratitude to Prof. Pandya for all the encouragement and support he accorded to me.

My thesis probably would have been much humbler had there not been the computer code-"FORTRAN PROGRAMMES FOR SPECTROSCOPIC CALCULATIONS IN (sdg)-BOSON SPACE: THE PACKAGE SDGIBM1" authored by Dr. Y. Durga Devi and Prof. V.K.B. Kota or my access to it. Chapter 4 of the thesis contains the cream of my results and owes its existence to this code. The numbers and results reported therein are of course my responsibility. I am deeply indebted to the authors of this code for allowing me to use it and helping me whenever I needed. I thank them also for executing the Shell Model program several times results of which are reported in Chapter 3. Many a discussion with Prof. Kota helped me swim across the waters I was in. Several suggestions by him made the thesis a lot better than what it would have been. I am also indebted to Dr. Durga Devi for many valuable discussions and suggestions.

I am also deeply grateful to Prof. C.R. Praharaj of Institute of Physics, Bhubaneswar, for providing me with the Hartree-Fock code and to my friends Bijay and

Ashwini who taught me, painstakingly, how to run it.

I recollect several educative discussions with Prof. S.B. Khadkikar. I also acknowledge very useful discussions I had with Prof. C.S. Warke and Prof. Y.K. Gambhir.

I recieved many helpful gestures and lots of encouraging words from Dr. Utpal Sarkar, Prof. B. Buti, Prof. A.C. Das, Prof. V. Sheorey, Prof D.P. Dewangan and Mr. S.V. Kasture. I thank them all. I am thankful to Mr. V.T. Vishwanathan, Mr. T.P. Muralidharan, Mr. K.J. Joseph, Mr. V. Sahadevan and Mr. Chunilal for all the help and friendly cooperation.

Computers, PCs and packages constitute the "system" on which theoretical physicists, especially the "Nuclear" type, now-a-days live. I did. In my efforts, I got all the help I required regarding these matters readily. I express my earnest gratitude to Dr. B.R. Sitaram and Dr. Sai Iyer for all the help and also for the encouragement it implied. My sincere thanks are also due to Mr. P.S. Shah and all his colleagues and trainees at the Computer Centre.

I acknowledge with deep gratitude the immense service rendered by the Library. "Current Contents" and "Research Alerts" promptly coming up at the counter helped me locating some fresh articles very important for the work presented here. The library staff were ready to help whenever needed smilingly and instantly. I thank Ms. Bharucha and all her colleagues in the Library.

I also thank the PRL authority, the Academic Committee, its chairman Dr. J.N. Goswami and administration for bearing with me through the inordinate delay in completing my work.

Personal relations stung by professional rivalry, suspicion and selfishness can create traumatic situations. On the otherhand, unplagued by such dark elements and marked by a basic respect and trust towards others can spring a prized friendship, create room for sharing varied emotions and propels one through tough days. My friendship with Viju and later on with Jitesh, Mathew, Raju, Ashwini and Janardan went a long way in doing this. Fond memories will echo in my mind.

If you are writing your thesis, then instictively you are offered help – tangible or otherwise, "materially" and "spiritually". The help I recieved from Ashwini, Janardan, Jitesh, Mathew, Rajagopalan, Raju, Sam, Shwetaketu and Viju greatly shortened my ordeal with giving the thesis a final form. Spirit-boosting wishes and offers for help came amply from all friends and colleagues in the hostel. I am especially grateful to Ajay, Anant, Anjan, Anshu, Bijay, Bhushan, Birendra, Dadu, Gautam, Himadri, Kiran, Kishan, Kishku, Mac, Mitaxi, Nagaraj, Nirjhari, Pallam, Rashmi, Seema, Shirley, Subba, Sushant, Sushma and Vinod for cheering me on. I also wish to

thank my friends and colleagues Biswa, Debabrata, Debashish (both), Ganguly, Guru, Krishnan, Lambodar, Manoharlal, Manoj, Poulose, Prahlad, Rama, Sandip, Shishir, Somesh, Srini, Stella, Supriyo, Varun and Watson even for the queries that at times annoyed me.

I shall always cherish many an event – sweet n' sour – and the lively atmosphere created by friends in the hostel and in the Laboratory. Jokes and passionate, "exothermic" debates on the dining table, over the cups of tea and the volley ball games shall ring in my memory.

I shall always remember the great time I spent with Ravi, Velu, IshwarBhai, Jitesh, Joseph, RamanBhai, Pauline and their families for the affection they showered on me.

I thank Prof. Indira J. Parikh for her encouragement and affection.

Outside the realm of Physics, I learnt a great deal about the world and the society, about great Prometheans of our times, about innumerable Heroes of mankind who loved Life, lived, struggled and sacrificed for its progress and about the crores of toiling people to whom, I understand, we are all indebted for our existence. My friendship with Ravi, Velu, Ishwarbhai, Bhaskaran, Mathew and many others, from and with whom I learnt all this, is of immesurable value to me.

With deep respect and gratitude I mention my parents, and with love and affection my dear sisters and brother for their ceaseless worry about my well-being and persistently urging me on with my work. Lots of thanks and love to Debasmita whose letters from afar full of proddings bathed with patience and affection kept me both steady and going.

List of Publications

1. **IBM and the Dynamic(HF) Fermion Basis for Zn isotopes** Subrata Sarangi and Jitendra C. Parikh 1990 in *DAE symposium in Nuclear Physics,* at Madras.

2. **IBM-2 spectra of $1\nu - 1\pi$ Boson Systems in Microscopic Basis** Subrata Sarangi and Jitendra C. Parikh 1991 in *DAE symposium in Nuclear Physics,* at Bombay.

3. **Dynamic Microscopic Basis for IBM-2: A New Approach** Subrata Sarangi and Jitendra C Parikh 1992 – Communicated.

4. **Shape Transition of Even-even $^{96-106}Mo$ and $^{146-154}Sm$ Isotopes in Dynamic Microscopic IBM** Subrata Sarangi and Jitendra C. Parikh 1992 – Under Preparation

Chapter 1

General Introduction

1.1 Background

The phenomenological Interacting Boson Model (IBM) of atomic nuclei proposed by Arima and Iachello (1975), to describe the low-lying collectivity of even-even medium and heavy mass nuclei, has been extensively studied (Iachello and Arima 1987,Casten and Warner 1988) and has earned its place as a standard model for analysis of experimental data. Corresponding to the pairing and quadrupole degrees of freedom, established to be the most dominant modes of nuclear collective motion, the IBM-1 assumes, for a pair of valence nucleons, a boson carrying angular momentum $J = 0(s\text{-boson})$ or $J = 2(d\text{-boson})$ respectively. The boson Hamiltonian and the other operators are then constructed by evaluating their parameters from fits to experimental data. This model has so far gone through several extensions (See Iachello and Arima 1987) such as (i) IBM-2, where neutron and proton bosons are distinguished (ii) IBM-3 and IBM-4, where bosons corresponding to neutron-proton

pairs are also incorporated, (iii) inclusion of g-bosons ($J = 4$) corresponding to hexadecapole collectivity and so on. The wide success of phenomenological IBM has also inspired, concurrent with the development of IBM-2, a great deal of activity and investigations into the microscopic foundations of IBM in terms of the valence neutrons(ν) and protons(π) (Iachello and Talmi 1987). In these calculations, one attempts to actually construct the boson states and the Hamiltonian together with other operators in terms of the valence neutron and proton pairs and the interaction amongst them. Several schemes and procedures have been proposed to carry out such calculations and have also been applied, with various degrees of success, to the study of nuclear vibrational and rotational collectivity and shape transitions between them. In the present thesis, an alternative procedure to carry out this construction is presented. This procedure has also been applied to study vibrational and rotational nuclei. The shape transition from vibrational to rotational in $even-A$ Mo and Sm isotopes is also studied.

It is well known that nuclear shell model calculations, although fundamental and microscopic, become prohibitive for the medium and heavy mass nuclei with the valence nucleons occupying closely spaced spherical single particle (s.p.) levels because of large matrix dimensions. For example, in ^{154}Sm, with 12 valence protons (relative to $Z = 50$) and 10 neutrons (relative to $N = 82$), the number of positive parity states with $J = 0$ and 2 are $\sim$ 41 *trillion* and $\sim$ 346 *trillion* respectively (Otsuka *et al.* 1978a)! However, in the study of low-lying spectra of such nuclei, we are concerned with only very few of these trillions of levels which are experimentally observed and identified. Hence it is obviously desirable to seek for a hypothesis which allows us to drastically truncate the SM space without losing much relevant information in the process and retrieve the properties of low-lying states from the truncated space. One effective and practicable method is the well established Hartree-Fock (HF) procedure along with the angular momentum projection and band mixing

techniques (Khadkikar *et al.* 1974, Khadkikar and Praharaj 1983, Sahu and Pandya 1984, Praharaj 1989, Rath 1991) where this problem of large multiplicity of states is circumvented by considering various low lying variational states and particle-hole excitations based on them.

In an alternative and very instructive Shell Model (SM) calculation, Hecht *et al.* (1972) demonstrated that the low-lying collective spectra can be generated to more than 90% accuracy in a drastically truncated SM space by choosing only a few low-lying and coherent "favored pairs" of protons and neutrons separately and then mixing them by neutron-proton term of the surface delta interaction (SDI) (Brussaard and Glaudemans 1977).

The basic premises of IBM-1 are reflections of the existence of such favoured pairs. As already stated, they are based on the fact that the pairing and the quadrupole degrees of freedom are the most dominant aspects of nuclear collectivity in the low energy regions of nuclei away from closed shell configurations. The most important achievement of this model has been that the Hamiltonian $\mathcal{H}_{\text{IBM}-1}$ with s- and d-bosons (sdIBM-1) has, as limiting cases, three dynamical symmetries — those of (i) $U(5)$, (ii) $SU(3)$ and (iii) $O(6)$ groups. These symmetry groups alongwith the angular momentum conservation given by the $O(3)$ subgroup correspond to three types of nuclear collective motion — vibrational, rotational and γ-unstable (Iachello and Arima 1987) as also shown by the Collective Model (CM) of Bohr and Mottelson (1975).

The complete set of basis states, constructed from the framework provided by the group reduction chain of any one of these symmetries also allows us to study the transitional nuclei as perturbative cases.

The obvious and natural extension of sdIBM-1 to sdIBM-2 (Arima *et al.* 1977,

Otsuka *et al.* 1978a, 1978b) where distinct neutron and proton bosons were incorporated brought it into closer correspondence with the SM and made it possible to carry out IBM calculation in microscopic basis and established its foundations in the fundamental nucleonic degrees of freedom. This extension also revealed further systematics in the nuclear collectivity such as F-spin symmetry among the neutron and proton bosons. It also led to a natural explanation of magnetic dipole (M1) transitions, and of the 'scissors' mode (in low-lying collective 1^+ states) in deformed nuclei (review by Lipas *et al.* 1990).

Otsuka *et al.* (1978a,1978b) initiated the microscopic IBM calculations and in fact pioneered the most popular procedure, known as the OAI mapping, to establish the correspondence between the valence nucleon pairs and the bosons and to construct the boson operators as images of the corresponding fermionic operators. With the valence nucleons in a single-j shell for every pair coupled to angular momenta 0 and 2, they demonstrated the method to construct the S- and D-pairs (Otsuka *et al.* 1978b) corresponding to the s- and d-bosons. The space constructed by these pairs, called the $S-D$ subspace, was shown by them to be a very good approximation to the full SM space. They also estąblished the Marumori mapping of states in the $S-D$ space onto those in the $s-d$ boson space. This mapping helped evaluate the parameters of the boson Hamiltonian through calculation of a few fermion matrix elements in the $S-D$ space. This method has since been developed and modified to address more and more complex situations by introducing necessary approximations. A different technique based on Dyson boson mapping (Ring and Schuck 1980) has also been employed to this end (Klein and Marshalek 1991).

The three most important questions addressed in most of these calculations are the following:

1. What are the physically dominant, and hence relevant, collective degrees of

freedom in terms of pairs of nucleons in the fermionic space which serve as the basis for the drastic truncation of SM space and are represented by bosons in the corresponding boson space?

2. How exactly do we realise the bosons in IBM as coupled pairs of valence nucleons distributed over the s.p. SM states?

3. How to construct operators in the boson space as images of the respective fermion operators acting on basis states constructed out of the nucleon pairs and spanning the truncated SM space?

As stated above, a great deal of endeavour has gone into the vast literature of microscopic IBM calculations addressing these questions. We shall discuss them at some length in the next chapter.

1.2 Scope of the Thesis

In this work, an alternative method to construct the identical nucleon pairs and the IBM-2 operators (Hamiltonian and the $E2$-transition operator) from microscopic fermion input is presented. A discussion of its merits and shortcomings compared to other approaches alongwith a brief survey of the latter is also presented. This new scheme is then applied to study the low-lying collective spectra and $E2$ transition probabilities of a large number of nuclei.

The identical nucleon pairs are constructed for each nucleus under consideration, by a prescription(Sarangi and Parikh 1990) from its prolate-deformed HF solutions. This is a general prescription and applies to any even-even nucleus with at least two valence nucleons of each kind. The energy of each pair and the interaction between a neutron and a proton pair are evaluated by employing standard

SM spectroscopy techniques. These matrix elements define the IBM-2 Hamiltonian through a Marumori mapping (Ring and Schuck 1980) from the identical nucleon pair space onto the boson space. The two-body identical boson matrix elements are, however, ignored as an approximation. These matrix elements cannot be evaluated from the fermion picture because the necessary one-to-one mapping from the nucleon pair space of two identical pairs onto the space of two identical bosons cannot be established.

This scheme of constructing the *sdg*IBM-2 Hamiltonian and other operators is then applied to study the low lying spectra of nuclei. The calculations for simple nuclei like ^{20}Ne, ^{44}Ti, ^{60}Zn and ^{94}Mo with only one boson of each kind reproduce the Yrast levels of these nuclei in very good agreement with experimental and SM results (Sarangi and Parikh 1991). The non-Yrast levels for ^{20}Ne, ^{44}Ti, ^{60}Zn are pushed up in energy, whereas those of ^{94}Mo are reproduced well. As the valence neutrons and protons in the three lighter nuclei occupy the same s.p. spherical shell model space, it is more appropriate to carry out the calculations in the IBM-3 domain (Elliott 1985, Elliott *et al.* 1987) where bosons corresponding to neutron-proton mixed pairs are incorporated. The IBM-2 Hamiltonian for these nuclei does not conserve the isospin symmetry. However, our isospin mixing analysis of the eigenstates of the Hamiltonian for these nuclei shows that for the Yrast levels the isospin still remains almost conserved. This explains their good agreement with the experimental and SM results. For non-Yrast levels, however, there is substantial mixing of different isospin states which explains the upward shift of these levels.

IBM studies of collective behaviour of nuclei in medium and heavy mass region is, quite obviously, numerous and varied. The s.p. shell model space available to the valence nucleons, even within a major shell is fairly large for these nuclei, and hence varied collective properties are observed in the isotopes and isotones in these regions.

A spectacular example is the shape transition of nuclei from spherical to axial rotor in $even-A\ Zr$ and Mo nuclei in the medium mass and $Nd-Sm-Gd$ nuclei in the heavier mass regions. There have been several phenomenological IBM studies (Casten and Warner 1988, Devi and Kota 1992) to study such phenomena. Several authors have also carried out microscopic IBM calculations to examine the vibrational and rotational spectra and the shape transitions (Scholten 1983, Pannert *et al.* 1985, Druce *et al.* 1987, Navrátil and Dobeš 1991). In fact, reproducibility of these observed phenomena of shape transitions in nuclei has been the test for the various schemes and procedures to construct the IBM from a microscopic basis.

We have applied our microscopic formulation to the study of the well-known shape transitions in even-A $^{96-108}Mo$ and $^{146-154}Sm$ isotopes. While microscopic IBM calculations have already been carried out for the the Sm isotopes (Scholten 1983, Navrátil and Dobeš 1991), we have carried out the first such calculations for the Mo isotopes.

Due to the lack of a suitable IBM-2 code explicitly incorporating g-bosons, we have carried out these calculations in the IBM-1 model. In the first step, to this end, we project the IBM-2 hamiltonian $\mathcal{H}_{\text{IBM}-2}$ and $E2$-transition operator $\mathcal{T}^{(E2)}_{\text{IBM}-2}$ onto those in IBM-1 by the projection techinque of Frank and Lipas (1990) based on F-spin symmetry. The parameters of the IBM-1 operators thus determined are then used in the SDGIBM1 code of Devi and Kota (1990) to generate the spectra and calculate the $B(E2)$ values.

We have been able to reproduce very closely the experimental and theoretically calculated spectra and $E2$-transition probabilities clearly showing the characteristics of shape transition. It may be noted here that the three formalisms – those of Scholten and of Navrátil and Dobeš and ours used for deriving the microscopic IBM parameters of Sm isotopes are mutually distinct and different. Yet the results agree with each

other quite well. We have also carried out detailed spectroscopic calculations for ^{148}Sm which is a spherical nucleus and ^{150}Nd and ^{152}Sm which are known to be rotational.

In these studies we find that in order to consistently reproduce the observed spectra of the full isotopic chain, we still have to vary a few of the fermion input parameters like the strength of the effective two-body interaction and the effective charges. Similar observations have also been made by Scholten(1983) and by Navrátil and Dobeš(1991).

In Chapter 2, a brief survey of earlier approaches in microscopic IBM calculations and details of the present scheme are discussed. Its merits and shortcomings *vis à vis* other procedures are also pointed out. The results of *sdg*IBM-2 calculations applying the formalism of Chapter 2 to ^{20}Ne, ^{44}Ti, ^{60}Zn and ^{94}Mo and the analysis are reported in Chapter 3. The study of shape transitions of even-A $^{96-108}Mo$ and $^{146-154}Sm$ isotopes and detailed spectroscopic calculations are presented and discussed in Chapter 4. We also present a comparative study of sdgIBM-2 and sdgIBM-1 spectra for ^{20}Ne and ^{94}Mo in this chapter. The thesis concludes with a summary and a short discussion of future calculations in Chapter 5.

1.3 References

1. Arima A and Iachello F 1975 *Phys. Rev. Lett.* **35** 1069

2. Arima A, Ohtsuka T, Iachello F and Talmi I 1977 *Phys. Lett.* **66B** 205

3. Bohr A and Mottelson B R 1975 in *Nuclear Structure* **Vol. II** (W. A. Benjamin, Reading, Mass.)

4. Brussaard P J and Glaudemans P W M 1977 in *Shell Model Applications in Nuclear Spectroscopy* (North Holland, Amsterdam), and the references therein

5. Casten R F and Warner D D 1988 *Rev. Mod. Phys.* **60** 389, and the references therein

6. Devi Y D and Kota V K B 1990 in FORTRAN PROGRAMMES FOR SPECTROSCOPIC CALCULATIONS IN (sdg)-BOSON SPACE – THE PACKAGE SDGIBM1 (Physical Research Laboratory) (PRL-TN-90-68)

7. Devi Y D and Kota V K B 1992 *Phys. Rev.* **C45** 2238

8. Druce C H, Pittel S, Barrett B R and Duval P D 1987 *Ann. Phys.* **176** 114

9. Elliott J P 1985 *Rep. Prog. Phys.* **48** 171

10. Elliott J P, Evans J A and Williams A P 1987 *Nucl. Phys.* **A469** 51

11. Frank W and Lipas P O 1990 *J. Phys.* **G16** 1653

12. Hecht K T, McGrory J B and Draayer J P 1972 *Nucl. Phys.* **A197** 369

13. Iachello F and Arima A 1987 in *The Interacting Boson Model* (Cambridge Univ. Press), and the references therein

14. Iachello F and Talmi I 1987 *Rev. Mod. Phys.* **59** 339, and the references therein

15. Khadkikar S B, Kulkarni D R and Pandya S P 1974 *Pramana* **2** 259

16. Khadkikar S B and Praharaj C R 1983 *Phys. Rev. Lett.* **50** 1254

17. Klein A and Marshalek E R 1991 *Rev. Mod. Phys.* **63** 375

18. Lipas P O, von Brentano P and Gelberg A 1990 *Rep. Prog. Phys.* **53** 1355

19. Navrátil P and Dobeš J 1991 *Nucl. Phys.* **A533** 223

20. Otsuka T, Arima A, Iachello F and Talmi I 1978a *Phys. Lett.* **76B** 139

21. Otsuka T, Arima A and Iachello F 1978b *Nucl. Phys.* **309** 1

22. Pannert W, Ring P and Gambhir Y K 1985 *Nucl. Phys.* **A443** 189

23. Praharaj C R 1989 *Pramana- J. Phys.* **32** 351

24. Rath A K 1991 Ph.D. Thesis, Institute of Physics, Bhubaneshwar

25. Ring P and Schuck P 1980 in *The Nuclear Many-Body Problem* (Springer-Verlag, New York Inc.)

26. Sahu R and Pandya S P 1984 *Nucl. Phys.* **A414** 240

27. Sarangi Subrata and Parikh Jitendra C 1990 in *DAE Symposium in Nuclear Physics* at Madras

28. Sarangi Subrata and Parikh Jitendra C 1991 *DAE Symposium In Nuclear Physics* at Bombay

29. Scholten O 1983 *Phys. Rev.* **C28** 1783

Chapter 2

Formulation

2.1 Earlier Approaches

Microscopic studies of IBM began with the extensive and elaborate paper by Otsuka, Arima and Iachello (1978b). They first demonstrated that truncation of the Shell Model (SM) space to $S-D$ subspace is a good approximation scheme and more importantly, they presented a seniority-based mapping technique of the SM states in the $S-D$ subspace with single-j shell configurations onto those in the $s-d$ boson space of IBM-1. By virtue of this mapping which is of Marumori type (Klein and Marshalek 1991), they constructed the boson image of the fermion operators in the $S-D$ space. This mapping technique has since been popularly known as the Otsuka-Arima-Iachello (OAI) mapping and has been developed and applied by many authors (Iachello and Talmi 1987).

The OAI mapping procedure can be described in three major steps. First the nucleon pair creation operators $S^\dagger$ and $D^\dagger_M$ with seniority $v = 0, 2$ respectively are

constructed from the single particle (s.p.) creation operators $a^\dagger_{jm}$

$$S^\dagger \equiv \sqrt{\Omega} A^\dagger_{00} = \sqrt{\frac{\Omega}{2}} (a^\dagger_j a^\dagger_j)^{J=0M=0} \tag{2.1}$$

and

$$D^\dagger_M \equiv \mathcal{P} A^\dagger_{2M} = \frac{1}{\sqrt{2}} \mathcal{P} (a^\dagger_j a^\dagger_j)^{2M} \tag{2.2}$$

where the terms $(a^\dagger_j a^\dagger_j)^{JM}$ stand for a coupled pair operator with angular momentum J and projection M. In eq. (2.1), the $S^\dagger$ operator is equivalent to the quasi-spin step up operator S_+ of the Racah seniority scheme, $2\Omega = 2j + 1$ is the degeneracy of the shell. The operator $\mathcal{P}$ in eq. (2.2) projects out that component of $A^\dagger_{2M}$ which acts on the highest seniority v-particle state $|j^v v J M'\rangle$ to generate the highest seniority state $|j^{v+2} v + 2 J' M''\rangle$. Thus $D^\dagger_M$ is the highest seniority generator with angular momentum $J = 2$. $S^\dagger$ and $D^\dagger_M$, operating on the fermionic vacuum (the core) $|0\rangle_F$, generate the corresponding pairs.

In the next step, the normalized $n(= even)$-particle states

$$|j^n (S^{\frac{1}{2}(n-v)} D^{\frac{1}{2}v}) \alpha J M\rangle = \sqrt{\frac{(\Omega - \frac{1}{2}(n+v))!}{(\frac{1}{2}(n-v))!(\Omega - v)!}} (S^\dagger)^{\frac{1}{2}(n-v)} |j^v (D^{\frac{1}{2}v}) \alpha J M\rangle \tag{2.3}$$

that span the $S-D$ subspace are constructed. In eq. (2.3) $|j^v (D^{\frac{1}{2}v}) \alpha J M\rangle$ is the normalized $v(= even)$-particle highest seniority state constructed by the operation of $(D^\dagger)^{\frac{1}{2}v}$ on $|0\rangle_F$ generating a set of intermediate angular momentum states $\alpha = \{J_1, J_2, ..., J_{\frac{1}{2}v-1}\}$.

Similarly, the boson states spanning the N-boson space with N_s s-bosons and N_d d-bosons $(N_s + N_d = N)$

$$|s^{N_s} d^{N_d} \alpha J M\rangle = \mathcal{N}^{-1}_{N_s} s^{\dagger N_s} |d^{N_d} \alpha J M\rangle \tag{2.4}$$

are constructed by acting with the corresponding boson creation operators $s^\dagger$ and $d^\dagger$ on the boson vacuum $|0\rangle_B$. However, for $N_d \geq 4$, d^{N_d} configuration gives rise to

multiple J states. In order to label them, the states are classified using the group chain $U(5) \supset O(5) \supset O(3) \supset O(2)$ (Iachello and Arima 1987) and labelled by the quantum numbers N_d , v_d (d-boson seniority), n_Δ (number of d-boson triplets coupled to angular momentum 0), J and M. Otsuka *et al.* demonstrated that one can relabel the D subspace states of eq. (2.3) with the boson quantum numbers through a one-to-one mapping onto the d-subspace. This mapping is realized by a similarity transformation on the states of eq. (2.3) with $v_d = 2N_d$.

$$|j^v(D^{\frac{1}{2}v})\,''\,v_d\,''\,''\,n_\Delta\,''\,JM\rangle = \sum_\alpha C_\alpha^{v_d n_\Delta JM} |j^v(D^{\frac{1}{2}v})\alpha JM\rangle \tag{2.5}$$

Substituting these states in eq. (2.3) and correspondingly in the boson states of eq. (2.4) we establish the Marumori mapping.

$$|j^n(s^{\frac{1}{2}(n-v)}D^{\frac{1}{2}v}\,''\,v_d\,''\,''\,n_\Delta\,''JM\rangle \Leftrightarrow |s^{N_s}d^{N_d}v_d n_\Delta JM\rangle \tag{2.6}$$

Here we recall that $N = N_s + N_d = n/2$ and $N_s = \frac{1}{2}(n - v)$.

In the third step, the boson images $\mathcal{O}^B$ of the fermion operators $\mathcal{O}^F$ are constructed. The above mapping being Marumori type, the parameters of $\mathcal{O}^B$ are determined by the requirement that its matrix elements (m.e.) in the boson space spanned by the states on the r.h.s. of eq. (2.6) reproduce the m.e. of $\mathcal{O}^F$ in the fermion space (l.h.s. of eq. (2.6)). In principle, $\mathcal{O}^B$ of the n'-body operator $\mathcal{O}^F$ should be a series expansion of n''-body boson operator $n'' > n'$. However, Otsuka *et al.* have demonstrated that for a number conserving $\mathcal{O}^F$, the zeroth order approximation to $\mathcal{O}^B$, *i.e.*, $n'' = n'$ is sufficient to produce good results in agreement with those of fermionic calculations. Evaluation of the parameters of $\mathcal{O}^B$ in zeroth order involves calculations of m.e. of $\mathcal{O}^F$ only in the lower j^n (typically, j^2 and j^4) configurations. This is possible because of the applicability of Racah seniority reduction formulae and their similarity with the reduction formulae for s-bosons. Once these parameters are fixed, the spectroscopic calculations are performed in the boson space which is

much simpler than that in the fermionic space and the results are almost as good.

Otsuka *et al.* (1978a) also employed a similar mapping technique in IBM-2 regime and reproduced the low-energy collective spectra of Ba isotopes. The valence nucleons here are assumed to be occupying a $j = \frac{31}{2}$ shell, an approximation for $Z = N$ =50-82 major shell. Yet, the qualitative features of the spectra of Ba isotopes including the observed vibrational to rataional shape transition in the neutron-rich isotopes are reproduced.

The OAI mapping procedure laid down a method for mapping from the nucleon pair space onto the boson space and to construct the boson operators as images of the fermion operators. Applicability of Racah seniority reduction formulae makes these calculations simple and analytically tractable. It is applicable for the case of single-j shell or degenerate multi-j shell calculations (Otsuka 1981). The matrix elements derive their dynamic character through the boson numbers N_{s_ρ} and N_{d_ρ}. Actual shell effects of the j-shells in the major shell are, however, glossed over. The pairs S_ρ and D_ρ do not get a dynamic character with the change of N_ρ.

Pittel *et al.* (1982) and Druce *et al.* (1987) generalised this method of seniority based mapping to realistic cases of non-degenerate multi-j shell configurations by invoking the concept of generalised seniority (Talmi 1971). The $S-D$ space of Pittel *et al.* (1982) is spanned by N pair states constructed out of the "dominant" collective pairs $S_\rho^\dagger|0\rangle_F$ and $D_\rho^\dagger|0\rangle_F$ (ρ=ν and π for a neutron and a proton pair respectively). These collective pairs are chosen to be the energetically lowest J= 0 and 2 eigenstates of the one-plus-two body Hamiltonian in identical 2-particle configurations of the model space $\{j^\rho\}$. The operators $S_\rho^\dagger$ and $D_\rho^\dagger$ are now correlated pair creation operators expressed as linear combinations of operators that create the nucleon pairs in specific

s.p. orbits

$$S^{\dagger}_{\rho} = \sum_{j^{\rho}} \alpha_{j^{\rho}} (a^{\dagger}_{j^{\rho}} \tilde{a}_{j^{\rho}})^{00} \tag{2.7}$$

and

$$D^{\dagger}_{\rho,M} = \sum_{j^{\rho} \leq j'^{\rho}} \beta_{j^{\rho} j'^{\rho}} (a^{\dagger}_{j^{\rho}} \tilde{a}_{j'^{\rho}})^{2M} \tag{2.8}$$

The generalised seniority v_{ρ} of a state of identical nucleons with N_{ρ} pairs is defined as twice the number of non-S_{ρ} pairs in that state. The OAI mapping is easily established among pair states of low generalised seniority $v_{\rho} \leq 2$, *i.e.*, states containing a maximum of one D_{ρ}-pair for $\rho = \nu$ and π and the corresponding bosons. Parameters of the zeroth order boson image $\mathcal{O}^B$ are determined by demanding that the low generalised seniority ($v_{\rho} \leq 2$, $v = v_{\nu} + v_{\pi} \leq 4$) m.e. of $\mathcal{O}^F$ be exactly reproduced by the m.e. of $\mathcal{O}^B$ with the corresponding boson states. Once these parameters are determined, the higher generalised seniority m.e. in the fermion space are approximated in terms of the rather easily calculated boson m.e. with higher boson seniority states. The low generalised seniority m.e. of $\mathcal{O}^F$ are calculated analytically by Pittel *et al.* through a technique of expanding $S^{\dagger N}_{\rho}$ in terms of $J = 0$ pair creation operators of the single-j orbits in the chosen model space $\{j^{\rho}\}$(Pittel *et al.* 1982; Allaart *et al* 1988). This expansion allows the application of seniority scheme to evaluate m.e. of the individual orbits. Druce *et al.* (1987) extended the truncated space to include the effects of G_{ρ} states pertubatively by renormalising the parameters of the *sd*IBM2 Hamiltonian.

A shortcoming of this procedure is that the structure of S_{ρ} and D_{ρ} pairs, *i.e.*, the coefficients $\alpha_{j^{\rho}}$ and $\beta_{j^{\rho} j'^{\rho}}$, do not reflect the presence of many valence nucleons and hence is not dynamic. This is especially so, in the case of deformed nuclei with many valence nucleons, where the coefficients evaluated from two-particle configurations have large discrepancies from their actual values. Pittel *et al.* attempted to overcome this problem by phenomenologically choosing the single particle energies (s.p.e.) such that they vary with the number of valence nucleons. In Scholten's iterative procedure

(1983) these coefficients are determined by self-consistently taking into account the presence of all the neutron and proton pairs.

The approach of Gambhir *et al.* (1982a, 1982b) and of Van Egmond and Allaart (1984) employing the Broken Pair Approximation (BPA) (Allaart *et al.* 1988) is clearly more general and dynamic compared to that of Pittel *et al.* (1982). Following the generalised seniority scheme of Talmi (1971), it is assumed here that the ground state ($J^\pi = 0^+$) of a semi-magic nucleus with $2N_\rho$ active identical nucleons consists of only S_ρ pairs (Allaart *et al.* 1988) and can be written as $(S_\rho^\dagger)^{N_\rho}|0\rangle_F$. The coefficients $\alpha_{j\rho}$ (eq. (2.7)) are then variationally evaluated by minimising ${}_F\langle 0|(\tilde{S}_\rho)^{N_\rho}\mathcal{H}_\rho(S_\rho^\dagger)^{N_\rho}|0\rangle_F$ where $\mathcal{H}_\rho$ is the one-plus-two body identical nucleon Hamiltonian. The broken pair basis states $|\Phi^{JM}_{j\rho j'\rho}\rangle$ are then constructed by replacing one S_ρ pair in the ground state by a two particle creation operator $A^{JM}_{j\rho j'\rho}{}^\dagger$ with total angular momentum $J > 0$

$$|\Phi^{JM}_{j\rho j'\rho}\rangle \propto A^{JM}_{j\rho j'\rho}{}^\dagger (S^\dagger)^{N_\rho - 1}|0\rangle_F \tag{2.9}$$

The structure coefficients $\beta_{j\rho j'\rho}$ (eq. (2.8)) of the D_ρ pair are determined by diagonalising the Hamiltonian $\mathcal{H}_\rho$ in the space spanned by $|\Phi^{2M}_{j\rho j'\rho}\rangle$ and choosing the energetically lowest eigenvector. Once these coefficients are determined, the OAI mapping is constructed from the $S-D$ space spanned by $(S_\rho^\dagger)^{N_\rho}|0\rangle_F$ and $(S_\rho^\dagger)^{N_\rho-1}D_\rho^\dagger|0\rangle_F$ onto the corresponding states in the boson space spanned by $(s_\rho^\dagger)^{N_\rho}|0\rangle_B$ and $(s_\rho^\dagger)^{N_\rho-1}d_\rho^\dagger|0\rangle_B$ and the parameters of the boson Hamiltonian are determined by equating the corresponding boson and fermion matrices (Gambhir *et al.* 1982a). Van Egmond and Allaart (1984) evaluate the coefficients $\alpha_{j\nu}$ and $\alpha_{j\pi}$ by minimising the energy of the $N_\nu + N_\pi$ pair states $(S_\nu^\dagger)^{N_\nu}(S_\pi^\dagger)^{N_\pi}|0\rangle_F$ with the Shell Model Hamiltonian. The coefficients $\beta_{j\rho j'\rho}$ of the D_ρ pairs are determined by minimising the SM Hamiltonian in the space of $A^{\dagger JM}_{j\rho j'\rho}(S_\rho^\dagger)^{N_\rho-1}(S_{\rho'}^\dagger)^{N_{\rho'}}|0\rangle_F$ with $(\rho \neq \rho' = \nu,\ \pi)$. The OAI mapping is then constructed in much the same way as done by Druce *et al.* (1987). The SM matrix elements which define the parameters of the Hamiltonian through this mapping are

calculated by the broken-pair formulae developed by Gambhir *et al.* (1969, 1971, 1973) and Lorazo (1970).

This procedure, as discussed by Gambhir *et al.* (1982b) and Van Egmond and Allaart (1984), holds good for vibrational nuclei where the ground state, to a very good approximation, consists of S-pairs only. The situation, however, changes in case of transitional and rotational nuclei where D-pairs do occur in the ground states also. Van Egmond and Allaart also present the correction schemes to modify the S-pair structure coefficients $\alpha_{j\rho}$ to account for the Pauli blocking effect caused by the presence of D-pairs in the ground state. They also present a renormalisation scheme to take into account effects of higher collective pairs such as G_ρ and other non-collective pairs in the *sd*IBM2 operators.

Recently, Skouras *et al.* (1990) and Bonatsos *et al.* (1991) have presented a method of mapping the non-orthogonal SM states of a nucleus of 4-active particles constructed out of two 2-particle (two-pair state) states with spin-isospin quantum number JT to a corresponding two-boson state. The nonorthogonal two-pair state is eventually orthonormalised by diagonalising the SM overlap matrix. This method does not assume, unlike the OAI mapping, any ordering of SM states according to number of S-pairs and, hence is named by the authors a "Democratic mapping". Apart from being applicable to odd-A nuclei (Boson-Fermion systems) (Skouras *et al.* 1990), this method has the potential of widening the boson space (Bonatsos *et al.* 1991) to include s' and d' bosons to handle the intruder states and band mixing calculations as well as the proton-neutron bosons of IBM-3 and IBM-4 construct. Applied to single-j shell nuclei (Skouras *et al.* 1990) and to 4-particle *sd*-shell (^{20}Ne) and fp-shell (^{44}Ti) (Bonatsos *et al.* (1991)) it has been successful. However, as discussed by the authors themselves (Bonatsos *et al.* (1991)), the real test of its merit will be when it is applied to heavier (even-even) *sd*- and fp-shell nuclei.

As discussed earlier, construction of the correlated pairs S_ρ, D_ρ and G_ρ following the seniority based procedures (generalised seniority or BPA) in spherical basis had the drawback that it could not apply to the cases of transitional and rotational nuclei satisfactorily. For such cases, there have been several attempts to construct the correlated pairs by first constructing a Cooper pair in deformed basis and then projecting out its good $J(=0,2,4..)$ components.

In the Nilsson-plus-BCS calculations (Otsuka *et al.* 1982, Bes *et al.* 1982) the deformed single particle orbits $a^\dagger_{k\rho}|0\rangle_F$ are generated in the $a^\dagger_{j\rho k\rho}|0\rangle_F$ basis space by diagonalising the Nilsson Hamiltonian. The BCS calculation is then performed on these states by minimising the energy of the BCS-Nilsson state

$$|\mathrm{BCS-Nil}\rangle = \prod_{k_\rho>0}(U_{k\rho} + V_{k\rho}a^\dagger_{k\rho}a^\dagger_{\bar{k}\rho})|0\rangle_F \tag{2.10}$$

where $U_{k\rho}$ and $V_{k\rho}$ are the non-occupation and occupation probability amplitudes of the state $a^\dagger_{k\rho}|0\rangle_F$, $a^\dagger_{\bar{k}\rho}$ is the operator which creates time reversal state of $a^\dagger_{k\rho}|0\rangle_F$. The normalised number-projected state $|\mathrm{BCS-Nil}\rangle$ with $2N_\rho$ particles is written as

$$|2N_\rho\rangle = \mathcal{N}(\Lambda_\rho{}^\dagger)^{N_\rho}|0\rangle_F \tag{2.11}$$

where $\Lambda^\dagger_\rho$ is the deformed Cooper pair operator

$$\Lambda^\dagger_\rho = \sum_{k>0} C_\rho \frac{V_{k\rho}}{U_{k\rho}} a^\dagger_{k\rho}a^\dagger_{\bar{k}\rho}|0\rangle_F \tag{2.12}$$

normalised by the condition ${}_F\langle 0|\Lambda_\rho\Lambda^\dagger_\rho|0\rangle_F = 1$. This operator is then expanded in terms of good-angular momentum coupled operators $A^{J0\dagger}_\rho$ with the projection quantum number M=0

$$\Lambda^\dagger_\rho = \sum_J x^J_\rho A^{J0\dagger}_\rho \tag{2.13}$$

and the coefficients x^J_ρ. The $A^{J0\dagger}_\rho$ with J=0,2,4,.. given by

$$A^{J0\dagger}_\rho = \sum_{j^\rho\le j'^\rho} \beta^J_{j^\rho j'^\rho}(a^\dagger_{j^\rho}a^\dagger_{j'^\rho})^J. \tag{2.14}$$

are identified as S_ρ, D_ρ, G_ρ,.. correlated pairs respectively. The expansion coefficients $\beta^J_{j^\rho j'^\rho}$ here are functions of C_ρ, x^J_ρ, $V_{k\rho}$ and $U_{k\rho}$. These calculations show that the S and D pairs together account for $\geq$ 85% of the deformed pair $\Lambda^\dagger_\rho$. Although G pairs contribute a very small amount $\sim$ 10%, their contribution is very crucial in reproducing the intrinsic quadrupole moment given by the full wave function.

More accurate procedure was followed by Pittel and Dukelsky (1983) and Pannert *et al.* (1985) in pursuing number-projected HFB calculations. These calculations also indicate the small but important role played by the G-pairs in the deformed nuclei (Sm isotopes as shown by Pittel and Dukelsky). Pannert *et al.* (1985), in their extensive calculations on $^{154-164}Dy$ and $^{148-154}Sm$ isotopes which exhibit shape transition in going from lighter to heavier mass A, extensively discuss and demonstrate the need to extend the truncation of the fermion space from $S-D$ to $S-D-G$ subspace.

Maglione *et al.* (1982) proposed a collective pair approximation with the pair creation operator $\Lambda^\dagger$ given by

$$\Lambda^\dagger = \alpha S^\dagger + \beta D^\dagger \tag{2.15}$$

and the ground state of a nucleus with $2N$ valence particles given by

$$|\Psi_{2N}\rangle = (\Lambda^\dagger)^N |0\rangle_F \tag{2.16}$$

The coefficient of expansion α, β in eq. (2.15) and the structure coefficients α_j, $\beta_{jj'}$ of the S- and D- pairs are determined by minimising

$$\frac{\langle\Psi_{2N}|\mathcal{H}|\Psi_{2N}\rangle}{\langle\Psi_{2N}|\Psi_{2N}\rangle} \tag{2.17}$$

with different values of N.

However, calculation of spectra have so far not been reported in sequence to these procedures in the deformed basis.

The OAI mapping technique applied in the work discussed so far is of Marumori type. An alternative method of mapping due to Belyaev and Zelevinsky (BZ) has also been applied by many authors (Klein and Mashalek 1991). Unlike the Marumori mapping where state vectors of correlated pairs are mapped onto those of the boson space and the matrix elements are equated, here the nucleon pair (or "bifermion") operators (namely, the pair creation, annihilation and multipole operators) are mapped onto appropriate operators in the boson space. These operators in the boson space are constructed out of the basic boson operators (which obey the standard boson commutation relations) in such a way that their commutation relations and those of their fermionic counterparts, in the respective spaces, are identical.

Our work to be presented in the next section, belongs to the domain of Marumori method. Hence, in the following, we shall for the sake of completeness very briefly review the work done in the BZ domain.

Out of several prescribed versions of this general method two have been reported (Navrátil and Dobeš 1990) to be successful. Bonatsos *et al.* (1984) presented a version, known as Holstein-Primakoff version where the bifermion operators in a single-j shell with symmetry $SO(2(2j+1))$ are mapped onto boson operators satisfying the same Lie algebra. This procedure has the satisfactory consequence that introduction of g bosons becomes a necessity in order to satisfy commutators to higher orders. This method has since been generalised to non-degenerate multi-j shell cases (Bonatsos and Klein 1987; Menezes *et al.* 1987)

The other successful version has been the Dyson boson mapping (Gambhir et al 1985, Geyer 1986, de Kock and Geyer 1988, Navrátil and Dobeš 1990, 1991). Here the nucleon pair operators are mapped onto the Dyson boson operators which are functions of the basic boson operators and are generated by a non-unitary transformation. The Dyson-boson image $\mathcal{O}^D$ is obtained by simply replacing the operators

in $\mathcal{O}^F$ by their corresponding Dyson boson operators . The non-unitarity involved gives rise to non- Hermitian boson Hamiltonian $\mathcal{H}^D$ expressed in terms of the basic boson operators. Gambhir *et al.* constructed the correlated identical nucleon pair operators (or the "collective bifermion excitations") employing the BPA method and then mapped them onto the boson space. They advocated construction of the $\mathcal{H}^D$ matrix in the bi-orthonormal physical boson basis(Dyson-transformed basis states of the fermion space) and then hermitisation of $\mathcal{H}^D$ by following Gambhir-Basavaraju (1979) prescription.

Geyer (1986) and de Kock and Geyer (1988) presented, for a single-j shell case, an alternative procedure to construct the seniority-boson operators (in the OAI sense) from the Dyson-boson operators. In their procedure, the pairing Hamiltonian $\mathcal{H}_p^F$ in the fermion space plays a special role. Decomposing the matrix H_p^D of its Dyson image which is tringular (non-Hermitian) into a diagonal part H_0 and off-diagonal part W, they construct a similarity transformation Z using H_0 and W. This transformation relates the eigenstates of H_0 (which are seniority-like) to those of H_p^D. This similarity transformation along with the hermitisation prescription (Gambhir and Basavaraju 1979) now can generate a Hermitian boson operator $\mathcal{O}^B$ from $\mathcal{O}^D$ and in particular any $\mathcal{H}^B$ from the corresponding $\mathcal{H}^D$. In this process the OAI results are recovered. Navrátil and Dobeš (1990,1991) have been able to generalise this procedure to non-degenerate multi-j shell for *sd*IBM-2 and *sdg*IBM-2 calculations respectively and have reported good results for rare-earth and actinide nuclei. Recently, Dobeš *et al.* (1992) have demonstrated the equivalence of this procedure with the OAI procedure in non-degenerate multi-j shell configurations.

The question as to how good is the $S-D$ subspace as an approximation of the large SM space has also attracted a great deal of attention. Shell model calculations carried out by McGrory (1978, 1979) showed that the S- and D- coupled nucleon pairs

exhaust only about 70% of the wave functions even for low spin states and indicated the necessity to include higher angular momentum pairs such as $J = 4(G)$ pairs in the truncated space. Sage and Barrett (1980) demonstrated the effect of g-bosons (or G-pairs) in their microscopic IBM calculations on Ba isotopes. Chakraborty *et al.* (1980) also found it necessary to include the g-bosons in order to correctly reproduce the spectra and the intrinsic mass quadrupole moments of deformed nuclei. It has now been conclusively established by numerous experimental (Todd Baker *et al.* 1985, Sethi *et al.* 1990, Sethi *et al.* 1991) and microscopic (Otsuka *et al.* 1982, Bes *et al.* 1982, Scholten 1983, Yoshinaga *et al.* 1984, Pannert *et al.* 1985, Druce *et al.* 1987, Dobaczewski and Skalski 1988, Navrátil and Dobeš 1991 and many others) investigations that the G-pairs (or the g-bosons) do play a crucial role in the reproduction of spectra and hence must also be taken into consideration in the truncation of the SM space. In the IBM literature, the effect of g-boson has been included in two ways. One method is to renormalise the parameters of the *sd*IBM Hamiltonian and other operators in order to include these effects (Otsuka 1984, Van Egmond and Allaart 1984, Druce *et al.* 1987). The other is to incorporate the g-bosons in the calculations explicitly (Scholten 1983, Navrátil and Dobeš 1991, Devi and Kota (1992)). With the development of *sdg*IBM-code (Devi and Kota 1990), such calculations have also been made possible. Explicit inclusion of g-bosons makes it possible to generate higher J levels in the spectrum which are outside the space of only d-boson configurations.

The *sd*IBM with the inclusion of g-bosons has been referred to as *sdg*IBM, or in short *g*IBM, in the literature. All the work presented in this thesis has been carried out in *g*IBM formalism with explicit inclusion of g-bosons. In the following, we sometimes use the terms "*g*IBM" and "IBM" interchangeably.

2.2 Our Scheme

We have developed an alternative microscopic method to construct the correlated S_ρ, D_ρ and G_ρ pairs and derive the parameters of the IBM-2 one- and two-body operators dynamically for every nucleus. This is a general procedure applicable to any *even-even* nucleus with at least two valence nucleons of each kind. It is carried out in three major steps as given below.

(1) We construct the correlated identical nucleon pair states $|B^\rho_J\rangle$ with $J = 0$, 2 and 4 (respectively, for S_ρ, D_ρ and G_ρ pairs) from the axially-deformed and prolate HF solutions by following a prescription (Sarangi and Parikh 1990).

(2) We then establish the Marumori mapping of single pair states $|B^\rho_J\rangle$ and $\nu\pi$ pair states $|(B^\nu_{J_1} B^\pi_{J_2})J\rangle$ (J_1 and J_2 coupled to J) onto the corresponding boson states $|b^\rho_J\rangle$ and $|(b^\nu_{J_1} b^\pi_{J_2})J\rangle$ respectively. This mapping equates the m.e. of the boson one- and two-body operators to the m.e. of the corresponding fermion operators with one- and two-pair states respectively. This equality gives us the parameters of the IBM-2 Hamiltonian and the transition operators.

(3) Finally, we calculate the m.e. of the fermion oparators with one- and two- pair states by employing standard methods of the SM spectroscopy.

The rest of this chapter is devoted to the detailed mathematical description of the procedure. In Section 2.2.1 the construction of the correlated nucleon pairs $|B^\rho_J\rangle$ is presented. In Section 2.2.2 the mapping from nucleon pair space onto the IBM-2 boson space is shown and the construction of $\mathcal{H}_{\rm IBM-2}$ and the $\mathcal{T}^{(E2)}_{\rm IBM-2}$ operators is described. The matrix elements of the corresponding operators in the fermion space involving $|B^\rho_J\rangle$ and $|(B^\nu_{J_1} B^\pi_{J_2})J\rangle$ are calculated in Section 2.2.3. The projection of these IBM-2 operators onto the corresponding IBM-1 operators is described in

Section 2.2.4.

2.2.1 Construction of the Correlated Identical Nucleon Pair States

The nuclear Hamiltonian $\mathcal{H}$ for a system of n_ρ ($\rho = \nu$ and π) valence nucleons is given by

$$\mathcal{H} = \sum_{\rho=\nu,\pi} \sum_{i=1}^{n_\rho} h_i^\rho + \frac{1}{2} \sum_{\rho=\nu,\pi} \sum_{i\neq j}^{n_\rho} \mathcal{V}_{ij}^{\rho\rho} + \sum_{i=1}^{n_\nu} \sum_{j=1}^{n_\pi} \mathcal{V}_{ij}^{\nu\pi} \tag{2.18}$$

Here h_i^ρ is the one-body part with the harmonic oscillator and ls-coupling potential. $\mathcal{V}_{ij}^{\rho\rho'}$ with i and j going over the appropriate particle indices are the residual two-body interaction operators. The one-body part of the above Hamiltonian is given by the set of single particle energies (s.p.e.) $\{\epsilon_{j^\rho}\}$ in the chosen single particle (s.p.) model space $\{j^\rho\}$. The axially-symmetric, good-parity prolate solutions are obtained by minimising variationally the expectation value of this Hamiltonian in the determinantal space of n_ρ nucleons in a major shell. This iterative procedure also gives the set of s.p. HF orbits $|\rho; \pm k\Pi\rangle$ with the HF s.p. energy $\epsilon_{k\Pi}^\rho$.

These HF orbits $|\rho; \pm k\Pi\rangle$, where k and Π are the angular momentum projection quantum number along the symmetry axis and the parity respectively, are linear superpositions of spherical s.p. model orbits

$$|\rho; k\Pi\rangle = \sum_{j_i^\rho} C_{j_i^\rho k} |j_i^\rho k\Pi\rangle \qquad [\text{time}-\text{like}] \tag{2.19}$$

and

$$|\rho; -k\Pi\rangle = \sum_{j_i^\rho} C'_{j_i^\rho k} |j_i^\rho -k\Pi\rangle \qquad [\text{time}-\text{reversed}] \tag{2.20}$$

where the summations run over all j_i^ρ orbits in the chosen model space. The single oscillator major shell with the set of s.p. levels $\{j^\rho\}$ contains at the most one intruder

j-shell from the higher major shell with a different parity π. However, as this intruder shell is always distinct from the rest of the j-shells in the set $\{j^\rho\}$, we do not need to explicitly carry the label π in the coefficients $C_{j_i^\rho k}$ with which we deal henceforth. These coefficients of expansion $C_{j_i^\rho k}$ and $C'_{j_i^\rho k}$ are related by the phase relation

$$C'_{j_i^\rho k} = (-1)^{j_i^\rho - k} C_{j_i^\rho k} \tag{2.21}$$

From the set of occupied orbits we evaluate the occupancy $X_{j_i^\rho}$ of each spherical orbit j_i^ρ

$$X_{j_i^\rho} = 2 \sum_{l=1}^{n_\rho/2} |C_{j_i^\rho}^{(l)}|^2 \tag{2.22}$$

where l is the index of the occupied orbit and the factor 2 accounts for the occupation of the time-like and time-reversed orbitals $\pm k$ of the spherical orbit j_i^ρ.

We now define the normalised s.p. deformed orbit $|\rho; k = \frac{1}{2}\rangle_{\text{eff}}$

$$|\rho; k = \tfrac{1}{2}\rangle_{\text{eff}} = \sum_{j_i^\rho} p_{j_i^\rho} \bar{C}_{j_i^\rho} |j_i^\rho \tfrac{1}{2}\pi\rangle \tag{2.23}$$

with the coefficients of expansion $\bar{C}_{j_i^\rho}$ given by

$$\bar{C}_{j_i^\rho} = +\sqrt{\frac{X_{j_i^\rho}}{n_\rho}} \tag{2.24}$$

and the relative phase factors $p_{j_i^\rho}$ fixed to be

$$p_{j_i^\rho} = \frac{C_{j_i^\rho}^{(1)}}{|C_{j_i^\rho}^{(1)}|} \tag{2.25}$$

In eq. (2.25), $C_{j_i^\rho}^{(1)}$ are the coefficients of expansion of the first (energetically lowest) HF orbit (see eq.(2.19)). In case of occupied intruder orbits $|\rho; \pm k\pi'\rangle$ the phase of the lowest $\epsilon_{k\Pi'}^\rho$ is chosen to be the corresponding p_{j^ρ}. Thus, it ought to be noted here, that the $|\rho; \frac{1}{2}\rangle_{\text{eff}}$ orbit of eq. (2.23) does not have good parity. The motivation behind choosing the phases p_{j^ρ} (eq.(2.25)) for the orbit $|\rho; k = \frac{1}{2}\rangle_{\text{eff}}$ is simply the

fact that the energetically lowest HF orbit with this phase choice is invariably the most deformed orbit with maximum intrinsic quadrupole moment. Thus the average field here is maximally deformed and the most collective which prompts us to make the choice. This may be put forth as a plausibility argument for the above phase choice. In our results presented in Chapter 4 we observe that this works. The time-reversed orbit $|\rho; k = -\frac{1}{2}\rangle_{\text{eff}}$ is related to the time-like $|\rho; k = \frac{1}{2}\rangle_{\text{eff}}$ by the usual phase relationship given by eq. (2.21).

From the two-particle determinant defined by these two deformed orbits, we project out the good angular momentum and positive parity correlated pair states $|B^{\rho}_{JM=0}\rangle$ with $J = 0$, 2 and 4 for the S_ρ-, D_ρ- and G_ρ-pairs respectively

$$|B^{\rho}_{J0}\rangle = \mathcal{N}^{\rho}_{J} \sum_{j^{\rho}_{k}, j^{\rho}_{l}; k \leq l} \sqrt{1+\delta_{kl}}\,(2-\delta_{kl})\,\langle j^{\rho}_{k}\ \tfrac{1}{2}\ j^{\rho}_{l}\ -\tfrac{1}{2}|J0\rangle \\ (-1)^{j^{\rho}_{l}-\frac{1}{2}} p_{j^{\rho}_{k}}\, p_{j^{\rho}_{l}}\, \bar{C}_{j^{\rho}_{k}}\, \bar{C}_{j^{\rho}_{l}}\, |(j^{\rho}_{k} j^{\rho}_{l})J0\rangle \qquad (2.26)$$

Here and henceforth k denotes a s.p. index and not the s.p. projection quantum number. $\mathcal{N}^{\rho}_{J}$ in eq. (2.26) is the normalisation constant and the quantity in triangular brackets is the Clebsch-Gordan coefficient. From the eq. (2.26), we define the coefficients $\mathcal{C}^{\rho}_{(kl)J}$

$$\mathcal{C}^{\rho}_{(kl)J} = \mathcal{N}^{\rho}_{J}\,(-1)^{j^{\rho}_{l}-\frac{1}{2}}\,\sqrt{1+\delta_{kl}}\,(2-\delta_{kl})\,\langle j^{\rho}_{k}\ \tfrac{1}{2}\ j^{\rho}_{l}\ -\tfrac{1}{2}|j^{\rho}_{k} j^{\rho}_{l} : J0\rangle\, p_{j^{\rho}_{k}}\, p_{j^{\rho}_{l}}\, \bar{C}_{j^{\rho}_{k}}\, \bar{C}_{j^{\rho}_{l}} \qquad (2.27)$$

and the state vector $|(\rho; kl)JM = 0\rangle$

$$|(\rho; kl)J0\rangle = |(j^{\rho}_{k} j^{\rho}_{l})J0\rangle \qquad (2.28)$$

Henceforth, we suppress the projection quantum number $M = 0$ and rewrite the eq. (2.26) using the definitions of eqs. (2.27) and (2.28)

$$|B^{\rho}_{J}\rangle = \sum_{(\rho;kl)} \mathcal{C}^{\rho}_{(kl)J} |(\rho; kl)J\rangle \qquad (2.29)$$

Note that the summation in eqs. (2.29) and (2.26) are identical. The isospin quantum numbers (T, T_3) of the constructed pairs are $(1, +1)$ and $(1, -1)$ for a ν- and a π-pair respectively.

This method of construction of correlated pairs, based as it is on the self-consistently generated HF solutions, is very similar to the procedure of Dukelsky and Pittel (1983) and of Pannert *et al.* (1985) based on the HFB solutions. Projecting out the good angular momentum states from the two-particle determinantal state defined by the effective deformed orbits $|k = \pm\frac{1}{2}\rangle_{\text{eff}}$ is in parallel with their way of isolating the correlated pairs from the expansion of the deformed Cooper pair Λ_ρ in terms of good angular momentum operators $A_\rho^{J0\dagger}$(eq. (2.13)). However, our procedure is rather simple-minded compared to the HFB procedure which is a better variational procedure explicitly incorporating the pairing interaction. Being based on the occupancies $X_{j_i^\rho}$ of the model orbits which vary with n_ρ, *i.e.*, from nucleus to nucleus, the correlated pairs $|B_J^\rho\rangle$ are dynamic in character. This procedure, as also those based on HFB or Nilsson-BCS calculations, does not demand that the ground state of the nucleus should comprise only of S-pairs. Thus it is well-suited for studying any *even-even* nucleus — whether spherical or deformed. In fact, our calculations show that even in cases of nuclei exhibiting vibrational spectra, the D- and G-pairs occur in the ground state although in a very small fraction. Van Egmond and Allaart (1984) take qualitative account of this fact by incorporating Pauli-blocking corrections into the S-pair structure. In our case these effects are taken care of through the prescription.

2.2.2 Marumori Mapping of Nucleon Pair States onto the Boson States and Construction of the IBM-2 Operators

Under Marumori mapping (Klein and Marshalek 1991), we have the following correspondence between the nucleon pair states and the boson states

nucleon pairs		bosons	
$\|B^{\rho}_{J}\rangle$	$\rightarrow$	$\|b^{\rho}_{J}\rangle$; $J = 0, 2, 4$	(2.30)
$\|(B^{\nu}_{J_1} B^{\pi}_{J_2})J\rangle$	$\rightarrow$	$\|(b^{\nu}_{J_1} b^{\pi}_{J_2})J\rangle$; $J_1, J_2 = 0, 2, 4$	(2.31)

In eq. (2.31), both the fermion pairs and the bosons being distinguishable, there is no (anti)symmetry requirement amongst them and the coupled total angular momentum J can take all the values allowed by the angular mometum coupling rules. Hence the one-to-one mapping of eq.(2.31) is straight forward. Mapping of two indentical pair states $|(B^{\rho}_{J_1} B^{\rho}_{J_2})J\rangle$ onto the identical bosons states $|(b^{\rho}_{J_1} b^{\rho}_{J_2})J\rangle$ is not possible, because the allowed values of J are not the same for the fermions (nucleons) and the bosons due to the respective symmetry requirements.

The above mapping makes the boson m.e. equal to their nucleon pair counterparts.

boson m.e.		nucleon pair m.e.	
$\langle b^{\rho}_{J}\|\mathcal{O}^{B}_{\rho}\|b^{\rho}_{J}\rangle$	$=$	$\langle B^{\rho}_{J}\|\mathcal{O}^{F}_{\rho}\|B^{\rho}_{J}\rangle$	(2.32)
$\langle(b^{\nu}_{J_1} b^{\pi}_{J_2})J\|\mathcal{V}^{B}_{\nu\pi}\|(b^{\nu}_{J_3} b^{\pi}_{J_4})J\rangle$	$=$	$\langle(B^{\nu}_{J_1} B^{\pi}_{J_2})J\|\mathcal{V}^{F}_{\nu\pi}\|(B^{\nu}_{J_3} B^{\pi}_{J_4})J\rangle$	(2.33)

Here $\mathcal{O}^{B}_{\rho}$ and $\mathcal{V}^{B}_{\nu\pi}$ denote the zeroth order one- and two-body boson images of the respective fermion operators $\mathcal{O}^{F}_{\rho}$ and $\mathcal{V}^{F}_{\nu\pi}$.

It is clear from eq. (2.30) and (2.31), that our mapping procedure, though of

Marumori type, is not an OAI mapping where N-pair states in the fermion space are mapped onto the N boson states.

Secondly, since it is not possible to establish a mapping between $|(B^{\rho}_{J_1} B^{\rho}_{J_2})J\rangle$ and $|(b^{\rho}_{J_1} b^{\rho}_{J_2})J\rangle$, we cannot determine the two-body identical boson interaction parameters of the IBM-2 Hamiltonian. However, this does not prove to be a severe handicap because it is known (Scholten 1980; Iachello and Talmi 1987) from the $2^+_1 \rightarrow 0^+_1$ level separation of the isotopes of semi-magic nuclei (Sn, Pb) and their neighbouring even-even nuclei that the interaction among identical bosons can be assumed to be negligible. On this ground, in the IBM-2 Hamiltonian we ignore the interaction amongst identical bosons.

Construction of IBM-2 Hamiltonian

The general IBM-2 Hamiltonian $\mathcal{H}_{\text{IBM}-2}$ can be written as

$$\mathcal{H}_{\text{IBM}-2} = \mathcal{H}^B_{\nu} + \mathcal{H}^B_{\pi} + \mathcal{V}^B_{\nu\pi} \tag{2.34}$$

Here $\mathcal{H}^B_{\rho}$ is the identical boson part of $\mathcal{H}_{\text{IBM}-2}$ and $\mathcal{V}^B_{\nu\pi}$ is the two-body interaction term amongst the ν and π bosons. The $\mathcal{H}^B_{\rho}$ term contains only the single boson (energy) term as the identical two-body part has been ignored.

The boson matrix elements $\langle b^{\rho}_J | \mathcal{H}^B_{\rho} | b^{\rho}_J \rangle$ and $\langle (b^{\nu}_{J_1} b^{\pi}_{J_2})J | \mathcal{V}^B_{\nu\pi} | (b^{\nu}_{J_3} b^{\pi}_{J_4})J \rangle$ are evaluated in eqs. (2.32) and (2.33) by calculating fermion (nucleon) pair matrix elements $\langle B^{\rho}_J | \mathcal{H}^F_{\rho} | B^{\rho}_J \rangle$ and $\langle (B^{\nu}_{J_1} B^{\pi}_{J_2})J | \mathcal{V}^F_{\nu\pi} | (B^{\nu}_{J_3} B^{\pi}_{J_4})J \rangle$ of the identical nucleon one-plus-two body Hamiltonian $\mathcal{H}^F_{\rho}$ and the neutron-proton interaction operator $\mathcal{V}^F_{\nu\pi}$ respectively. We shall refer to these matrix elements as identical nucleon pair energy and the neutron-proton pair interaction matrix elements respectively. The evaluation of these fermion (nucleon) pair matrix elements is discussed in the next subsection.

The IBM-2 Hamiltonian, in terms of the boson creation and annhilation operators $b_J^{\rho\dagger}$ and $\tilde{b}_J^{\rho}$ and the conventional tensor coupling notations, is given by

$$\mathcal{H}_{\text{IBM}-2} = \sum_J (-1)^J \epsilon_J^{\nu} \, (b_J^{\nu\dagger} \cdot \tilde{b}_J^{\nu}) + \sum_J (-1)^J \epsilon_J^{\pi} \, (b_J^{\pi\dagger} \cdot \tilde{b}_J^{\pi}) + \sum_{J_1 J_2 J_3 J_4; J'} (-1)^{J'} W^{J'}_{J_1 J_2 J_3 J_4} \left((b_{J_1}^{\nu\dagger} \times b_{J_2}^{\pi\dagger})^{J'} \cdot (\tilde{b}_{J_3}^{\nu} \times \tilde{b}_{J_4}^{\pi})^{J'} \right) \quad (2.35)$$

where J_1, J_2, J_3, J_4 and$J = 0, 2, 4$. The total coupled angular momentum J' in the third term assumes all the values allowed by the angular momentum coupling rules. The scalar product between the tensor operators U^k and V^k of angular momentum rank k is defined in terms of the standard coupled tensor operators as

$$(U^k \cdot V^k) = (-1)^k \sqrt{2k+1} (U^k \times V^k)^0_0 \quad (2.36)$$

The matrix elements ϵ_J^{ρ} and $W^{J'}_{J_1 J_2 J_3 J_4}$ in eq.(2.35) are the boson matrix elements of the boson operators $\mathcal{H}_{\rho}^{B}$ and $\mathcal{V}_{\nu\pi}^{B}$ evaluated in eqs. (2.32) and (2.33) respectively. In the *sdg*IBM-2 Hamiltonian, the eq.(2.35) will have 6 single boson energies ϵ_J^{ρ} and 82 distinct two-body $(\nu\pi)$-boson interaction matrix elements $W^{J'}_{J_1 J_2 J_3 J_4}$.

Construction of the E2-Transition Operator

The E2-transition operator $\mathcal{T}^{(E2)}_{\text{IBM}-2}$ in IBM-2 can be written as

$$\mathcal{T}^{(E2)}_{\text{IBM}-2} = \mathcal{T}^{(E2),B}_{\nu} + \mathcal{T}^{(E2),B}_{\pi} \quad (2.37)$$

where $\mathcal{T}^{(E2),B}_{\rho}$ are the boson transition operators in the ρ-boson space given by

$$\mathcal{T}^{(E2),B}_{\rho} = \sum_{JJ'} e^{\rho}_{JJ'} (b_J^{\rho\dagger} \tilde{b}_J^{\rho})^2_0. \quad (2.38)$$

with J and J' going over the values 0,2 and 4 for the s, d and g bosons. This operator can be rewritten in expanded form

$$\mathcal{T}^{(E2)}_{\rho} = e^{\rho}_{sd}(s^{\dagger}_{\rho}\tilde{d}_{\rho} + d^{\dagger}_{\rho}\tilde{s}_{\rho})^2_0 + e^{\rho}_{dd}(d^{\dagger}_{\rho}\tilde{d}_{\rho})^2_0 + e^{\rho}_{dg}(d^{\dagger}_{\rho}\tilde{g}_{\rho} + g^{\dagger}_{\rho}\tilde{d}_{\rho})^2_0 + e^{\rho}_{gg}(g^{\dagger}_{\rho}\tilde{g}_{\rho})^2_0 \quad (2.39)$$

The parameters $e^{\rho}_{JJ'}$ in eq.(2.38) are calculated microscopically in the fermion basis by using eq.(2.32) which now reads

$$\langle b^{\rho}_{J_1}|\mathcal{T}^{(E2),B}_{\rho}|b^{\rho}_{J_2}\rangle = \langle B^{\rho}_{J_1}|\mathcal{T}^{(E2),F}_{\rho}|B^{\rho}_{J_2}\rangle \tag{2.40}$$

where $\mathcal{T}^{(E2),F}_{\rho}$ on the r.h.s. is the fermion electric quadrupole operator. Substituting for $\mathcal{T}^{(E2),B}_{\rho}$ from eq.(2.38) in the boson matrix elements of eq.(2.40), we have, by Wigner-Eckart theorem

$$\langle b^{\rho}_{J_1}|\mathcal{T}^{(E2),B}_{\rho}|b^{\rho}_{J_2}\rangle = \sum_{JJ'} e^{\rho}_{JJ'}\langle J_2\,0\,2\,0|J_1\,0\rangle[J_1]^{-\frac{1}{2}}\langle b^{\rho}_{J_1}\|(b^{\rho}_{J}b^{\rho}_{J'})^2\|b^{\rho}_{J_2}\rangle \tag{2.41}$$

with

$$[J_1] = 2J_1 + 1 \tag{2.42}$$

By intermediate state expansion, with the only possible intermediate state$|\lambda\rangle\equiv|0_B\rangle$ we have

$$\langle b^{\rho}_{J_1}||(b^{\rho}_{J}b^{\rho}_{J'})^2||b^{\rho}_{J_2}\rangle = (-1)^{J_1+J_2-2}\begin{Bmatrix} J_1 & J & 0 \\ J' & J_2 & 2 \end{Bmatrix}[2J_1J_2]^{\frac{1}{2}}\delta_{J_1J}\delta_{J_2J'} \tag{2.43}$$

where the Wigner $6-j$ symbol alongwith the Kronecker delta's reduces to

$$\begin{Bmatrix} J_1 & J_1 & 0 \\ J_2 & J_2 & 2 \end{Bmatrix} = (-1)^{J_1+J_2+2}[J_1J_2]^{-\frac{1}{2}} \tag{2.44}$$

with the quantities $\left[\frac{a}{b\,c}\right]$ given by

$$\left[\frac{a}{b\,c}\right] = \frac{[a]}{[b]\,[c]} \tag{2.45}$$

The boson matrix element in eq.(2.41) with substitution from eq.(2.43) yields

$$\langle b^{\rho}_{J_1}|\mathcal{T}^{(E2),B}_{\rho}|b^{\rho}_{J_2}\rangle = \left[\frac{2}{J_1}\right]^{\frac{1}{2}}\langle J_2\,0\,2\,0|J_1\,0\rangle t^{\rho}_{J_1J_2} \tag{2.46}$$

Eq.(2.40) along with eq.(2.46) finally gives

$$e^{\rho}_{J_1J_2} = \left[\frac{J_1}{2}\right]^{\frac{1}{2}}\frac{\langle B^{\rho}_{J_1}|\mathcal{T}^{(E2)}_{\rho}|B^{\rho}_{J_2}\rangle}{\langle J_2\,0\,2\,0|J_1\,0\rangle} \tag{2.47}$$

The nucleon pair $E2$-transition matrix element $\langle B^{\rho}_{J_1}|\mathcal{T}^{(E2),F}_{\rho}|B^{\rho}_{J_2}\rangle$ of the fermion $\mathcal{T}^{(E2),F}_{\rho}$ operator is evaluated in the next section.

2.2.3 Calculation of the Nucleon Pair Matrix Elements in the Fermion Basis

We shall calculate here the nucleon pair matrix elements, namely,

1. The identical nucleon pair energy $\langle B^{\rho}_{J}|\mathcal{H}^{F}_{\rho}|B^{\rho}_{J}\rangle$
2. The neutron proton pair interaction matrix element

$$\langle (B^{\nu}_{J_1}B^{\pi}_{J_2})J|\mathcal{V}^{F}_{\nu\pi}|(B^{\nu}_{J_3}B^{\pi}_{J_4})J\rangle$$

3. The nucleon pair $E2$-transition matrix element $\langle B^{\rho}_{J_1}|\mathcal{T}^{(E2),F}_{\rho}|B^{\rho}_{J_2}\rangle$.

These matrix elements are calcualted,using standard techniques of Shell Model spectroscopy (French 1966; French *et al.* 1969). We shall henceforth omit the superscript ^{F} denoting the fermion operator because in this subsection we shall deal only with fermion operators.

The identical nucleon pair energy

By virtue of the Marumori mapping eqs.(2.30) and (2.32), we have the single boson energy ϵ^{ρ}_{J} equal to the identical nucleon pair energy

$$\epsilon^{\rho}_{J} = \langle B^{\rho}_{J}|\mathcal{H}_{\rho}|B^{\rho}_{J}\rangle \tag{2.48}$$

Using eq.(2.29), the linear expansion of $|B^{\rho}_{J}\rangle$ states we have

$$\epsilon^{\rho}_{J} = \sum_{(\rho;k_1l_1)}\sum_{(\rho;k_2l_2)} \mathcal{C}^{\rho}_{(k_1l_1)J}\,\mathcal{C}^{\rho}_{(k_2l_2)J}\,\langle(\rho;k_1l_1)J|\mathcal{H}_{\rho}|(\rho;k_2l_2)J\rangle \tag{2.49}$$

The Hamiltonian operator $\mathcal{H}_{\rho}$ contains the one -and two-body part, i.e, $\mathcal{H}^{(1)}_{\rho} + \mathcal{H}^{(2)}_{\rho}$. Recalling the notation of eq. (2.28), we write the m.e. of $\mathcal{H}_{\rho}$ on the r.h.s. of eq.

(2.49).

$$\langle(\rho;k_1l_1)J|\mathcal{H}_\rho|(\rho;k_2l_2)J\rangle = (\epsilon_{j^\rho_{k_1}} + \epsilon_{j^\rho_{l_1}})\delta_{j^\rho_{k_1}j^\rho_{k_2}}\delta_{j^\rho_{l_1}j^\rho_{l_2}} + V^J_{j^\rho_{k_1}j^\rho_{l_1}j^\rho_{k_2}j^\rho_{l_2}} \tag{2.50}$$

where $\epsilon_{j^\rho_k}$ is the s.p.e. of the SM orbit j^ρ_k and $V^J_{j^\rho_{k_1}j^\rho_{l_1}j^\rho_{k_2}j^\rho_{l_2}}$ is the two body matrix element (t.b.m.e.) of the model residual interaction connecting the identical 2-particle states $|(j^\rho_{k_1}j^\rho_{l_1})JT=1\rangle$ and $|(j^\rho_{k_2}j^\rho_{l_2})JT=1\rangle$.

The neutron-proton pair interaction matrix element

Following the notation of French (1966) (p.330, eq. 5.103) of the article), the two-body operator $\mathcal{V}_{\nu\pi}$ that mediates the interaction between two-pair states $(|B^\nu_{J_1}B^\pi_{J_2})J\rangle$ is

$$\mathcal{V}_{\nu\pi} = \sum_{j^\nu j^\pi j'^\nu j'^\pi;J'} [J']^{\frac{1}{2}} V^{J'}_{j^\nu j^\pi j'^\nu j'^\pi}\left((a^\dagger_{j^\nu}\times a^\dagger_{j^\pi})^{J'}\times(\tilde{a}_{j'^\nu}\times\tilde{a}_{j'^\pi})^{J'}\right)^0 \tag{2.51}$$

The summation over j^ν, j'^ν and j^π, j'^π runs through the ν,π model spaces $\{j^\nu\}$ and $\{j^\pi\}$ and the set of coupled angular momentum values J' simultaneously allowed by j^ν, j^π and j'^ν, j'^π coupling. The fermion two-body interaction matrix elements $V^{J'}_{j^\nu j^\pi j'^\nu j'^\pi}$, in $\nu\pi$ formalism, are related to those in JT formalism by

$$V^{J'}_{j^\nu j^\pi j'^\nu j'^\pi} = \frac{1}{2\zeta_{j^\nu j^\pi}\zeta_{j'^\nu j'^\pi}}\left(V^{J'T=0}_{j^\nu j^\pi j'^\nu j'^\pi} + V^{J'T=1}_{j^\nu j^\pi j'^\nu j'^\pi}\right) \tag{2.52}$$

where

$$\zeta_{j^\nu j^\pi} = \frac{1}{\sqrt{1+\delta_{j^\nu j^\pi}}} \tag{2.53}$$

For our purpose, we need to go over to multipole form of the operator from the normal-ordered form in eq. (2.51) by recoupling the tensor operators therein

$$\mathcal{V}_{\nu\pi} = \sum_{j^\nu j^\pi j'^\nu j'^\pi;J'} [J'] V^{J'}_{j^\nu j^\pi j'^\nu j'^\pi} \sum_{J''}(-1)^{j^\pi+j'^\nu+J'+J''}[J'']^{\frac{1}{2}}$$
$$\left\{\begin{array}{ccc} j^\nu & j^\pi & J' \\ j'^\pi & j'^\nu & J'' \end{array}\right\}\left((a^\dagger_{j^\nu}\times\tilde{a}_{j'^\nu})^{J''}\times(a^\dagger_{j^\pi}\times\tilde{a}_{j'^\pi})^{J''}\right)^0 \tag{2.54}$$

The neutron-proton pair interaction m.e., with the notation of eq. (2.29) can be written as

$$\langle (B^{\nu}_{J_1} B^{\pi}_{J_2}) J | \mathcal{V}_{\nu\pi} | (B^{\nu}_{J_3} B^{\pi}_{J_4}) J \rangle$$

$$= \sum_{(\nu;k_1 l_1)} \sum_{(\pi;k_2 l_2)} \sum_{(\nu;k_3 l_3)} \sum_{(\pi;k_4 l_4)} \mathcal{C}^{\nu}_{(k_1 l_1) J_1} \mathcal{C}^{\pi}_{(k_2 l_2) J_2} \mathcal{C}^{\nu}_{(k_3 l_3) J_3} \mathcal{C}^{\pi}_{(k_4 l_4) J_4}$$

$$\langle ((\nu; k_1 l_1) J_1, (\pi; k_2 l_2) J_2) J | \mathcal{V}_{\nu\pi} | ((\nu; k_3 l_3) J_3, (\pi; k_4 l_4) J_4) J \rangle \quad (2.55)$$

The m.e. on the r.h.s. of the eq. (2.55) will, henceforth, be referred to as the basic matrix element (b.m.e).

We now apply the Wigner-Eckart theorem to reduce the (single bar) basic matrix element of $\mathcal{V}_{\nu\pi}$ from eq. (2.54)

$$\langle ((\nu; k_1 l_1) J_1, (\pi; k_2 l_2) J_2) J | \mathcal{V}_{\nu\pi} | ((\nu; k_3 l_3) J_3, (\pi; k_4 l_4) J_4) J \rangle$$

$$= \frac{1}{[J]^{\frac{1}{2}}} \sum_{j^{\nu} j^{\pi} j'^{\nu} j'^{\pi}; J'} [J'] V^{J'}_{j^{\nu} j^{\pi} j'^{\nu} j'^{\pi}} \sum_{J''} (-1)^{j^{\pi} + j'^{\nu} + J' + J''} [J'']^{\frac{1}{2}} \begin{Bmatrix} j^{\nu} & j^{\pi} & J' \\ j'^{\pi} & j'^{\nu} & J'' \end{Bmatrix}$$

$$\langle\langle ((\nu; k_1 l_1) J_1, (\pi; k_2 l_2) J_2) J \| \left((a^{\dagger}_{j^{\nu}} \times \tilde{a}_{j'^{\nu}})^{J''} \times (a^{\dagger}_{j^{\pi}} \times \tilde{a}_{j'^{\pi}})^{J''} \right)^{0} \| ((\nu; k_3 l_3) J_3, (\pi; k_4 l_4) J_4) J \rangle\rangle \quad (2.56)$$

The m.e. on the r.h.s. of eq. (2.56) gets further factorised into m.e. in the neutron and proton space.

$$\langle ((\nu; k_1 l_1) J_1, (\pi; k_2 l_2) J_2) J | \mathcal{V}_{\nu\pi} | ((\nu; k_3 l_3) J_3), (\pi; k_4 l_4) J_4) J \rangle$$

$$= (-1)^{J_2 + J_3 + J} \sum_{j^{\nu} j^{\pi} j'^{\nu} j'^{\pi}; J'} (-1)^{j^{\pi} + j'^{\nu} + J'} [J'] V^{J'}_{j^{\nu} j^{\pi} j'^{\nu} j'^{\pi}} \sum_{J''} \begin{Bmatrix} J_1 & J_2 & J \\ J_4 & J_3 & J'' \end{Bmatrix} \begin{Bmatrix} j^{\nu} & j^{\pi} & J' \\ j'^{\pi} & j'^{\nu} & J'' \end{Bmatrix}$$

$$\langle (\nu; k_1 l_1) J_1 \| (a^{\dagger}_{j^{\nu}} \times \tilde{a}_{j'^{\nu}})^{J''} \| (\nu; k_3 l_3) J_3 \rangle \langle (\pi; k_2 l_2) J_2 \| (a^{\dagger}_{j^{\pi}} \times \tilde{a}_{j'^{\pi}})^{J''} \| (\pi; k_4 l_4) J_4 \rangle \quad (2.57)$$

The matrix elements on the r.h.s. of eq. (2.57) are evaluated by employing standard techniques of SM spectroscopy i.e., intermediate state expansion, recoupling of the spherical tensors and application of the fermion anticommutation relations. The detailed procedure of the evaluation of this matrix element is presented in Appendix - A. The final result of this calculation is

$$\langle(\rho;k_rl_r)J_r||(a^\dagger_{j^\rho}\times\tilde{a}_{j'^\rho})^{J''}||(\rho;k_sl_s)J_s\rangle$$
$$=-(-1)^{j^\rho_{k_r}+j^\rho_{l_r}+J_s-J''}[J_rJ_sJ'']^{\frac{1}{2}}\zeta_{k_rl_r}\zeta_{k_sl_s}$$
$$\left\{\begin{array}{ccc} J_r & j^\rho & j^\rho_{l_r} \\ j'^\rho & J_s & J'' \end{array}\right\}\mathcal{E}_{k_rl_rJ_r}\mathcal{E}_{k_sl_sJ_s}\delta_{j^\rho_{k_r}j^\rho}\delta_{j'^\rho j^\rho_{k_s}}\delta_{j^\rho_{l_r}j^\rho_{l_s}} \qquad (2.58)$$

with $\mathcal{E}_{klJ}$ defined as the exchange operator (French 1966,Appendix)

$$\mathcal{E}_{klJ}f(k,l,J)=f(k,l,J)-(-1)^{j_k+j_l-J}f(l,k,J) \qquad (2.59)$$

By substituting from the matrix element eq. (2.58), we write down the final expression for the b.m.e.

$$\langle((\nu;k_1l_1)J_1,(\pi;k_2l_2)J_2)J|\mathcal{V}_{\nu\pi}|((\nu;k_3l_3)J_3,(\pi;k_4l_4)J_4)J\rangle$$
$$=(-1)^{J_1+J_4+J+1}\prod_{i=1}^{4}\zeta_{k_il_i}\,[J_i]^{\frac{1}{2}}\mathcal{E}_{k_il_iJ_i}$$
$$\sum_{J'J''}(-1)^{j^\nu_{k_1}+j^\nu_{k_3}+j^\nu_{l_1}+j^\pi_{l_2}+J'}\,[J'J'']\,V^{J'}_{j^\nu_{k_1}j^\pi_{k_2}j^\nu_{k_3}j^\pi_{k_4}}\left\{\begin{array}{ccc} J_1 & J_2 & J \\ J_4 & J_3 & J'' \end{array}\right\}$$
$$\left\{\begin{array}{ccc} j^\nu_{k_1} & j^\pi_{k_2} & J' \\ j^\pi_{k_4} & j^\nu_{k_3} & J'' \end{array}\right\}\left\{\begin{array}{ccc} J_1 & j^\nu_{k_1} & j^\nu_{l_1} \\ j^\nu_{k_3} & J_3 & J'' \end{array}\right\}\left\{\begin{array}{ccc} J_2 & j^\pi_{k_2} & j^\pi_{l_2} \\ j^\pi_{k_4} & J_4 & J'' \end{array}\right\}\delta_{j^\nu_{l_1}j^\nu_{l_3}}\delta_{j^\pi_{l_2}j^\pi_{l_4}} \qquad (2.60)$$

Finally by using eq. (2.60) in eq. (2.55) we evaluate the neutron-proton pair interaction matrix element.

The nucleon pair E2-transition matrix element

Here we shall evaluate the matrix elements of the fermion E2-transition operator in the $\rho(\nu$ or $\pi)$ model space $\{j^\rho\}$. The operator $\mathcal{T}^{(E2)}_\rho$ is given by

$$\mathcal{T}^{(E2)}_\rho=-\frac{e_\rho}{\sqrt{5}}\sum_{j^\rho j'^\rho}\langle j^\rho||r^2Y^2||j'^\rho\rangle(a^\dagger_{j^\rho}\times\tilde{a}_{j'^\rho})^2_0 \qquad (2.61)$$

In this expression for the operator, e_ρ is the effective neutron or proton charge. The term $\langle j^\rho||r^2Y^2||j'^\rho\rangle$ is the reduced quadrupole m.e. in single nucleon space calculated

in units of oscillator size parameter b_ρ^2 and will, henceforth be referred to as $q_{j^\rho j'^\rho}$. For a nucleus of mass number A with N neutrons and Z protons, the oscillator size parameters can be expressed in units of $barns(b)$ ($1b = 10^{-24}cm^2$) (Baranger and Kumar 1968, Ring and Schuck 1980)

$$b_\nu^2 = 0.0102(\frac{2N}{A^2})^{-\frac{1}{3}} \tag{2.62}$$

$$b_\pi^2 = 0.0102(\frac{2Z}{A^2})^{-\frac{1}{3}} \tag{2.63}$$

The matrix elements of this operator in the correlated pair space $|B_J^\rho\rangle$ is

$$\langle B_{J_1}^\rho|T_\rho^{(E2)}|B_{J_2}^\rho\rangle = \sum_{(\rho;k_1l_1)}\sum_{(\rho;k_2l_2)} C^\rho_{(k_1l_1)J_1}C^\rho_{(k_2l_2)J_2}\langle(\rho;k_1l_1)J_1|T_\rho^{(E2)}|(\rho;k_2l_2)J_2\rangle \tag{2.64}$$

The basic matrix element on the r.h.s. of the eq. (2.64) is evaluated by applying Wigner- Eckart theorem and then substituting for the $T_\rho^{(E2)}$ from eq. (2.61)

$$\begin{aligned}&\langle(\rho;k_1l_1)J_1|T_\rho^{(E2)}|(\rho;k_2l_2)J_2\rangle \\ &= -\frac{e_\rho}{\sqrt{5}}[J_1]^{-\frac{1}{2}}\langle J_2\,0\,2\,0\,|J_1\,0\rangle\sum_{j^\rho} \\ &\qquad \sum_{j'^\rho} q_{j^\rho j'^\rho}\langle(\rho;k_1l_1)J_1||(a^\dagger_{j^\rho}\times\tilde{a}_{j'^\rho})^2||(\rho;k_2l_2)J_2\rangle\end{aligned} \tag{2.65}$$

We write down the m.e. on the r.h.s. of eq. (2.65) by applying the general formula of eq. (2.58) and carry out the summation over j^ρ and j'^ρ. The final result is

$$\begin{aligned}&\langle(\rho;k_1l_1)J_1|T_\rho^{(E2)}|(\rho;k_2l_2)J_2\rangle \\ &= e_\rho[J_2]^{\frac{1}{2}}\langle J_2\,0\,2\,0\,|J_1\,0\rangle(-1)^{j^\rho_{k_1}+j^\rho_{l_1}+J_2}q_{j^\rho_{k_1}j^\rho_{k_2}} \\ &\qquad \zeta_{k_1l_1}\zeta_{k_2l_2}\begin{Bmatrix} j^\rho_{k_1} & j^\rho_{l_1} & J_1 \\ J_2 & 2 & j^\rho_{k_2}\end{Bmatrix}\mathcal{E}_{k_1l_1J_1}\mathcal{E}_{k_2l_2J_2}\delta_{j^\rho_{l_1}j^\rho_{l_2}}\end{aligned} \tag{2.66}$$

Substitution of eq. (2.66) in eq. (2.64) finally yields the value of $\langle B_{J_1}^\rho|T_\rho^{(E2)}|B_{J_2}^\rho\rangle$.

We first apply this formalism to a few simple cases where the chosen nuclei

have only one boson of each kind($N_\nu = N_\pi = 1$). The Hamiltonian matrices in various J subspaces are easily set up and then diagonalised (Sarangi and Parikh 1991).

In the calculations for many boson ($N_\nu \geq N_\pi \geq 1$) systems, we encounter the problem of unavailability of a suitable IBM-2 code . The code developed by Otsuka (1977), though available, does not explicitly incorporate g-bosons. We, therefore, carry out the studies with IBM-1 operators. The parameters of these operators are calculated from those in IBM-2 by a projection technique based on F-spin symmetry (Frank and Lipas 1990) and then used in the SDGIBM1 code developed and documented by Devi and Kota (1990). This code incorporates the g-bosons in the IBM-1 formalism.

2.2.4 Projection of IBM-2 operators to IBM-1 operators

The projection technique (Frank and Lipas 1990) exploits the F-spin symmetry between the proton and the neutron bosons in IBM-2 construct. The $\nu(\pi)$ bosons are attributed the quantum numbers $F = \frac{1}{2}$, $M_F = -\frac{1}{2}(\frac{1}{2})$ respectively as those of an $SU(2)$ doublet. First conjectured by Arima *et al.* (1977, 1978a, 1978b), it has been further developed by many authors (Van Isacker *et al.* 1986, Lipas *et al.* 1990).

As discussed by Lipas *et al.* (1990), the remarkable success of the phenomenological IBM-1 which does not distinguish between neutron and proton bosons suggests the existence of this symmetry. The IBM-2 spectra which are much richer compared to IBM-1, also exhibit in the low-lying regions almost pure symmetry (Frank *et al.* 1988, Lipas *et al.* 1990, Harter 1990) with respect to interchange of neutron and proton labels of the bosons. The $M1$ transitions which are generated by the $\nu\pi$ distinguishing operators like $(d^\dagger_\nu \tilde{d}_\pi)^1$, are very weak in these low-lying regions of IBM-2 spectra and stronger at higher energies where collective dipole states occur. These

observations strongly suggest that F-spin is indeed a good symmetry in the low-lying regions of IBM-2 spectra which is of our interest. They also indicate that to the extent F-spin symmetry is good in these regions, the IBM-1 Hamiltonian can be treated as a good approximation to the IBM-2 Hamiltonian. This motivates us to establish the relationship between the parameters of the operators in IBM-2 and IBM-1 and construct the projection from the former to the latter in a good F-spin limit.

The present projection technique of Frank and Lipas (1990) is derived with the assumption that the low-lying IBM-2 levels are completely symmetric under interchange of ν-π labels. For a given nucleus with N_ν and N_π number of neutron and proton bosons, a completely F-symmetric state corresponds to a state with F and its projection quantum number M_F given by

$$F = F_{max} = \frac{1}{2}(N_\nu + N_\pi) = \frac{1}{2}N \tag{2.67}$$

$$M_F = \frac{1}{2}(N_\pi - N_\nu) \tag{2.68}$$

This symmetry can be realised (Lipas *et al.* 1990) by either constructing a F-scalar Hamiltonian or, as a more realistic case, include in a non-F-scalar Hamiltonian a large Majorana force $M_{\nu\pi}$ (Iachello *et al.* 1979, Frank *et al.* 1988). The Majorana force given by

$$M_{\nu\pi} = \sum_{J_1 \neq J_2} \sum_{J=even} \xi_J \left((b^{\nu\dagger}_{J_1} b^{\pi\dagger}_{J_2})^J - (b^{\nu\dagger}_{J_2} b^{\pi\dagger}_{J_1})^J \right) \cdot \left((\tilde{b}^{\nu}_{J_1} \tilde{b}^{\pi}_{J_2})^J - (\tilde{b}^{\nu}_{J_2} \tilde{b}^{\pi}_{J_1})^J \right) + \sum_{J_1=2,4} \sum_{J=odd} \xi_J (b^{\nu\dagger}_{J_1} b^{\pi\dagger}_{J_1})^J \cdot (\tilde{b}^{\nu}_{J_1} \tilde{b}^{\pi}_{J_1})^J \tag{2.69}$$

in the sdg space, does not affect the F-symmetric ($F = F_{max}$) basis states, but pushes those with $F < F_{max}$ up in energy making the low-lying levels almost pure $F = F_{max}$. The microscopically derived IBM-2 Hamiltonians with valence nucleons in different major shells are quite clearly non-F-scalar. In these calculations the Majorana term automatically comes up in the IBM-2 Hamiltonian (Pittel *et al.* 1982, Scholten 1983, Van Egmond and Allaart 1984, Druce *et al.* 1987) although its strength coefficients ξ_J

(eq. (2.69)) evaluated microscopically come out to be comparable or less in magnitude compared to other coefficients of the Hamiltonian. The calculations of Scholten (1983) and Van Egmond and Allaart (1984) suggest that Majorana forces arise due to the renormalisation effects of truncation of the SM space. Novoselsky and Talmi (1986) in their semi-microscopic calculations of Ba and Xe isotopes, were able to reproduce the experimental results to quite good accuracy without including a Majorana term. Yet, as shown by Lipas *et al.* (1990), the eigenstates in their calculations corresponding to the low-lying levels consisted of $\sim 93\%$ (or less) of the amplitude corresponding to $F = F_{max}$. The IBM-2 Hamiltonian constructed in our microscopic procedure is clearly non-F-scalar. However, we presume that the low-lying levels and, in particular, the Yrast levels among them that we are interested in do have $F = F_{max}$ and proceed to project out the IBM-1 Hamiltonian from the IBM-2 Hamiltonian. Those terms in the expansion of the IBM-2 Hamiltonian which give the Majorana operator (eq. (2.69)), collapse in IBM-1 because of symmetry requirements of the IBM-1 states. Out of the 82 parameters of the two-body part of $\mathcal{H}_{\rm IBM-2}$ only 68 contribute to $\mathcal{H}_{\rm IBM-1}$ m.e. and the rest are mapped to zero. As we shall see in Chapter 4, the spectrum generated by the IBM-1 Hamiltonian, and the $B(E2)$ values calculated with the projected $\mathcal{T}^{(E2)}_{\rm IBM-1}$ operator are in quite good agreement with experimental and other theoretical results in the ground state and the first excited bands.

The projection of the IBM-2 operators to those of IBM-1, following Frank and Lipas(1990) can be summarised as follows

1. First we decompose the second quantised 'F-decoupled' ν-π operators of one-body type $(b^{\rho\dagger}_{J_1}\tilde{b}^{\rho}_{J_2})^J$ and two-body type $\left((b^{\nu\dagger}_{J_1}b^{\pi\dagger}_{J_2})^J(\tilde{b}^{\nu}_{J_3}\tilde{b}^{\pi}_{J_4})^J\right)^0$ in eq. (2.35) and (2.38) into linear combinations of 'coupled' operators in the $SU(2)$ F-spin space.

$$\mathcal{O} = \sum_f \mathcal{O}^{fM_f=0} \tag{2.70}$$

where f is the F-spin quantum number and M_f is its projection. The operators concerned conserve N_ν and N_π separately. Hence M_f=0. For one-body operators f=0, 1 and for two-body operators f=0, 1 and 2 .

2. Assuming that IBM-2 states of our interest are $F = F_{max} = \frac{1}{2}N$ states, we denote them as $|\alpha F_{max} M_F\rangle$ with $M_F = \frac{1}{2}(N_\pi - N_\nu)$ where α represents the spatial quantum numbers . We note that the state $|\alpha F_{max} F_{max}\rangle$ will denote a state with all proton bosons and being a symmetric state with bosons of one kind, it corresponds to an IBM-1 state. Applying the Wigner-Eckart theorem twice we relate the general m.e. of $\mathcal{O}^{f0}$ for any states with F quantum numbers $F_{max}M_F$ with that of $F_{max}F_{max}$:

$$\langle \alpha_1 F_{max} M_F | \mathcal{O}^{f0} | \alpha_2 F_{max} M_F \rangle = C_f(F_{max} M_F) \langle \alpha_1 F_{max} F_{max} | \mathcal{O}^{f0} | \alpha_2 F_{max} F_{max} \rangle \tag{2.71}$$

where

$$C_f(F_{max} M_F) = (-1)^{2(F_{max} - M_F)} \frac{\langle F_{max} - M_F f 0 | F_{max} - M_F \rangle}{\langle F_{max} - F_{max} f 0 | F_{max} - F_{max} \rangle} \tag{2.72}$$

3. Now we write $\mathcal{O}^{f0}$ back in the form of ν-π (F-spin decoupled) operators. The states in the m.e. on the r.h.s. of eq. (2.71) are pure proton boson states. Hence only the pure proton boson states in the decoupled expression of $\mathcal{O}^{f0}$ contribute to the m.e. on the r.h.s. and the others ($\nu\nu$ and $\nu\pi$ terms) drop out. With this, on the r.h.s., we are left with only proton labels in the m.e. which are then dropped making the m.e. correspond to that of IBM-1. It is related to the IBM-2 m.e. through the coefficients of eq. (2.71).

Denoting the above operation by the projection operator $\mathcal{P}$, the final results can be compiled as below (from Frank and Lipas 1990)

$$\begin{aligned} & \text{IBM}-2 \qquad \text{IBM}-1 \\ \mathcal{P}(b^{\rho\dagger}_{J_1}\tilde{b}^{\rho}_{J_2})^J\mathcal{P} &= \frac{N_\rho}{N}(b^\dagger_{J_1}\tilde{b}_{J_2})^J \qquad (2.73) \\ \mathcal{P}\Big((b^{\nu\dagger}_{J_1}b^{\pi\dagger}_{J_2})^J(\tilde{b}^{\nu}_{J_3}\tilde{b}^{\pi}_{J_4})^J\Big)^0\mathcal{P} &= \zeta_{J_1J_2}\zeta_{J_3J_4}\frac{N_\nu N_\pi}{N(N-1)}\Big((b^\dagger_{J_1}b^\dagger_{J_2})^J(\tilde{b}_{J_3}\tilde{b}_{J_4})^J\Big)^0 \qquad (2.74) \end{aligned}$$

The normalisation factor $\zeta_{J_1J_2}\zeta_{J_3J_4}$ is not explicitly stated in the formulae of Frank and Lipas. With this we now write our projected IBM-1 operators corresponding to the IBM-2 operators in eq. (2.35) and eq. (2.37).

$$\begin{aligned} \mathcal{H}_{\text{IBM}-1} &= \frac{1}{N}\sum_J(-1)^J(N_\nu\epsilon^\nu_J + N_\pi\epsilon^\pi_J)(b^\dagger_J\cdot\tilde{b}_J) \\ &+ \frac{1}{N(N-1)}\sum_{J_1J_2J_3J_4;J'}(-1)^{J'}\bar{W}^{J'}_{J_1J_2J_3J_4}\zeta_{J_1J_2}\zeta_{J_3J_4}N_\nu N_\pi(b^\dagger_{J_1}b^\dagger_{J_2})^{J'}\cdot(\tilde{b}_{J_3}\tilde{b}_{J_4})^{J'} \qquad (2.75) \end{aligned}$$

and

$$\mathcal{T}^{E2}_{\text{IBM}-1} = \frac{1}{N}\sum_{JJ'}(N_\nu e^\nu_{JJ'} + N_\pi e^\pi_{JJ'})(b^\dagger_J\tilde{b}'_J)^2_0 \qquad (2.76)$$

In eq. (2.75), the paremeter $\bar{W}^{J'}_{J_1J_2J_3J_4}$ is the sum of all the parameters $W^{J'}_{J_1J_2J_3J_4}$ in the $\mathcal{H}_{\text{IBM}-2}$ with distinct permutations of $(J_1,\ J_2)$ and $(J_3,\ J_4)$. In this manner, out of the 68 parameters of $\mathcal{H}_{\text{IBM}-2}$, we construct the 32 two-body matrix elements (t.b.m.e.) of the $\mathcal{H}_{\text{IBM}-1}$.

The single boson energies ϵ_J, the boson two body matrix elements $V^{J'}_{J_1J_2J_3J_4}$ and the boson effective charges $e_{JJ'}$ that are finally fed into the SDGIBM1 code of Devi and Kota (1990) are given by

$$\epsilon_J = \frac{1}{N}(N_\nu\epsilon^\nu_J + N_\pi\epsilon^\pi_J) \qquad (2.77)$$

$$V^{J'}_{J_1J_2J_3J_4} = \frac{N_\nu N_\pi}{N(N-1)}\bar{W}^{J'}_{J_1J_2J_3J_4} \qquad (2.78)$$

$$e_{JJ'} = \frac{1}{N}(N_\nu e^\nu_{JJ'} + N_\pi t^\pi_{JJ'}) \qquad (2.79)$$

Thus we shall have the 3 single boson energies and 32 two-body parameters of $\mathcal{H}_{\text{IBM}-1}$ and the 4 parameters of $\mathcal{T}^{(E2)}_{\text{IBM}-1}$ all microscopically determined.

2.3 References

1. Allaart K, Boeker E, Bonsignori G, Savoia M and Gambhir Y K 1988 *Phys. Rep.* **169** 209, and references therein

2. Arima A, Ohtsuka T, Iachello F and Talmi I 1977 *Phys. Lett.* **66B** 205

3. Baranger M and Kumar K 1968 *Nucl. Phys.* **A110** 490

4. Bes D R, Broglia R A, Maglione E and Vitturi A 1982 *Phys. Rev. Lett.* **48** 1001

5. Bonatsos D and Klein A 1987 *Nucl. Phys.* **A469** 253

6. Bonatsos D, Klein A and Li C T 1984 *Nucl. Phys.* **A425** 521

7. Bonatsos D, Skouras L D, Van Isacker P and Nagarajan M A 1991 *J. Phys.* **G17** 1803

8. Chakraborty Manab, Brahmam Kota V K and Parikh Jitendra C 1981 *Phys. Lett.* **100B** 201

9. de Kock E A and Geyer H B 1988 *Phys. Rev.* **C38** 2887

10. Devi Y D and Kota V K B 1990 FORTRAN PROGRAMMES FOR SPECTROSCOPIC CALCULATIONS IN (sdg)-BOSON SPACE: THE PACKAGE SDGIBM1 (PRL-TN-90-68)

11. Devi Y D and Kota V K B 1992 *Phys. Rev.* **C45** 2238

12. Dobaczewski J and Skalski J 1988 *Phys. Rev.* **C38** 580

13. Dobeš J, Navrátil P and Scholten O 1992 *Phys. Rev.* **C45** 2795

14. Druce C H, Pittel S, Barrett B R and Duval P D 1987 *Ann. Phys.* **176** 114

15. Frank W and Lipas P O 1990 *J. Phys.* **G16** 1653, and references therein

16. Frank W, von Brentano P, Gelberg A and Harter H 1988 *Phys. Rev.* **C38** 2358

17. French J B 1966 in *Multipole and Sum Rule Methods in Spectroscopy*, Proceeding of the International School of Physics, Enrico Fermi, Course **36**, Varenna, 1965, ed. C. Bloch (Academic Press, New York, 1966) New York

18. French J B, Halbert E C, McGrory J B and Wong S S M 1969 *Complex Spectroscopy, Adv. Nucl. Phys.* **Vol. 3, Chap. 3**

19. Gambhir Y K and Basavaraju G 1979 *Pramana* **13** 47

20. Gambhir Y K and Rimini A and Weber T 1969 *Phys. Rev.* **188** 1573; 1971 *Phys. Rev.* **C3** 1965; 1973 *Phys. Rev.* **C7** 1454

21. Gambhir Y K, Ring P and Schuck P 1982a *Phys. Rev.* **C25** 2858

22. Gambhir Y K, Ring P and Schuck P 1982b *Nucl. Phys.* **A384** 37

23. Gambhir Y K, Sheikh J A, Ring P and Schuck P 1985 *Phys. Rev.* **C31** 1519

24. Geyer H B 1986 *Phys. Rev.* **C34** 2373 and references therein

25. Harter H 1990 *Il Nuovo Cimento* **104A** 1265

26. Iachello F, Puddu G, Scholten O, Arima A and Otsuka T 1979 *Phys. Lett.* **89B** 1

27. Iachello F and Talmi I 1987 *Rev. Mod. Phys.* **59** 339

28. Klein A and Marshalek E R 1991 *Rev. Mod. Phys.* **63** 375

29. Lipas P O, von Brentano P and Gelberg A 1990 *Rep. Prog. Phys.* **53** 1355 and references therein

30. Lorazo B 1970 *Nucl. Phys.* **A153** 255

31. Maglione E, Catara F, Insolia A and Vitturi A 1983 *Nucl. Phys.* **A397** 102

32. McGrory J B 1978 *Phys. Rev. Lett.* **41** 533

33. McGrory J B 1979 in *Interacting Bosons in Nuclear Physics* (Ed. F. Iachello) (Plenum, 1979)

34. Menezes D P, Bonatsos D and Klein A 1987 *Nucl. Phys.* **A474** 381

35. Navrátil P and Dobeš J 1990 *Nucl. Phys.* **A507** 340

36. Navrátil P and Dobeš J 1991 *Nucl. Phys.* **A533** 223

37. Novoselsky A and Talmi I 1986 *Phys. Lett.* **172B** 139

38. Otsuka T 1977 *Computer Programme NPBOS*, University of Tokyo, Japan

39. Otsuka T 1981 *Phys. Rev. Lett.* **46** 710

40. Otsuka T 1984 *Phys. Lett.* **138B** 1

41. Otsuka T, Arima A, Iachello F and Talmi I 1978a *Phys. Lett.* **76B** 139

42. Otsuka T, Arima A and Iachello F 1978b *Nucl. Phys.* **A309** 1

43. Otsuka T, Arima A and Yoshinaga N 1982 *Phys. Rev. Lett.* **48** 387

44. Pannert W, Ring P and Gambhir Y K 1985 *Nucl. Phys.* **A443** 189

45. Pittel S and Dukelsky J 1983 *Phys. Lett.* **128B** 9

46. Pittel S, Duval P D and Barrett B R 1982 *Ann. Phys.* **144** 168

47. Ring P and Schuck P 1980 in *The Nuclear Many-Body Problem* (Springer-Verlag New York Inc.)

48. Sage K A and Barrett B R 1980 *Phys. Rev.* **C22** 1765

49. Sarangi Subrata and Parikh Jitendra C 1990 *DAE Symposium in Nuclear Physics*, at Madras

50. Sarangi Subrata and Parikh Jitendra C 1991 *DAE Symposium in Nuclear Physics*, at BomBay

51. Scholten O 1980 Ph.D. Thesis, University of Groningen, The Netherlands.

52. Scholten O 1983 *Phys. Rev.* **C28** 1783

53. Sethi A, Hintz N M, Mihailidis D N, Mack A M, Gazzaly M, Jones K W, Pauletta G, Santi L and Goutte D 1991 *Phys. Rev.* **C44** 700

54. Sethi A, Todd Baker F, Emery G T, Jones W P, Grimm M A 1990 *Nucl. Phys.* **A518** 536

55. Skouras L D, Van Isacker P and Nagarajan M A 1990 *Nucl. Phys.* **A516** 255

56. Talmi I 1971 *Nucl. Phys.* **A172** 1

57. Todd Baker F, Sethi A, Penumetcha V, Emery G T, Jones W P, Grimm M A, Whiten M L 1985 *Phys. Rev.* **C32** 2212

58. Van Egmond A and Allaart K 1984 *Nucl. Phys.* **A425** 275

59. Van Isacker P, Heyde K, Jolie J and Sevrin A 1986 *Ann. Phys.* **171** 253

60. Yoshinaga N, Arima A and Otsuka T 1984 *Phys. Lett.* **143B** 5

Chapter 3

sdgIBM2 Studies of Some Simple Nuclei

3.1 Introduction

The scheme developed in the previous chapter has been applied to a few cases of simple nuclei to study their low-lying collective spectra in IBM-2 domain and the results are presented in this chapter.

Our sample nuclei are (i) ^{44}Ti in single-j shell and (ii) ^{20}Ne, ^{60}Zn and ^{94}Mo in multi-j shell configurations. These nuclei are chosen by the criterion that they have only two valence neutrons and two valence protons. In other words, they are nuclei with one neutron and one proton boson ($N_\nu = N_\pi = 1$). The parameters of $\mathcal{H}_{\text{IBM-2}}$, namely ϵ^ρ_J and $W^{J'}_{J_1 J_2 J_3 J_4}$ (eq. (2.35)) derived in the previous chapter are precisely the matrix elements of the Hamiltonian in the two-boson configurations $|(b^\nu_{J_1} b^\pi_{J_2})J\rangle$

of these nuclei.

$$\langle (b^{\nu}_{J_1} b^{\pi}_{J_2}) J | \mathcal{H}_{\text{IBM}-2} | (b^{\nu}_{J_3} b^{\pi}_{J_4}) J \rangle = (\epsilon^{\nu}_{J_1} + \epsilon^{\pi}_{J_2}) \delta_{J_1 J_3} \delta_{J_2 J_4} + W^{J}_{J_1 J_2 J_3 J_4} \qquad (3.1)$$

Thus the matrices in different J-subspaces are easily set up and diagonalised. Because of this straight forward correspondence between the boson states $|(b^{\nu}_{J_1} b^{\pi}_{J_2})J\rangle$ and the nucleon pair states $|(B^{\nu}_{J_1} B^{\pi}_{J_2})J\rangle$, we can equivalently say that these spectroscopic calculations are carried out in the nucleon pair space spanned by the latter. The low-lying spectra are then compared with the results of available theoretical and experimental results.

The Yrast levels of all the four nuclei are reproduced to very good accuracy. The non-Yrast levels of the lighter nuclei, *viz.*, ^{20}Ne, ^{44}Ti and ^{60}Zn are pushed up in energy whereas those of ^{94}Mo are comparable to observed experimental values.

The inclusion of g-bosons in these calculations is found to be essential to produce not only the levels of low angular momenta ($J \leq 4$) to good accuracy but also the higher levels ($J > 4$) which lie outside of the $(d^{\dagger}_{\nu} d^{\dagger}_{\pi})^{J} \mid 0\rangle_{B}$ configuration space.

The IBM-2 does not include any bosons corresponding to the mixed ($\nu\pi$) pairs. It has been discussed by Elliott (1985) and Elliott *et al.* (1987) that when the valence neutrons and protons are in the same j-shell(s) (as is the case for ^{20}Ne, ^{44}Ti and ^{60}Zn in our calculations) one ought to include the mixed pairs alongwith the identical particle pairs in order to preserve the isospin symmetry and carry out the IBM-3 or IBM-4 calculations. On the other hand, the recent calculations of Skouras *et al.* (1990) in single-j ($= f_{\frac{7}{2}}$) shell for Ti, Cr and V isotopes and Bonatsos *et al.* (1991) in the *sd*-shell and *fp*-shell for ^{20}Ne and ^{44}Ti respectively indicate that the effects of mixed pairs are very small. Bonatsos *et al.* demonstrate that apart from

the s_ρ, d_ρ and g_ρ ($\rho = \nu$ or π) bosons, the higher identical particle ($T = 1$) non-collective and collective bosons, *i.e.*, d'_ρ and i_ρ respectively play more dominant role than the bosons corresponding to mixed pairs ($T = 0$) in reproducing the low-lying levels including the non-Yrast levels.

Carrying out IBM-3 and IBM-4 calculations or incorporating the higher bosons is out of the scope of our work. In analysing the results of the IBM-2 calculations for these light nuclei, we calculate the expectation values of $\mathcal{T}^2$ ($\mathcal{T}$ is the total isospin opertor) in the eigenstates of the Yrast and other low-lying levels. Ideally, this value should be zero for the low-lying states of the nuclei considered. Because of the isospin mixing mentioned above they turn out to be non-zero. We find that for the Yrast levels, $\langle \mathcal{T}^2 \rangle$ is typically $\sim 10^{-2}$, very close to zero, whereas for the non-Yrast levels it is substantial, typically of order unity. This explains why the former agree with other theoretical and experimental results so well and why the latter do not.

The rest of this chapter is organised as follows. In Sec. 3.2, the spectra of the nuclei, starting with that of ^{44}Ti as a single-j shell case, are presented. In case of the non-degenerate multi-j shell calculations, we also compare the correlated pairs determined in our procedure with those of the generalised seniority method (Pittel *et al.* 1982). In Sec. 3.3, the $\mathcal{T}^2$ operator and its matrix elements are calculated and $\langle \mathcal{T}^2 \rangle$ values for the three light nuclei are tabulated.

Table 3.1: SM matrix elements $\langle(\frac{7}{2})^2 JT \mid V \mid (\frac{7}{2})^2 JT\rangle$.

J	T	ME(MeV)	J	T	ME(MeV)
0	1	−3.11	4	1	−0.26
1	0	−2.50	5	0	−1.60
2	1	−1.52	6	1	+0.14
3	0	−1.62	7	0	−2.49

3.2 Spectra of the Sample Nuclei

3.2.1 ^{44}Ti

Assuming ^{40}Ca to be an inert core, ^{44}Ti is regarded as having two valence neutrons and protons in $\{f_{\frac{7}{2}}\}$ shell. Because of the single-j shell, there is no need to follow the HF procedure here. The nucleon pairs $|B^{\rho}_{J}\rangle$ are, then, given by eq. (2.29) with $C^{\rho}_{(kl)J} = 1$. We have used the SM m.e. $\langle(\frac{7}{2})^2 JT \mid V \mid (\frac{7}{2})^2 JT\rangle$ listed by Skouras *et al.* (1990). These m.e. are reproduced in table 3.1.

Being a single-j shell case, the identical nucleon pair energies of the S-, D- and G- pairs, by eq. (2.50) are the J= 0, 2 and 4 ($T = 1$) two-body matrix elements (t.b.m.e.) listed in table 3.1. Thus the single boson energies ϵ^{ρ}_{J} of the s_ρ, d_ρ and g_ρ bosons are (in MeV) −3.11, −1.52 and −0.26 respectively. The m.e. listed in table 3.1 are then transformed to the $\nu\pi$-basis by eq. (2.52). The neutron-proton pair interaction matrix element, is calculated using eqs. (2.55), (2.59) and (2.60). These m.e., through the Marumori mapping (eq. (2.33)) are the t.b.m.e. $W^{J}_{J_1 J_2 J_3 J_4}$ of eq. (3.1). The eigenstates of $\mathcal{H}_{\mathrm{IBM-2}}$ (eq. (3.1)) with eigenvalues E_J of the level J can

be written as

$$|E_J^{(i)}\rangle = \sum_{J_1,\, J_2=0,\, 2,\, 4} C^{(i)}_{(J_1 J_2)J} |(b^{\nu}_{J_1} b^{\pi}_{J_2})J\rangle \tag{3.2}$$

where i is the index of the eigenstate assigned in increasing order of energy E_J. The spectrum generated by this Hamiltonian is plotted in fig. 3.1 (labelled IBM-2) alongwith the SM and "Model-2" ((sdg)IBM-1) results of Skouras *et al* (1990). The agreement of the Yrast levels produced by our calculation, barring the $J = 6$ level, is quite good. The non-Yrast levels ($2_2^+, 4_2^+$ and 0_2^+) are pushed up by a small amount. This is due to the loss of isospin symmetry mentioned before. This shift of non-Yrast will be more prominent in the multi-j shell cases to which we now turn.

3.2.2 ^{20}Ne

The ^{20}Ne calculations, with ^{16}O core, are carried out in $\{d_{\frac{5}{2}}, s_{\frac{1}{2}}, d_{\frac{3}{2}}\}$ SM space with Wildenthal's Universal-sd interaction and his choice of s.p.e.(in MeV) -3.95, -3.16 and 1.65 (Wildenthal 1984), respectively. This set of s.p.e. and t.b.m.e. have been determined by Wildenthal by fitting to the observed data and work well in the entire sd shell. The occupied time-like HF s.p. orbits, following the notation of Eq.(2.19), are

$$|\ \rho;\ k = \tfrac{1}{2}\rangle = 0.777\ |\ \rho;\ \tfrac{5}{2}\ \tfrac{1}{2}\rangle - 0.523\ |\ \rho;\ \tfrac{1}{2}\ \tfrac{1}{2}\rangle - 0.350\ |\ \rho;\ \tfrac{3}{2}\ \tfrac{1}{2}\rangle \quad (\rho = \nu,\ \pi) \tag{3.3}$$

The occupied time-reversed orbits are related to these time-like orbits through phase relationship given in eq. (2.21). These orbits as well as the correlated pair states to be constructed from them are identical for the neutrons and the protons because the valence nucleons occupy the same shell.

There being only two valence particles of each kind, the $|\rho; k = \frac{1}{2}\rangle_{\text{eff}}$ orbit eq. (2.23) is identical to the occupied HF orbit eq. (3.3). The correlated identical nucleon pair states $|B^{\rho}_J\rangle$ are then constructed from these orbits following eqs. (2.27)

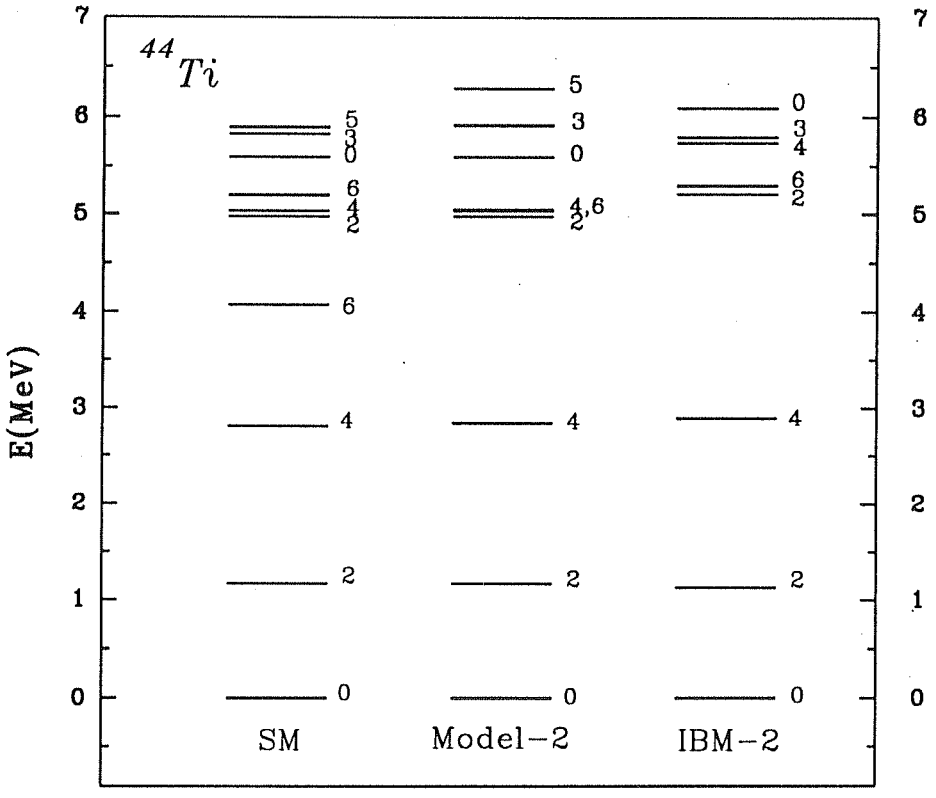

Figure 3.1: Spectrum of ^{44}Ti. The plots labelled 'SM' and 'Model-2' are the Shell Model and (sdg)IBM-1 spectra of Skouras *et al.*(1990). The plot labelled 'IBM-2' is the spectrum generated by our scheme with s, d, g bosons.

and eq. (2.29). The collectivity built into these states through our procedure is certainly better than that of the generalised seniority (g.s.) pairs $|B^{\rho}_{J}\rangle_{\text{g.s.}}$ (Pittel *et al.* 1982), i.e. the lowest J=0, 2 and 4 eigenstates of the two-particle (^{18}O) Hamiltonian. For the sake of illustration of this point, we plot in fig. (3.2) (a)-(c) the occupation probabilities of the components $|\mathcal{C}_{(kl)J}|^2$ for the two particle configurations $(kl)J$ (notation of eqs. (2.27) and (2.28) given by $|B^{\rho}_{J}\rangle$ and $|B^{\rho}_{J}\rangle_{\text{g.s.}}$). The participation of the higher s.p. orbits ($s_{\frac{1}{2}}$ and $d_{\frac{3}{2}}$) in the $|B^{\rho}_{J}\rangle$ states (denoted 'dynamic') compared to the g.s. states as seen in the plots is clearly more significant.

The identical nucleon pair energy is evaluated using the procedure outlined in sec. 2.2.3. The neutron proton pair interaction matrix elements are calculated from the Universal-*sd* m.e. as outlined in the case of ^{44}Ti above. The parameters of $\mathcal{H}_{\text{IBM}-2}$ in eq. (3.1), namely ϵ^{ρ}_{J} and $W^{J}_{J_1J_2J_3J_4}$ are, by the Marumori mapping, equal to the identical nucleon pair energy and the ν-π pair interaction m.e. respectively (eqs. (2.32) and (2.33)). The spectrum generated by this Hamiltonian is presented in fig. 3.3 (labelled IBM-2) alongwith the experimental (Halbert *et al.* 1971; Lederer and Shirley 1978) and the SM results.

It may be noted here that the dimensionalities of the SM matrices for angular momentum states J = 0, 2, 4, 6, 8 and T = 0 are 21, 56, 44, 17 and 3 (Sebe and Harvey 1968) respectively. In comparison the dimensionalities of the IBM Hamiltonian with the s, d and g bosons are 3, 6, 6, 3 and 1 respectively. Yet the Yrast levels match quite well with experimental and SM levels. These levels also match well with the phenomenological results of Devi *et al.* (1989). However, the non-Yrast levels (of which we have plotted only a few of the lower ones) are all pushed high up with the lowest of them, with J = 2 coming at 12.68 MeV. We shall examine these levels more closely in the next section.

Just as we generated the above spectrum by mapping $|B^{\rho}_{J}\rangle$ states onto the

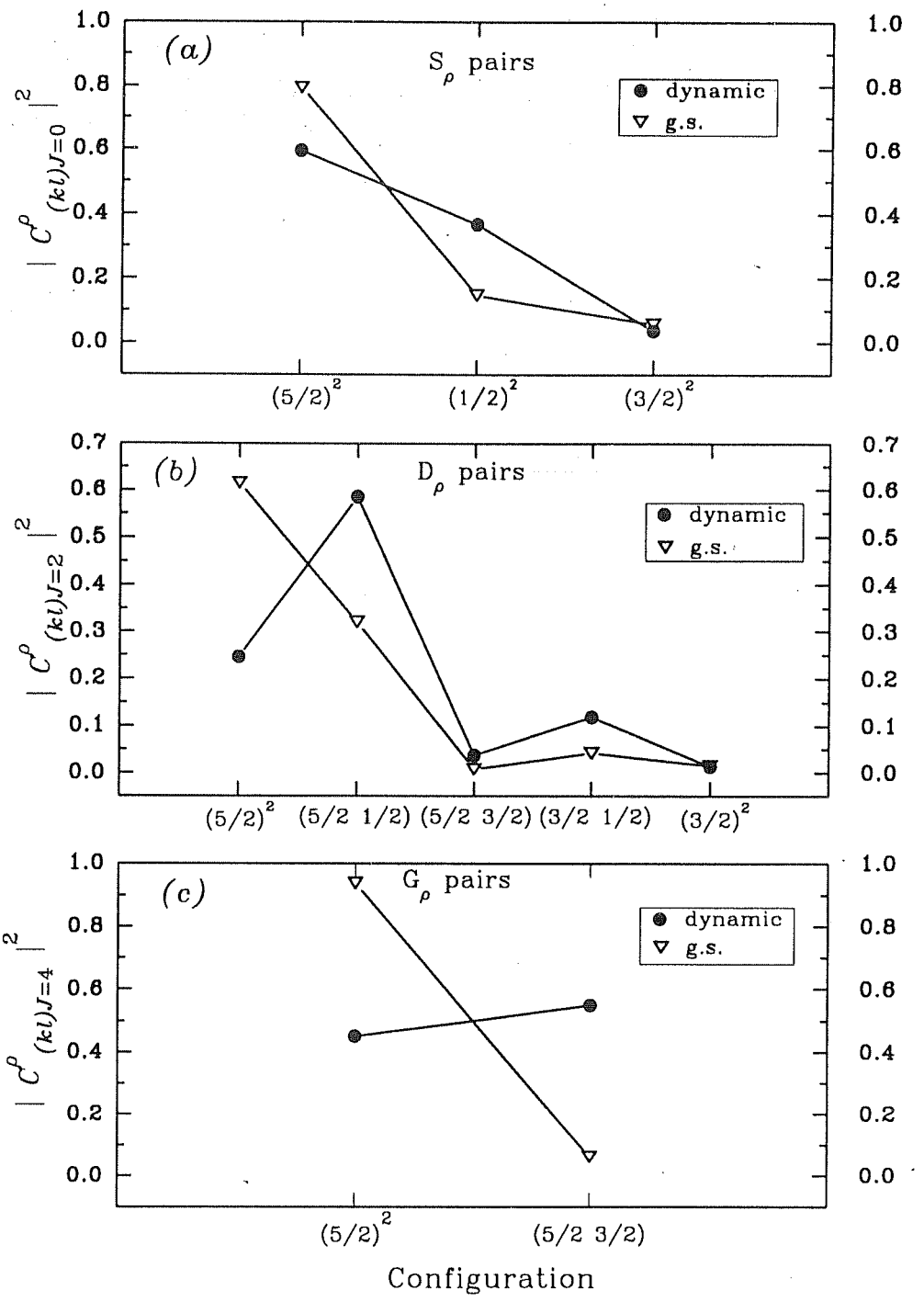

Figure 3.2: A Comparison of the correlated pairs $|B^\rho_J\rangle$ determined by our procedure from HF solutions of ^{20}Ne (denoted 'dynamic') and the eigenstates $|B^\rho_J\rangle_{\text{g.s.}}$ of the two-identical particle Hamiltonian of ^{18}O (denoted 'g.s.'). Figs. (a)-(c) show this comparison between the S, D and G correlated pairs respectively.

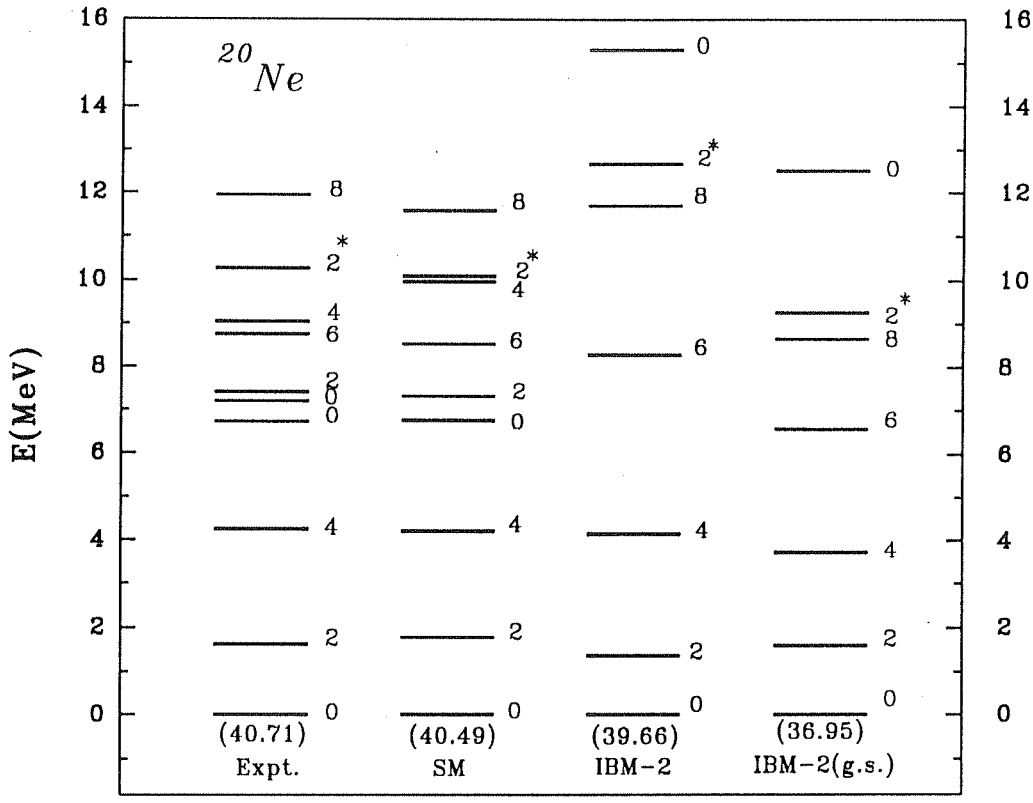

Figure 3.3: Spectrum of ^{20}Ne. Our results labelled 'IBM-2' are plotted alongside experimental (labelled 'Expt.') (Halbert *et al* 1971; Lederer and Shirley 1978) and SM (labelled 'SM') results. The absolute energies of the ground states w.r.t. that of ^{16}O are given in parentheses. The levels marked asterisk are $T = 1$ states. All the rest 'IBM-2' non-Yrast levels occur above the $J = 2$, $T = 1$ level. The Yrast and a few lower levels generated with $|B^{\rho}_{J}\rangle_{g.s.}$ are plotted (labelled 'IBM-2(g.s.)') for comparison.

bosons, we can generate the spectrum with the g.s. pairs $|B^{\rho}_{J}\rangle_{\text{g.s.}}$. The Yrast levels and a few higher levels of the spectrum generated in this calculation are plotted in fig. 3.3 and are labelled 'IBM-2(g.s.)'. The ground state of 'IBM-2(g.s.)' is pushed up by 3.5 MeV compared to that of SM whereas that of IBM-2 matches well. The collectivity of the $|B^{\rho}_{J}\rangle$ pairs plays the role in pushing the ground state down. The relative positions of the J=6 and 8 levels of the IBM-2 and IBM-2(g.s.) differ substantially. This is clearly because of the enhanced participation of the $d_{\frac{3}{2}}$ shell in the D_{ρ} and G_{ρ} pairs of IBM-2, as is clear from fig. 3.2 (b)-(c). This shell occurs at a high energy (5.7 MeV) above the $d_{\frac{5}{2}}$ shell and stronger participation of this shell in the states generating the higher J lavels pushes those levels higher up in energy. Overall, the IBM-2 spectrum, generated with the $|B^{\rho}_{J}\rangle$ states constructed by our procedure is very close to that of the SM calculations.

3.2.3 ^{60}Zn

The ^{60}Zn calculations, are done in $\{p_{\frac{3}{2}}\ f_{\frac{5}{2}}\ p_{\frac{1}{2}}\}$ SM space with ^{56}Ni as the core. Following Koops and Glaudemans (1977), the s.p.e. of the model orbits are chosen to be (in MeV) -10.24, -9.46 and -9.14 and the ASDI as t.b.m.e. for the calculations. The occupied time-like HF orbits for the neutrons and protons are calculated to be

$$|\ \rho;\ k=\tfrac{1}{2}\rangle = 0.733\ |\ \rho;\ \tfrac{3}{2}\ \tfrac{1}{2}\rangle - 0.504\ |\ \rho;\ \tfrac{5}{2}\ \tfrac{1}{2}\rangle - 0.457\ |\ \rho;\ \tfrac{1}{2}\ \tfrac{1}{2}\rangle \qquad (3.4)$$

The construction of the correlated nucleon pairs, calculation of their energies and the interaction matrix elements amongst the neutron and the proton pairs, construction of IBM-2 Hamiltonian follow according to the procedure outlined in the previous subsection.

The occupation probabilities $|C^{\rho}_{(kl)J}|^2$ of the $|B^{\rho}_{J}\rangle$ pairs calculated through our procedure and the $|B^{\rho}_{J}\rangle_{\text{g.s.}}$ pair states (the lowest J= 0, 2 and 4 eigenstates of 2-particle

(^{58}Ni) Hamiltonian) are plotted in fig. 3.4. The collectivity of the model orbits in both the cases is similar. In fact, the $|B^{\rho}_{J=0}\rangle_{\text{g.s.}}$ seems to be more collective than $|B^{\rho}_{J=0}\rangle$. The spectrum generated by the IBM-2 Hamiltonian is plotted in Fig. 3.5 alongwith the available experimental data (Lederer and Shirley 1978) and the SM results. These SM results have also been produced by Van Hienen *et al* (1976). Once again, the Yrast levels match well with the corresponding experimental and SM levels, whereas our non-Yrast levels are pushed up.

The spectrum generated by the $|B^{\rho}_{J}\rangle_{\text{g.s.}}$ pairs are also plotted in fig. 3.5 (labelled 'IBM-2(g.s.)'). Whereas the absolute energies of the ground states match more or less, the J=2 level generated through our procedure is clearly closer to that of SM than its g.s. counterpart. The higher J levels match well and much better than they do in the case of ^{20}Ne. This is because of the closer resemblance of the D and G pairs in our procedure and g.s. which in turn is rooted in the closer proximity of the s.p. levels $p_{\frac{3}{2}}$ and $f_{\frac{5}{2}}$. The overall agreement of the 'IBM-2' and the 'IBM-2(g.s.)' spectra may be ascribed to the approximately vibrational character of the ^{60}Zn spectrum for which the g.s. states are expected to work well.

3.2.4 ^{94}Mo

The calculations for ^{94}Mo, with ^{90}Zr core, are carried out in inequivalent model spaces for protons and neutrons. The two valence protons, outside the (semi-)closed shell at $Z = 40$, are in $\{g_{\frac{9}{2}}\}$ orbit with s.p.e. 0.0 MeV. The two valence neutrons, outside the closed shell at $N = 50$, are in $\{d_{\frac{5}{2}}\ s_{\frac{1}{2}}\ d_{\frac{3}{2}}\ g_{\frac{7}{2}}\ h_{\frac{11}{2}}\}$ space with s.p.e. of the orbits (in MeV) 0.0, 1.0, 2.5, 3.0 and 3.6 respectively (following Khosa *et al.* (1982) in their studies of shape transitions in Mo and Zr isotopes). But the HF procedure which conserves parity excludes the odd parity $h_{\frac{11}{2}}$ orbit from the lowest occupied HF orbit. The Surface Delta Interaction (SDI) with the $\nu - \pi$ interaction strength

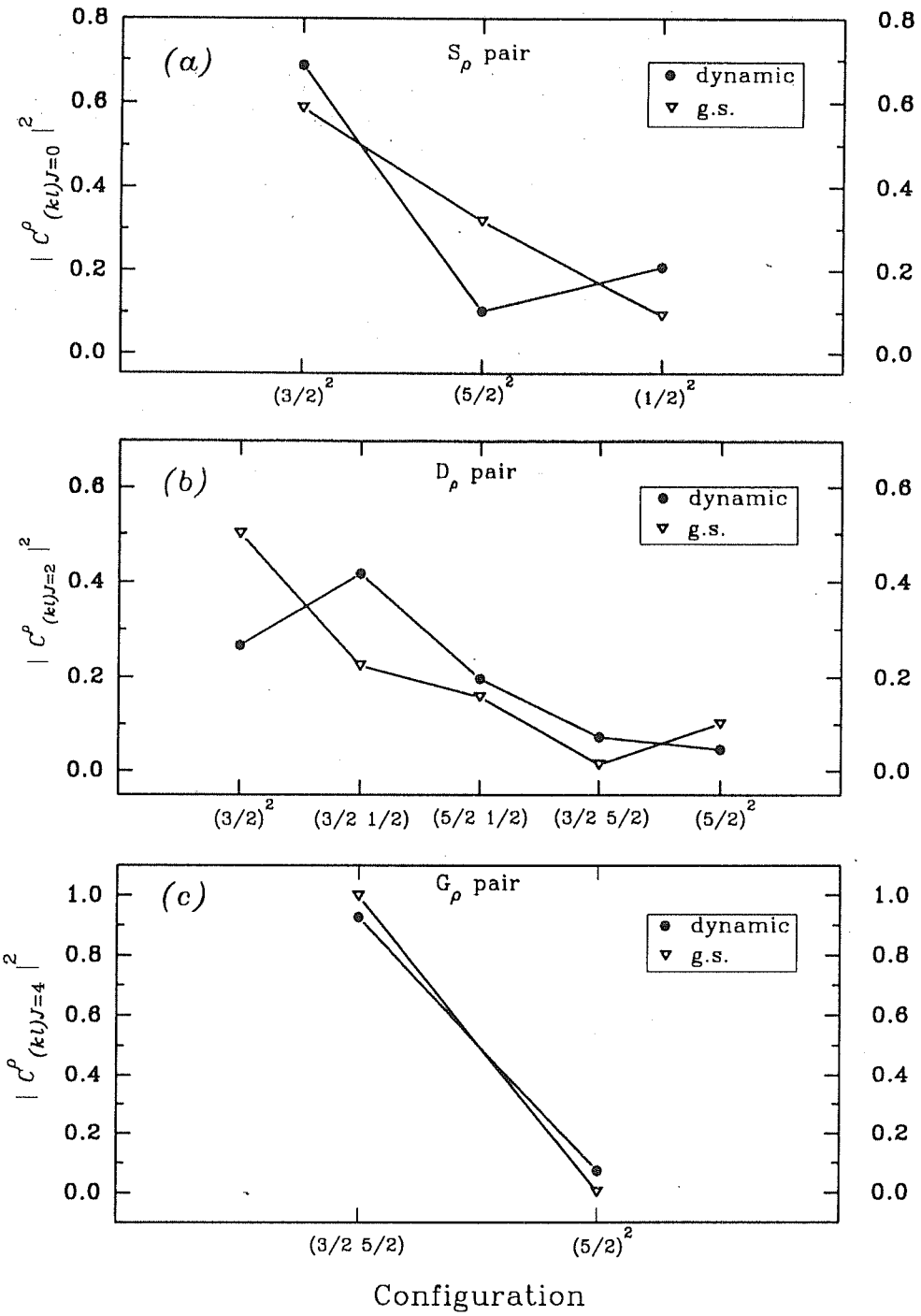

Figure 3.4: A Comparison of in the correlated pairs $|B^{\rho}_{J}\rangle$ determined by our procedure from HF solutions of ^{60}Zn ('dynamic') and the eigenstates $|B^{\rho}_{J}\rangle_{\text{g.s.}}$ of two-identical particle Hamiltonian of ^{58}Ni ('g.s.'). Figs. (a)-(c) show this comparison between the S, D and G correlated pairs respectively.

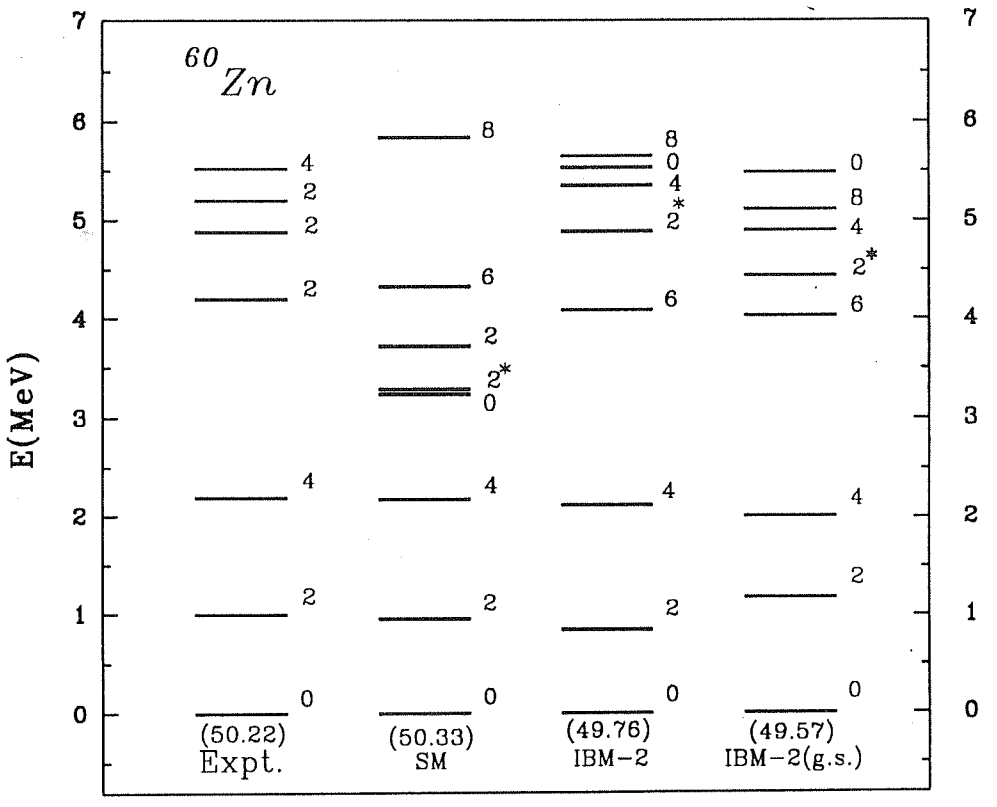

Figure 3.5: Spectrum of ^{60}Zn. Our results labelled 'IBM-2' are plotted alongside experimental (labelled 'Expt.') (Lederer annd Shirley 1978) and SM (labelled 'SM') results. The absolute energies of the ground states w.r.t. that of ^{56}Ni are given in parentheses. Levels marked asterisk are $T = 1$ states. All the rest IBM-2 non-Yrast levels are above the $J = 2$, $T = 1$ level. The spectrum generated by the $|B^{\rho}_{J}\rangle_{\text{g.s.}}$ states (labelled 'IBM-2(g.s.)') are also plotted.

$A_{\nu\pi} = 0.6MeV$ and identical particle interation strength $A_{\nu\nu} = A_{\pi\pi} = 0.35MeV$ chosen by Federman and Pittel (1978) as the residual two-body interaction produces a rather stretched spectrum. For better reproduction of the spectrum, a different choice of $A_{\nu\pi}$ is found necessary and it is chosen to be $0.4MeV$. With this choice of the strength parameters, the occupied time-like HF orbit for the neutrons is

$$| \nu;\ k = \tfrac{1}{2}\rangle = 0.891\ |\ \nu;\ \tfrac{5}{2}\ \tfrac{1}{2}\rangle + 0.343\ |\ \nu;\ \tfrac{1}{2}\ \tfrac{1}{2}\rangle - 0.228\ |\ \nu;\ \tfrac{3}{2}\ \tfrac{1}{2}\rangle - 0.191\ |\ \nu;\ \tfrac{7}{2}\ \tfrac{1}{2}\rangle \quad (3.5)$$

The construction of the correlated neutron pairs from the HF solutions, the calculation of their matrix elements, and the construction of IBM-2 Hamiltonian are accomplished following the same lines as given in Sec. 2.2.3.

The valence protons being in a single-j shell, the $|B^{\pi}_{J}\rangle$ and the $|B^{\pi}_{J}\rangle_{\text{g.s.}}$ are identical and are given by $|(\frac{9}{2})^2 J = 0, 2, 4\rangle$. The $|B^{\nu}_{J}\rangle$ and $|B^{\nu}_{J}\rangle_{\text{g.s.}}$ pairs exhibit similar structure (fig. 3.6).

The spectrum given by the IBM-2 Hamiltonian is plotted in Fig. 3.7 along with the experimentally observed energy levels (Lederer and Shirley 1978). For comparison we have also plotted the spectrum obtained by Chen *et al.* (1986) in their IBM-1 calculation with boson SDI(BSDI). The Yrast levels agree fairly well with the corresponding experimental levels. However, the distinguishing feature in this case is that the non-Yrast levels like 2^+_2, 4^+_2 and 4^+_3 levels, in contrast with the other sample nuclei, also are reproduced by our calculation to fairly good accuracy. The 3^+_1 level also comes close to the experimental value. Because of the unavailability of the fermion SM results, it is hard to interprete the gross disagreement of our 0^+_2 level. However, as we shall see in the next subsection, the overall good agreement of the non-Yrast levels is because isospin here is a good quantum number, unlike the case of the other sample nuclei.

The spectrum given by the $|B^{\rho}_{J}\rangle$ and the $|B^{\rho}_{J}\rangle_{\text{g.s.}}$ pairs denoted 'IBM-2' and

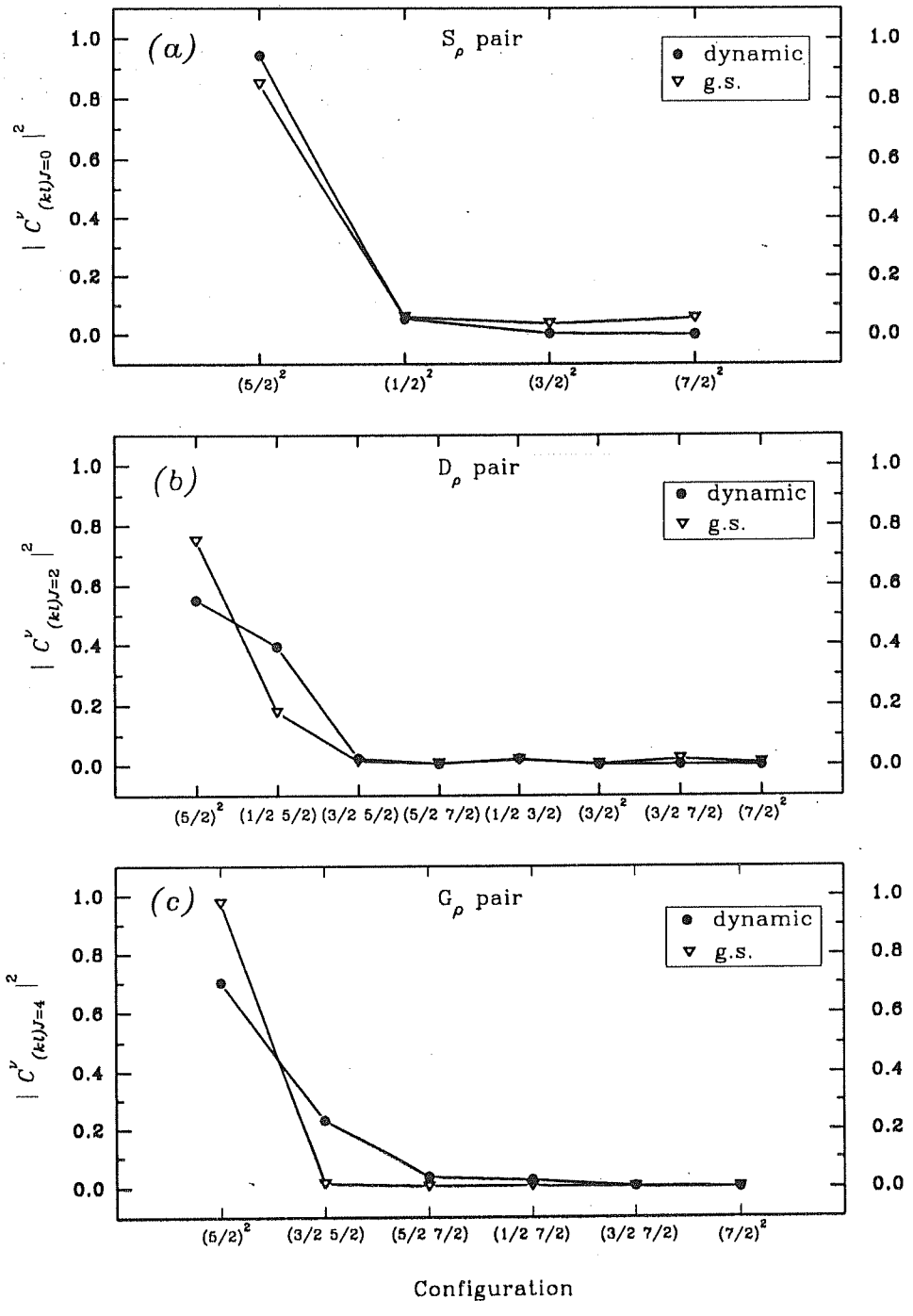

Figure 3.6: A comparison of the correlated neutron pairs $|B^{\nu}_J\rangle$ determined by our procedure from HF solutions of ^{94}Mo ('dynamic') and the eigenstates $|B^{\nu}_J\rangle_{\text{g.s}}$ of two-neutron Hamiltonian of ^{92}Zr ('g.s.'). Fig. (a)-(c) show this comparison between the S, D and G correlated pairs respectively.

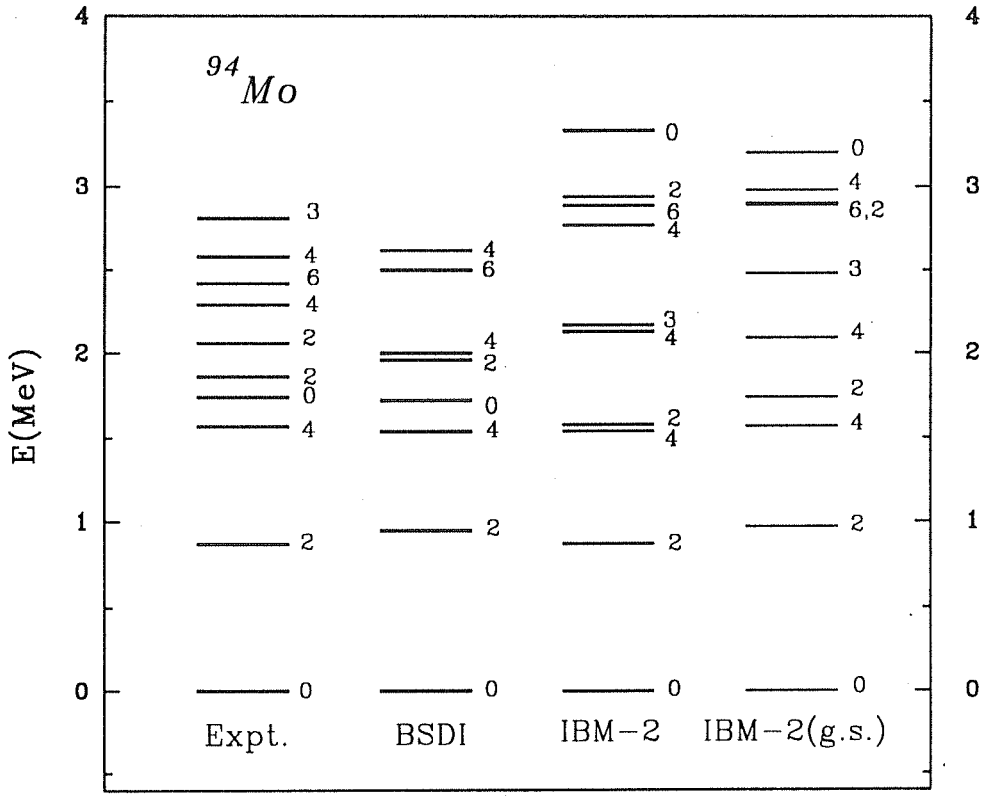

Figure 3.7: Spectrum of ^{94}Mo. Our results 'IBM-2' are plotted alongwith the experimental ('Expt.') and IBM-1 spectrum of Chen *et al.* (1986) generated by Boson Surface Delta Interaction (labelled 'BSDI'). The 'IBM-2(g.s.)' spectrum is also plotted for comparison.

'IBM-2(g.s.)' are very similar, akin to the case of ^{60}Zn. This is only to be expected as the neutron pairs generated in both these methods are very similar (fig. 3.6) and the proton pairs are identical. This may be ascribed to the vibrational character of ^{94}Mo.

In the next section, we discuss the loss of isospin symmetry in the Hamiltonian which affects the non-Yrast levels of the lighter nuclei substantially.

3.3 Loss of Isospin symmetry in IBM-2 states

As explained in Chap. 2, Sec. 2.2.1, we construct identical nucleon pairs $\mid B^{\rho}_{J}\rangle$ having $(T, T_3) = (1, \pm 1)$ and associate them with the IBM-2 boson states $\mid b^{\rho}_{J}\rangle$, $\rho = \nu, (\pi)$ for $T_3 = +1(-1)$ respectively. In the IBM-2 formalism, the concept of δ boson(Elliott *et al.* 1987) corresponding to a $\nu\pi$ pair is not included. Correspondingly, we do not have these pairs in our construction. As explained by Elliott (1985) and Elliott *et al.* (1987), in heavy nuclei, where the valence neutrons and protons are in different oscillator shells, absence of a $\nu\pi$ pair may not be of a serious consequence. All SM configurations in such cases will have definite isospin $T = \frac{1}{2}(N-Z)$ and $T_3 = \frac{1}{2}(N-Z)$. Amongst our sample nuclei, the model spaces for the valence protons and neutrons of ^{94}Mo are inequivalent and hence the IBM-2 states of ^{94}Mo correspond to good isospin SM states giving better agreement of the calculated spectrum with the experimental data. However, for the lighter nuclei, with valence neutrons and protons in the same oscillator shells, inclusion of the $\nu\pi$ pair alongwith the $\nu\nu$ and $\pi\pi$ pair is essential to preserve the $T = 1$ (triplet) symmetry. Absence of this pair, and correspondingly the δ boson causes loss of isospin symmetry in the IBM-2 Hamiltonian and affects the spectrum adversely.

This loss of isospin symmetry is the reason why our non-Yrast levels of ^{20}Ne,

^{44}Ti and ^{60}Zn are pushed up in energy. As for the Yrast levels, it is known that in the even-even nuclei, the higher $T(=1,2)$ states are well separated from the $T=0$ states which form the Yrast levels. This fact qualitatively explains the relatively good agreement of the Yrast levels of our calculations with the experimental and SM levels.

Calculations involving the δ bosons are out of the scope of the present work. In the following, we construct the $\mathcal{T}^2$ operator (where $\mathcal{T}$ stands for the total isospin operator) in the model spaces considered for our sample nuclei and calculate their expectation values in the energy eigenstates of the IBM-2 Hamiltonian. These expectation values enable us to identify the energy eigenstates with good or nearly good T and the extent of T-mixing in others as well.

3.3.1 $\mathcal{T}^2$ operator

The $\mathcal{T}^2$ operator ($\mathcal{T}$ being the total isospin oprator) for a nucleus having n_1 valence neutrons and n_2 valence protons is derived by French (1966) (See Appendix-B). In multipole form, it is given as

$$\begin{aligned}\mathcal{T}^2 &= \frac{1}{4}((n_1-n_2)^2+2(n_1+n_2)) \\ &\quad -\sum_{jj';J'}(-1)^{j-j'+J'}\,[J']^{\frac{1}{2}}\left((a^{\dagger}_{j\nu}\times\tilde{a}_{j'\nu})^{J'}\times(a^{\dagger}_{j'\pi}\times\tilde{a}_{j\pi})^{J'}\right)^{0} \qquad (3.6)\end{aligned}$$

The first term on the right hand side is the direct term which is clearly diagonal. The second (exchange) term which annihilates a proton in j orbit and creates a neutron in its place, will give a non-zero contribution only when the orbits j and j' occur simultaneously in both the model spaces for neutrons and protons. In other words, the orbits j and j' which are model orbits for protons, if already filled for neutrons, cannot accomodate any more neutrons in them according to Pauli principle thus causing the exchange term to vanish. For this reason, the summation variables and the phase factor in the second term of the equation (3.6)do not carry any superscripts.

The creation and annihilation operators, however, carry the superscipts to denote that they are neutron and proton operators.

Derivation of the matrix elements of the operator follows the same procedure as in Sec. 2.2.3. The matrix element of $\mathcal{T}^2$ in $\mid (B^{\nu}_{J_1} B^{\pi}_{J_2})J\rangle$ space is given by the equation (2.55) with the operator $\mathcal{V}_{\nu\pi}$ now replaced by $\mathcal{T}^2$. The expression for the basic matrix element is derived using the equation (3.6). The nondiagonal (second) term, P_2 say, in the expression for $\mathcal{T}^2$ in eqn. (3.6) gets simplified by factorisation

$$P_2 = (-1)^{J_2+J_3+J} \sum_{jj';J'} (-1)^{j-j'} \begin{Bmatrix} J_1 & J_2 & J \\ J_4 & J_3 & J' \end{Bmatrix}$$
$$\langle (\nu; k_1 l_1) J_1 \mid\mid (a^{\dagger}_j \times \tilde{a}_{j'})^{J'} \mid\mid (\nu; k_3 l_3) J_3 \rangle$$
$$\langle (\pi; k_2 l_2) J_2 \mid\mid (a^{\dagger}_{j'} \times \tilde{a}_j)^{J'} \mid\mid (\pi; k_4 l_4) J_4 \rangle \qquad (3.7)$$

The calculation of the m.e. on the r.h.s. of the eq. (3.7) follows the same procedure as described in (Appendix-A) and can be written down from the eq. (2.58). Summing over the s.p. orbits in the resulting expression, we write the final expression for the b.m.e. of $\mathcal{T}^2$

$$\langle ((\nu; k_1 l_1) J_1, (\pi; k_2 l_2) J_2) J \mid \mathcal{T}^2 \mid ((\nu; k_3 l_3) J_3, (\pi; k_4 l_4) J_4) J \rangle$$
$$= 2\, \delta_{k_1 k_3} \delta_{l_1 l_3} \delta_{J_1 J_3} \delta_{k_2 k_4} \delta_{l_2 l_4} \delta_{J_2 J_4}$$
$$-((-1)^{J_2+J_4+J} \prod_{i=1}^{4} \zeta_{k_i l_i} [J_i]^{\frac{1}{2}}\, \mathcal{E}_{k_i l_i J_i} \sum_{J'} (-1)^{j^{\nu}_{l_1} + j^{\nu}_{k_3} + j^{\pi}_{k_2} + j^{\pi}_{l_2}} [J'] \begin{Bmatrix} J_1 & J_2 & J \\ J_4 & J_3 & J' \end{Bmatrix}$$
$$\begin{Bmatrix} J_1 & j^{\nu}_{k_1} & j^{\nu}_{l_1} \\ j^{\nu}_{k_3} & J_3 & J' \end{Bmatrix} \begin{Bmatrix} J_2 & j^{\nu}_{k_3} & j^{\pi}_{l_2} \\ j^{\nu}_{k_1} & J_4 & J' \end{Bmatrix} \delta_{j^{\nu}_{k_1} j^{\pi}_{k_4}} \delta_{j^{\nu}_{l_1} j^{\nu}_{l_3}} \delta_{j^{\pi}_{l_2} j^{\pi}_{l_4}} \delta_{j^{\nu}_{k_3} j^{\pi}_{k_2}}) \qquad (3.8)$$

With these m.e. the $\mathcal{T}^2$ matrices for different angular momenta J are set up and the expectation values $\langle \mathcal{T}^2 \rangle$ of these matrices in the eigenstates of the Hamiltonian (eq. (3.1) are then calculated for ^{44}Ti, ^{20}Ne and ^{60}Zn. These values for the lowest

Table 3.2: $\langle T^2 \rangle$ values and eigenenergies of the relevant eigenstates of the ^{44}Ti Hamiltonian. For comparison, we have also tabulated the SM (T=0) eigen energies published by Skouras *et al.* (1990).

J	E(SM) ($T = 0$) in(MeV)	E(IBM-2) in (MeV)	$\langle T^2 \rangle$
0	**0.0**	**0.0**	**0.03**
0	5.61	6.09	0.7
2	**1.16**	**1.13**	**0.02**
2	4.98	5.21	0.17
2*	–	5.2	2.0
3	5.85	5.8	0.00
4	**2.8**	**2.9**	**0.07**
4	5.02	5.74	0.58
5	5.9	7.44	1.27
5	–	7.07	2.0
6	**4.09**	**5.3**	**0.19**
6	5.22	8.12	1.25

few eigenstates alongwith the corresponding eigenenergies are tabulated in tables 3.2 - 3.4. For comparison, we have also tabulated the SM eigenenergies of the $T = 0$ state.

The $\langle T^2 \rangle$ for $J =$ *even* Yrast states (high-lighted in the tables) are quite close to zero which explains the good agreement of the corresponding energy eigenvalues with experiment. The $J = 8$ level has $\langle T^2 \rangle$ identically equal to zero. The non-Yrast $J =$ *even* levels have strong mixtures of $T = 0$ and $T = 2$ states and these levels are pushed up in the spectrum. Note that the $T =$ *even*$(0, 2)$ and $T =$ *odd*(1) eigenstates dissociate and the former mix amongst themselves. This is also evident

Table 3.3: $\langle T^2 \rangle$ values and the eigenenergy values of some low-lying eigen states of ^{20}Ne IBM-2 Hamiltonian with the corresponding SM ($T = 0$) energies.

J	E(SM)($T = 0$) in(MeV)	E(IBM-2) in (MeV)	$\langle T^2 \rangle$
0	**0.0**	**0.0**	**0.01**
0	6.76	15.31	2.37
2	**1.78**	**1.36**	**0.002**
2*	7.32	12.68	2.0
3	10.23	14.3	2.0
4	**4.25**	**4.15**	**0.005**
4	9.97	14.37	2.0
5	11.59	17.33	2.0
6	**8.78**	**8.28**	**0.000**
6	12.94	17.37	2.0
8	**11.59**	**11.7**	**0.0**

Table 3.4: Eigenenergies and $\langle T^2 \rangle$ values of some low-lying eigenstates of ^{60}Zn sdgIBM-2 Hamiltonian with the SM energies for $T = 0$.

J	E(SM)($T = 0$) in (MeV)	E(sdgIBM-2) in (MeV)	$\langle T^2 \rangle$
0	**0.0**	**0.0**	**0.04**
0	3.24	5.53	2.47
2	**0.96**	**0.85**	**0.007**
2*	3.29	4.89	2.0
3	4.29	5.67	2.0
4	**2.18**	**2.12**	**0.02**
4	4.31	5.37	2.0
5	5.25	6.75	2.0
6	**4.33**	**4.09**	**0.003**
6	6.23	6.9	2.0
8	**5.84**	**5.65**	**0.0**

from the fact that all $\langle T^2 \rangle$ values corresponding to the $T = 1$ states are exactly equal to 2, (*i.e.* $= T(T+1)$). The $J = even(odd)$ states are symmetric (antisymmetric) linear combinations of configurations $| (b^{\nu}_{J_1} b^{\pi}_{J_2}) J \rangle$ when $T = even$ and *vice versa* for $T = odd$. The $J = 2$ levels with $\langle T^2 \rangle = 2$ marked asterisk correspond to the ground state energies of ^{44}Sc (3.2), ^{20}F (3.3) and ^{60}Cu (3.4) with respect to those of ^{44}Ti, ^{20}Ne and ^{60}Zn respectively.

In the next chapter, we apply our formulation to nuclei with many bosons of each type and present the results of these calculations.

3.4 References

1. Bonatsos D, Skouras L D, Van Isacker P and Nagarajan M A 1991 *J. Phys.* **G17** 1803

2. Chen Hsi-Tseng, Kiang L L, Yang C C, Chen L M, Chen T L and Jiang C W 1986 *J. Phys.* **G12** L217

3. Devi Y D, Kota V K B and Sheikh J A 1989 *Phys. Rev.* **C39** 2057

4. Elliott J P 1985 *Rep. Prog. Phys.* **48** 171

5. Elliott J P, Evans J A and Williams A P 1987 *Nucl. Phys.* **A469** 51

6. Federman P and Pittel S 1978 *Phys. Lett.* **77B** 29

7. French J B 1966 in *Multipole and Sum Rule Methods in Spectroscopy, Proceeding of the International School of Physics, Enrico Fermi*, Course **36**, Varenna 1965, ed. C. Bloch (Academic Press, New York, 1966) p. 278 New York

8. Halbert E C, McGrory J B, Wildenthal B H and Pandya S P in *An s-d-Shell-Model Study of A=18-21, Adv. Nucl. Phys.* **Vol. 4, Chap. 6**

9. Khosa S K, Tripathi P N and Sharma S K 1982 *Phys. Lett.* **119B** 257

10. Koops J E and Glaudemans P W M 1977 *Z. Physik* **A280** 181

11. Lederer C M and Shirley V S 1978 (Ed.) *Table of Isotopes(Seventh edition)* (John Wiley & Sons, Inc.)

12. Pittel S, Duval P D and Barrett B R 1982 *Ann. Phys.*(N.Y.) **144** 168

13. Sebe T and Harvey M 1978 in *Notes of Atomic Energy of Canada Limited* **AECL-3007**

14. Skouras L D, Van Isacker P and Nagarajan M A 1990 *Nucl. Phys.* **A516** 255

15. Van Hienen J F A, Chung W and Wildenthal B H 1976 *Nucl. Phys.* **A269** 159

16. Wildenthal B H 1984 *Prog. Part. Nucl. Phys.* **11** 5

Chapter 4

Shape Transition in Even – A Mo and Sm Isotopes

4.1 Introduction

The onset of transition from spherical to axially deformed shape in the even-even neutron rich $Sr - Zr - Mo - Ru$ nuclei at mass $A \simeq 100$ has been well established by several experimental investigations (Cheifetz *et al.* 1970, Wohn *et al.* 1990, Liang *et al.* 1991). The lighter Mo isotopes, $^{96-98}Mo$ exhibit low lying level energies typical of a spherical nucleus,*i.e.*, $E_{4_1^+} \simeq 2E_{2_1^+}$. The level energies of heavier $^{104-108}Mo$ isotopes, on the other hand, show a trend $\frac{E_{4_1^+}}{E_{2_1^+}} \simeq 3$, characteristic of rotational nuclei. Recent compilation of $E2$ transition probabilities from 0_1^+ to 2_1^+ levels ($B(E2)\uparrow$) (Raman *et al.* 1987,1989) demonstrate the enhancement of these values across the $A \simeq 100, 102$ range. As Scholten *et al.* (1978) point out, for ideal cases of spherical and axial rotor shapes $B(E2)\uparrow$ increases as N and N^2 (N is the total number of valence pairs or

bosons) respectively, thus exhibiting the sudden enhancement for the latter. Federman and Pittel (1977,1978) and later Khosa *et al.*(1982) carried out investigations on Zr and Mo isotopes in the fermion space by performing Hartree-Fock-Bogoliubov (HFB) calculations and attempted to theoretically explain this onset of deformation. In the IBM domain, Sambataro and Molnár (1982) carried out phenomenological *sd*IBM-2 calculations on $^{96-104}Mo$ isotopes which have been recently extended upto ^{108}Mo (Liang *et al.* 1991). Casten *et al.*(1985) carried out phenomenological *sd*IBM calculations for global fitting of the IBM parameters for nuclei in $A \simeq 100$ and 150 regions including Mo isotopes. All these calculations have reproduced the experimental results of the onset of deformation in neutron rich Mo isotopes at mass $A \simeq 100-102$. We have carried out the first microscopic *sdg*IBM calculations on $^{96-108}Mo$ isotopes and our results match with the experimental and theoretical results very well.

Similar onset of shape transition in rare-earth nuclei like Nd, Sm, Gd at mass $A \simeq 150$ region is experimentally well established (Lederer and Shirley 1978, Raman *et al.* 1987). There have been numerous theoretical investigations (Kumar 1974) to explore and understand it in the fermion picture. There have also been several phenomenological *sd*IBM (-1 and -2) studies of these nuclei (Scholten *et al.* 1978, Scholten 1980, Casten *et al.* 1985). Otsuka and Sugita (1988) have applied self-consistent angular momentum projection method in *sdg*IBM framework to study the shape transition in $^{146-158}Sm$ isotopes. Recently Devi and Kota (1992) have carried out full *sdg*IBM-1 shell model calculations for $^{146-158}Sm$ isotopes to study the shape transition as well as the $E4$-strength distributions in these nuclei.

There have also been several microscopic IBM calculations to this end. In fact, as Navrátil and Dobeš (1991) put it, "the Sm isotopic chain is .... used as a testing ground for various theoretical (phenomenological and microscopic) approaches (of IBM) quite frequently." Pittel and Dukelsky (1983) first applied their nucleon

pair construction procedure (discussed in Chapter 2 earlier) from HFB solutions to construct the S_ρ and D_ρ pairs for Sm isotopes and then derived the structure of boson quadrupole operator for the isotopes using these pairs. Pannert *et al.* (1985) applied the same procedure to construct the S_ρ, D_ρ and G_ρ pairs for $^{148-154}Sm$ and studied their structure, the importance of G_ρ pairs and the effects of the angular momentum projection from HFB solutions in the transition region from spherical to deformed nuclei.

Scholten (1983) developed a method to determine self-consistently the correlated pairs from the generalized seniority pairs to produce the spectra of $^{146-154}Sm$ isotopes that exhibited the shape transition characteristics. Recently Navrátil and Dobeš (1991) have applied the similarity transformed Dyson-boson mapping technique to derive the *sdg*IBM-2 Hamiltonian and have reproduced the shape transition by carrying out calculations in *sdg*IBM-1 formalism through the IBM-2 $\rightarrow$ IBM-1 projection. The calculation using our prescription to construct the correlated pair and the *sdg*IBM-2 Hamiltonian reproduces very similar patterns as have been obtained by Scholten and by Navrátil and Dobeš.

These results of our calculations and their analyses are presented in the following sections of the chapter. In Sec. (4.2), the procedure of our calculation is described. As mentioned earlier, (Sec. 2.2.4) due to the lack of a suitable boson shell model code, all our calculations have been carried out in the *sdg*IBM-1 space by projecting the operators from the *sdg*IBM-2 space. In Sec. 4.3, we present a comparison of the results of the IBM-2 and IBM-1 calculations for ^{20}Ne and ^{94}Mo. The IBM-2 results for these nuclei are presented in the previous chapter. In Sec. 4.4, we present the results of calculations for the Mo and Sm isotopic chains, compare them with experimental and/or theoretical results, study and analyse the shape transitions. We have also

carried out detailed spectroscopic calculations on a few individual spherical and rotational nuclei. We discuss these results alongwith other available experimental and theoretical results in Sec. 4.5. The chapter ends with concluding remarks in Sec. 4.6.

4.2 Calculational Procedure

The *sdg*IBM-2 Hamiltonian $\mathcal{H}_{\text{IBM}-2}$ is constructed for each nucleus in the $^{96-108}Mo$ and $^{146-154}Sm$ isotopic chains following our procedure formulated in Chapter 2 Sec. (2.2) and explained in Chapter 3. The model orbits $\{j^\rho\}$ for the valence neutrons ($\rho = \nu$) and protons ($\rho = \pi$), the spherical s.p. energies associated $\{\epsilon_{j^\rho}\}$ for each isotopic chain are given alongwith the results in the next section. The *Surface Delta Interaction* (SDI) (Brussaard and Glaudemans 1977) with strength parameters $A_{\nu\nu}$ and $A_{\pi\pi}$ is used as the effective residual two-body interaction among the valence neutrons and protons. In microscopic IBM calculations, $A_{\nu\nu}$ and $A_{\pi\pi}$ are chosen to be different (Pittel and Dukelsky 1983, Druce *et al.* 1987). However, we choose $A_{\nu\nu} = A_{\pi\pi}$ throughout our calculations with a wish to minimize the number free parameters. Navrátil and Dobeš (1991) use the same strength parameter in SDI with the quadrupole term enhanced by a multiplication factor. However, we obtain almost identical results for Sm isotopes as theirs, with the simple choice $A_{\nu\nu} = A_{\pi\pi}$. As for the residual two-body interaction amongst the neutrons and protons, it is customary in IBM microscopic calculations to use the quadrupole-quadrupole ($Q^{(2)}.Q^{(2)}$) interaction. We, however, choose the SDI m.e. $V_{\nu\pi}$ with a single strength parameter $A_{\nu\pi}$ for the same. It has been advocated by Scholten (1983), Druce *et al.* (1987), Navrátil and Dobeš (1991) that the hexadecapole-hexadecapole component of the $\nu\pi$- interaction should also be included in the unlike-boson interaction terms. In this vein, the choice of the SDI with strength $A_{\nu\pi}$ (which means both isospin T=0 and 1 part) is most general as it contains multipole components of all orders. This choice yields results as good as

theirs. The numerical values of $A_{\nu\nu}$, $A_{\nu\pi}$ and $A_{\pi\pi}$ for the two isotopic chains are tabulated in the next section alongwith the results.

In case of all the isotopes considered, the HF solutions with the lowest energy ϵ_{HF} were found to be prolate solutions. These results vindicate similar findings of Federman and Pittel (1978) for the Mo isotopes and of Pittel and Dukelsky (1983) for the Sm isotopes. As discussed in Sec.(2.2), the prolate HF solution is a prerequisite for the applicability of our scheme. These results demonstrate that this necessity is not all that restrictive as it may *a priori* appear.

Alongwith $\mathcal{H}_{\rm IBM-2}$, we also construct the E2-transition operator $\mathcal{T}^{(E2)}_{\rm IBM-2}$(eq. 2.37) as described in Sec. (2.2.2) of Chapter 2. Its parameters $e^{\rho}_{jj'}$ (eq. 2.38) are determined for each nucleus following the procedure described in Sec. (2.2.3), eqs. (2.64) and (2.66).

As discussed in Chapter 2, we finally carry out the spectroscopic calculations in IBM-1 regime using the SDGIBM-1 boson shell model code of Devi and Kota (1990). To this end, we first project our IBM-2 operators $\mathcal{H}_{\rm IBM-2}$ and $\mathcal{T}^{(E2)}_{\rm IBm-2}$ onto the corresponding IBM-1 operators. This mapping procedure (Frank and Lipas 1990) is discussed in Sec. (2.2.4) and the formulae used to carryout the projection are summed up in eqs. (2.75)–(2.76). The single boson energies ϵ_J, the boson two-body matrix elements (t.b.m.e.) $V^J_{J_1J_2J_3J_4}$ and effective boson $E2$-charges $e_{JJ'}$ fed as parameters of the $\mathcal{H}_{\rm IBM-1}$ and $\mathcal{T}^{(E2)}_{\rm IBM-1}$ of the code are related to our microscopically calculated parameters through eqs. (2.77)–(2.79).

Before proceding to discuss the results of our calculation, a brief account of the SDGIBM1 code of Devi and Kota is in order.

4.2.1 The SDGIBM1 Code

The SDGIBM1 code treats the s, d and g bosons on equal footing. Given the total number of bosons N for a nucleus, it generates all allowed basis states

$$|\{B\}\rangle \equiv |N_s;\ N_d v_d \alpha_d L_d;\ N_g v_g \alpha_g L_g : J\rangle \tag{4.1}$$

with the boson number conservation constraint

$$N_s + N_d + N_g = N \tag{4.2}$$

where N_s, N_d and N_g are the number of s, d and g bosons in a given configuration. The above states are constructed with quantum numbers provided by the group reduction given by Kota *et al.* (1987) of the completely symmetric U(15) representation $\{N\}$.

$$\begin{array}{ccccccccc} U(15) & \supset & \left\{\begin{array}{c} U_s(1) \\ \{N_s\} \\ \oplus \\ U_d(5) \\ \{N_d\} \\ \oplus \\ U_g(9) \\ \{N_g\} \end{array}\right. & \supset & \begin{array}{c} \\ \\ \\ O_d(5) \\ [v_d] \\ \oplus \\ O_g(9) \\ [v_g] \end{array} & \supset & \begin{array}{c} \\ \\ \\ O_d(3) \\ (\alpha_d L_d) \\ \oplus \\ O_g(3) \\ (\alpha_g L_g) \end{array} \left.\begin{array}{c} \\ \\ \\ \\ \\ \\ \\ \\ \end{array}\right\} & \supset & \begin{array}{c} O_{sdg}(3) \\ J \end{array} \\ \{N\} & & & & & & & & \end{array} \tag{4.3}$$

The quantum numbers (labels) corresponding to each group in the reduction chart (4.3) are given below the group notations. Given the $U_d(5)$ and $U_g(9)$ representations $\{N_d\}$ and $\{N_g\}$, the reduction to the corresponding orthogonal groups $O_d(5)$ and $O_g(9)$ with representations $[v_d]$ and $[v_g]$ is straightforward:

$$v_b = N_b,\ N_b - 2, \ldots 1 \text{ or } 0 \ (b = d \text{ or } g) \tag{4.4}$$

Here v_b represents the boson seniority quantum number. The reduction $O_d(5) \supset O_d(3)$ and $O_g(9) \supset O_g(3)$, i.e. generating all possible angular momenta L_d and L_g with the

respective multiplicities α_d and α_g from v_d and v_g is done by a procedure given by Kota *et al.* (1987). Finally, the total angular momentum J are generated by coupling L_d and L_g. The code then calculates the m×1 $\rightarrow$ $m+1$ 1-particle coefficients of fractional parentage (CFP's) by the procedure of Bayman and Lande (1966). A symmetric state vector $|m+1, v_f, \alpha_f, L_f\rangle$ of $m+1$ identical bosons each carrying an angular momentum l can be expressed as a linear combination of product states $|m, v_i, \alpha_i, L_i;\ 111l;\ L_f\rangle$ of the symmetric state of first m bosons and the last boson.

$$|m+1, v_f, \alpha_f, L_f\rangle = \sum_{v_i \alpha_i L_i} \langle m, v_i, \alpha_i, L_i; 111l|\}m+1, v_f, \alpha_f, L_f\rangle \; |m, v_i, \alpha_i, L_i;\ 111l;\ L_f\rangle \tag{4.5}$$

The coefficients of expansion $\langle ...|\}...\rangle$ in eq. (4.5) are the $m \times 1 \rightarrow m+1$ 1-particle CFP's. Recognising that the states $|mv\alpha L\rangle$ correspond to the group chain $U(2l+1) \supset SU(2l+1) \supset O(2l+1) \supset O(3)$, the CFP's are calculated by diagonalizing the linear superposition $aC_2(SU(2l+1)) + bC_2(O(2l+1))$ of the quadratic Casimir operators $C_2(SU(2l+1))$ and $C_2(O(2l+1))$ in the basis space $|m, v_i, \alpha_i, L_i;\ 111l;\ L_f\rangle$. The coefficients a and b are chosen to be 1 and 0.055 respectively in order to distinguish between eigenvalues corresponding to the symmetric representation $\{m+1\}$ and mixed symmetric $\{m, 1\}$. Using the boson single particle energies ϵ_J, t.b.m.e. $V^J_{J_1 J_2 J_3 J_4}$ and the CFP's, the code then calculates the matrix elements of $\mathcal{H}_{\text{IBM}-1}$ in the basis space $|\{B\}\rangle$ and diagonalises the matrices. Following the notation of Devi and Kota, we have the eigenstates $|\psi^J_E\rangle$ with total angular momentum J and energy E

$$|\psi^J_E\rangle = \sum_{\{B_i\}} C^E_{\{B_i\}} |\{B_i\}\rangle \tag{4.6}$$

The $E2$ transition probability from the initial state $|\psi^{J_i}_E\rangle$ to the final state $|\psi^{J_f}_{E'}\rangle$, $B(E2; J_i \rightarrow J_f)$, are then calculted by using the relation

$$B(E2; J_i \rightarrow J_f) = \frac{1}{2J_i+1} |\langle \psi^{J_f}_{E'} || \mathcal{T}^{(E2)}_{\text{IBM}-1} || \psi^{J_i}_E \rangle|^2 \tag{4.7}$$

Although the SDGIBM1 code is capable of treating the g-bosons at par with other bosons, in actual calculations we restrict the number of g-bosons $N_g \leq 2$. This choice, as discussed by Devi and Kota (1990), appears to be adequate for a large number of nuclei. In the calculations for Sm isotopes, we further restrict the basis space by imposing $N_s \geq 2$. The calculations of expectation value for the number operator $\hat{N}_s$ suggest that for nuclei with boson number $N \geq 6$, it can be taken as a valid approximation (Kota 1991). However, it should also be stated here that with availability of better and faster computational facilities than available to us, these restrictions on the boson states could be removed.

4.3 IBM-1 and IBM-2 Spectra—Comparison for Simple Nuclei

The IBM-2 spectra of a few simple nuclei are presented in Chapter 3. As all the calculations presented in this Chapter are carried out in IBM-1 regime, it is in order to compare the IBM-1 and IBM-2 spectra for these nuclei where it is possible for us to carry out both the calculations. In this section, we present these results for ^{20}Ne and ^{94}Mo. In Figs. 4.1(a)-(b), respectively, we present the comparison of their spectra. The model spaces and the residual two body interactions are chosen to be exactly the same as in the corresponding cases in Chapter 3 (Sec. 3.2.2 and Sec. 3.2.4 respectively). The case of ^{20}Ne with the two neutrons and two protons in the same major shell, is an ideal case of F-spin symmetry which explains the exact agreement of the IBM-2 and IBM-1 levels and their close agreement with the experimental and SM levels. This symmetry can also be seen in the eigenstates tabulated in Tables 4.1 and 4.2.

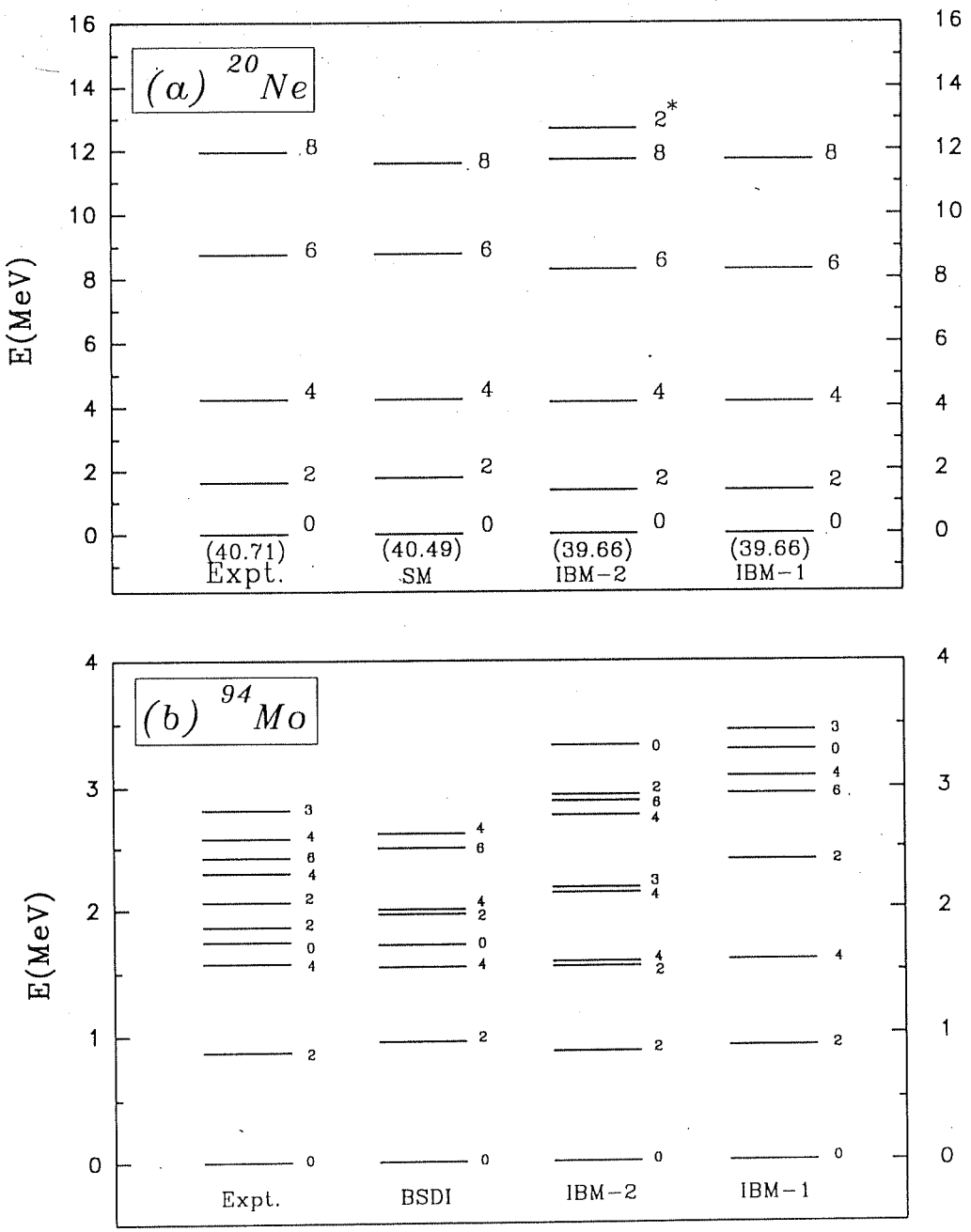

Figure 4.1: Comparison between IBM-1 and IBM-2 spectra of (a)^{20}Ne and ^{94}Mo. The Experimental (Expt.) results for both, the Shell-Model (SM) spectrum for ^{20}Ne and BSDI (Chen *et al.* 1986) spectrum for ^{94}Mo are also plotted.

The symmetry (antisymmetry) with respect to interchange of ν and π labels in the first (second) $J = 2$ and 4 eigenstates of ^{20}Ne is clearly seen. The F-spin antisymmetric $J = 2, 4$ levels do not occour in the IBM-1 spectrum. The $J = 2_2^+$ level marked asterisk in the IBM-2 spectrum of Fig. 4.1(a) is an $F = 0$ level and hence drops out in the IBM-1 spectrum. As discussed in Chapter 3, the non-Yrast levels of ^{20}Ne have substantial isospin mixing in the fermion space. Hence we do not discuss them here.

In the case of ^{94}Mo, however, the symmetry is not exact and our assumption stands on test. The spectrum Fig.(4.1(b)) shows that the Yrast levels ($J = 0_1^+$, 2_1^+, 4_1^+, 6_1^+) in IBM-1 spectrum are very close to those of IBM-2 indicating that the assumption of F-symmetry is good. They also agree well with the experimental (Lederer and Shirley 1978) and calculated levels with Boson Surface Delta Interaction (BSDI) of Chen *et al.* (1986). The other higher levels of IBM-1 are however shifted up because of mixing of F-spin symmetric and antisymmetric states. As seen in tables (4.1) and (4.2), the $J = 2_1^+$, 4_1^+(Yrast) levels (with energies $E_{2_1^+} = 0.95MeV$ and $E_{4_1^+} = 1.89MeV$), though not completely symmetric with respect to interchange of ν-π labels, are close to it. The relevant components of ($s_\nu d_\pi$, $d_\nu s_\pi$, and $d_\nu g_\pi$, $g_\nu d_\pi$ etc.) are quite comparable to each other and their phases are the same. In $J = 2_2^+$ and 4_2^+ states, the relative phases between such components are opposite. In $J = 4_2^+$

Table 4.1: J=2 IBM-2 Eigenstates.

Nucleus	E(MeV)	$s_\nu d_\pi$	$d_\nu s_\pi$	$d_\nu d_\pi$	$d_\nu g_\pi$	$g_\nu d_\pi$	$g_\nu g_\pi$
^{20}Ne	1.36	−0.54	−0.54	0.45	−0.31	−0.31	0.16
	12.68	0.53	−0.53	0.0	0.47	−0.47	0.0
^{94}Mo	0.95	−0.51	−0.73	0.18	−0.28	−0.27	0.12
	1.72	−0.62	0.29	−0.64	−0.17	0.02	−0.29

level, the absolute values of these components are quite comparable which means that this state is more closely F-spin antisymmetric. As no other phenomenological or microscopic IBM-2 results for ^{94}Mo are available in the literature, it is hard to make a better comparative study of these states here.

However, it can be ascertained that for the Yrast levels which are of prime interest to us here, the assumption of complete F-symmetry is a very good approximation. This point will be demonstrated in the following subsections where the spectra of IBM-1 operators with this approximation are seen to match very well with experimental and other theoretical results.

4.4 The Shape Transitions

4.4.1 *Mo* isotopes

The calculations for the even-A $^{96-108}Mo$ isotopes are carried out in the model space of $\{g_{\frac{9}{2}}\}$ for the two valence protons and $\{d_{\frac{5}{2}}s_{\frac{1}{2}}d_{\frac{3}{2}}g_{\frac{7}{2}}h_{\frac{11}{2}}\}$ for the neutrons. The s.p. energies of these orbits are (in MeV) $\{0.0\}$ and $\{0.0, 1.0, 2.5, 3.0, 3.6\}$ respectively following the choice of Khosa *et al.* (1982). The set

Table 4.2: $J = 4$ IBM-2 Eigenstates.

Nucleus	E(MeV)	$s_\nu g_\pi$	$g_\nu s_\pi$	$d_\nu d_\pi$	$d_\nu g_\pi$	$g_\nu d_\pi$	$g_\nu g_\pi$
^{20}Ne	4.15	0.40	0.40	0.67	−0.32	−0.32	0.17
	14.37	−0.64	0.64	0.00	0.29	−0.29	0.00
^{94}Mo	1.89	−0.64	−0.55	−0.51	0.16	0.05	−0.05
	2.61	−0.57	0.52	−0.02	−0.37	0.47	0.21

Table 4.3: Adopted SDI strength Parameters for $^{96-108}Mo$ isotopes.

Isotope	$A_{\nu\nu}(=A_{\pi\pi})$ (in MeV)	$A_{\nu\pi}$ (in MeV)
^{96}Mo	0.37	0.60
^{98}Mo	0.37	0.60
^{100}Mo	0.33	0.60
^{102}Mo	0.10	0.40
^{104}Mo	0.05	0.40
^{106}Mo	0.05	0.40
^{108}Mo	0.05	0.40

of SDI strength parameters $A_{\nu\nu} = A_{\pi\pi} = 0.35\,MeV$ and $A_{\nu\pi} = 0.6\,MeV$ used by Federman and Pittel (1978) were taken. However, it was observed that while this choice produced fairly good agreement with experimental spectra for the lighter isotopes ie.,$^{96-100}Mo$, for heavier isotopes, $^{104-108}Mo$, it yielded scaled up spectra indicating too small moments of inertia. In order to reproduce spectra close to observed ones, we varied these parameters while generally observing economy on such variations. The adopted set of strength parameters for each isotope is tabulated in Table 4.3 .

Note that we have to vary the parameters at $A = 100-102$ precisely where the shape transition is known to occur. The necessity of similar variation of the strength parameters of model interactions in order to produce agreeable results with observed ones has also been seen by Scholten (1983), Navrátil and Dobeš (1991) and by us in the calculations for the Sm isotopes.

The HF calculations were carried out in each case to obtain the lowest energy

axially-deformed prolate solutions with good parity. In none of the isotopes we observed occupation of the intruder $h_{\frac{11}{2}}$ orbit by the valence neutrons. The normalised occupancies $|\bar{C}_{j_i^\nu}|^2$ (eq. (2.24)) calculated from the $|\nu; k = \frac{1}{2}\rangle_{\rm eff}$ orbit (eq. (2.23)) for every valence orbit j_i^ν are plotted for all the isotopes in Fig. 4.2(a). In case of ^{98}Mo the $d_{\frac{5}{2}}$ orbit gets almost filled with very little participation of the rest of the model orbits and we observe a shell effect here. With addition of more neutrons, more collectivity sets in and for $A = 106$, 108 the $d_{\frac{3}{2}}$ and $g_{\frac{7}{2}}$ orbits also take part substantially. The subshell effect (as seen in ^{98}Mo) at $Z = 38$, 40, and $N = 56$, 58 have been observed and discussed by Mach *et al.*(1991) for Sr and Zr isotopes and are, according to them, responsible for the delay in the onset of shape transition in Mo isotopes.

The IBM-1 d- and g-boson energies ϵ_d, ϵ_g with respect to the s-boson energies are calculated from the corresponding IBM-2 quantities by eq. (2.77). Barring the case of ^{98}Mo, these quantities vary smoothly (fig. 4.2(b)). It is to be noted that for $^{104-108}Mo$, with the SDI strength parameters kept constant (Table (4.3)), there is gradual decrease in the ϵ_d-ϵ_g gap. This decrease facilitates a stronger mixing of the d- and g- bosons and probably helps the onset and sustenance of the deformation.

The effective (IBM-1) boson $E2$-charges $e_{JJ'}$ ($J \leq J' = 0$, 2 and 4 for s-, d- and g-bosons) of $\mathcal{T}^{(E2)}_{\rm IBM-1}$ in units of eb (e= electron charge and $b = 1barn = 10^{-24}cm^2$) are calculated from the IBM-2 charges $e^\rho_{JJ'}$ by eq. (2.79) with fermionic charges $e^F_\nu = 0.9e$ and $e^F_\pi = (1 + e^F_\nu) = 1.9e$. Barring the initial cases of $^{96-100}Mo$, for the heavier isotopes, these parameters remain constant and are of the same order (Fig. 4.2(c)). It is gratifying to note that these microscopically calculated $e_{JJ'}$ have the same relative phases as the $SU(3)$ $E2$-transition operator (Wu 1981)

$$\begin{aligned} \mathcal{T}^{(E2)}(SU(3)) &= e^B(4(\frac{7}{15})^{\frac{1}{2}}(s^\dagger\tilde{d} + d^\dagger\tilde{s})^2_0 - 11(\frac{2}{27})^{\frac{1}{2}}(d^\dagger\tilde{d})^2_0 \\ &+ \frac{36}{\sqrt{105}}(d^\dagger\tilde{g} + g^\dagger\tilde{d})^2_0 - 2(\frac{33}{7})^{\frac{1}{2}}(g^\dagger\tilde{g})^2_0) \end{aligned} \tag{4.8}$$

and with the choice of the free parameter $e^B = 0.04eb$ the two sets of parameters

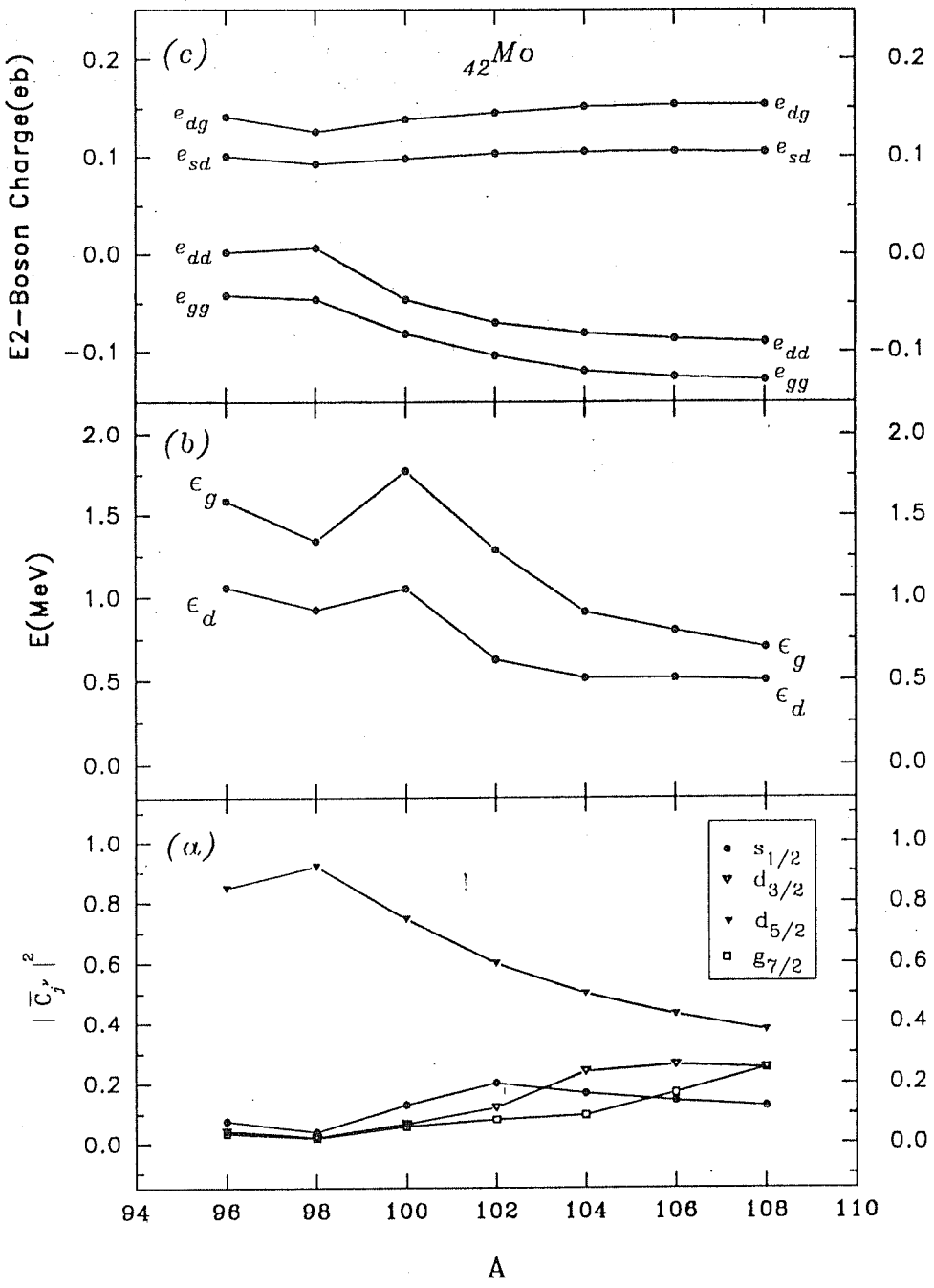

Figure 4.2: (a)Effective occupancies $|\bar{C}_{j_i^\nu}|^2$ of s.p. neutron orbits from $|\nu; k = +\frac{1}{2}\rangle_{\text{eff}}$ orbit; (b) The IBM-1 d- and g- boson energies ϵ_d and ϵ_g w.r.t. ϵ_s and (c) The IBM-1 effective boson charges for $E2$-transitions are plotted against the atomic number A.

become comparable for cases like $^{106-108}Mo$.

The $J = 2_1^+, 4_1^+$ and 6_1^+ calculated and experimental (Lederer and Shirley 1978, Liang *et al.* 1991) levels are plotted in Fig. 4.3(a). The lowering of these levels indicating higher moments of inertia for the heavier isotopes and the apparent $E_{J_1^+} \approx KJ(J+1)$ relation with K constant for $^{104-108}Mo$ indicate the shape transition. The ratio $R = \frac{E_{4_1^+}}{E_{2_1^+}}$ (Fig. 4.3(b)) clearly changes from $\simeq 2$ (vibrational limit) to $\simeq 3.3$ (rotational limit). The $B(E2; 0_1^+ \rightarrow 2_1^+)$ ($\equiv (B(E2)\uparrow)$) in units of e^2b^2 calculated with $\mathcal{T}^{(E2)}_{\mathrm{IBM}-1}$ operator also show (Fig. 4.3(c)) the characteristic enhancement at $A \simeq 100, 102$. However, the observed saturation of this $B(E2)\uparrow$ value for $^{106-108}Mo$ is not reproduced. It should be noted that these calculations have been carried out basically with only one parameter $e_\nu^F = 0.9e$ and e_π^F has been fixed at $1 + e_\nu^F$.

4.4.2 The Sm Isotopes

The s.p. model spaces and the s.p. energies of the levels for the valence neutrons (w.r.t. $N = 82$) and the valence protons (w.r.t. $Z = 50$) chosen in the calculations for $^{146-154}Sm$ isotopes are given in Table 4.4. The s.p.e. are chosen to be the BSSP (beginning-shell single-particle) energies for both neutrons and protons given by Pittel *et al.* (1982). The SDI with interaction strength $A_{\nu\nu} = A_{\pi\pi} = 0.3MeV$ and $A_{\nu\pi} = 0.12MeV$ is chosen throughout the calculation. As mentioned earlier, for isotopes like $^{152-154}Sm$, the $A_{\nu\nu}$ and $A_{\pi\pi}$ at 0.3 MeV do yield scaled up spectra although the $E_{J_1^+}$ levels exhibit rotational character. Again, like the case of Mo isotopes, one ought to vary these parameters in order to produce the spectra closer to experiment. We have carried out the calculations in both ways – with constant parameters and with a suitable variation. While studying the shape transitions in the isotopic chain, we keep these parameters fixed at the values quoted above in order to draw a closer comparison with the results of Scholten (1983). Scholten has carried out these calculations with

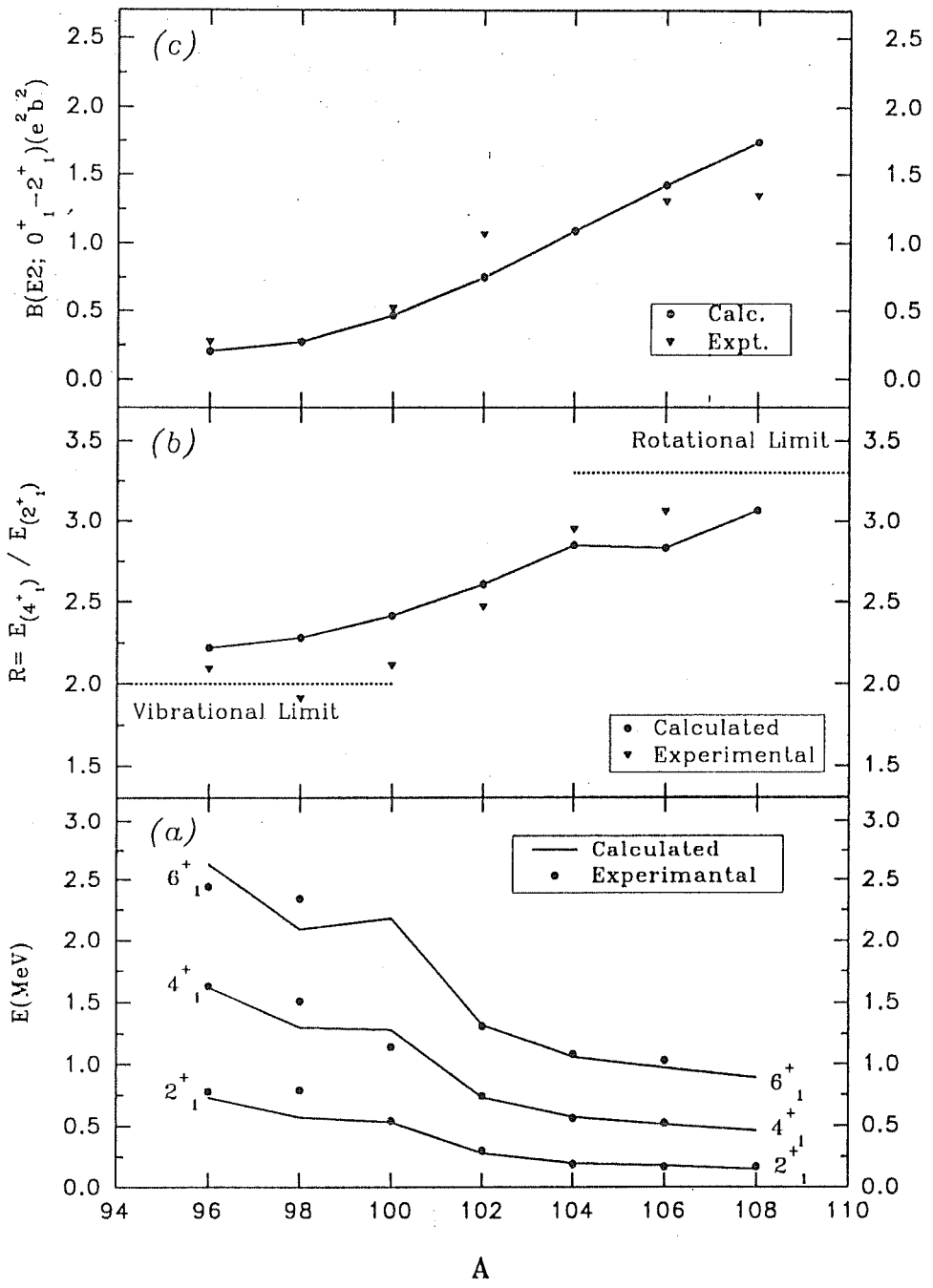

Figure 4.3: The experimental and calculated (a) Yrast spectrum; (b) Ratio of the energies of the 4_1^+ and 2_1^+ levels; and (c) The $E2$-transition probability ($B(E2)\uparrow$.

Table 4.4: The neutron and proton model spaces for $^{146-154}Sm$ and the s.p.e.

Neutrons		Protons	
orbits	energies(MeV)	orbits	energies(MeV)
$^3p_{\frac{1}{2}}$	2.25	$^3s_{\frac{1}{2}}$	2.99
$^3p_{\frac{3}{2}}$	1.50	$^2d_{\frac{3}{2}}$	2.69
$^2f_{\frac{5}{2}}$	2.60	$^2d_{\frac{5}{2}}$	0.96
$^2f_{\frac{7}{2}}$	0.00	$^1g_{\frac{7}{2}}$	0.00
$^1h_{\frac{9}{2}}$	2.45	$^1h_{\frac{11}{2}}$	2.76
$^1i_{\frac{13}{2}}$	2.80	–	–

constant strength parameters and has obtained scaled up spectra just like ours. In the detailed calculations for individual nuclei like ^{148}Sm and ^{152}Sm, we vary the parameters suitably so that the observed spectra are approximately reproduced.

In these calculations, we again do not find any occupation of the intruder orbit– either of $\pi-(^1h_{\frac{11}{2}})$ or $\nu-(^1i_{\frac{13}{2}})$. The normalised occupancies $|\bar{C}_{j_i^\pi}|^2$ and $|\bar{C}_{j_i^\nu}|^2$ of the $|\nu,\pi;k=+\frac{1}{2}\rangle_{\text{eff}}$ orbit are plotted for all j_i^π and j_i^ν orbits as functions of A in Fig. 4.4(a) and (b). As the proton number $Z=62$ does not vary, the $|\bar{C}_{j_i^\pi}|^2$ remain almost constant throughout. The $|\bar{C}_{j_i^\nu}|^2$ vary with A and indicate a subshell closure at $A=150$ with $^2f_{\frac{7}{2}}$ orbit almost filled. For $A=152$, higher orbits like $^2f_{\frac{5}{2}}$ and $^1h_{\frac{9}{2}}$ play an important role in building collectivity while for $A=146$, 148, $^3p_{\frac{3}{2}}$ orbit is more active.

The IBM-2 single boson energies e_d^ρ, e_g^ρ with respect to the s-boson energy e_s^ρ, ($\rho=\nu$ and π) are plotted in Fig. 4.5(a) and (b). While the $e_d^\pi-e_g^\pi$ separation remains essentially constant, that between the ν-boson energies increases. This enhances the $\epsilon_d-\epsilon_g$ separation in IBM-1 regime, unlike the Mo isotopes. Such effects are also

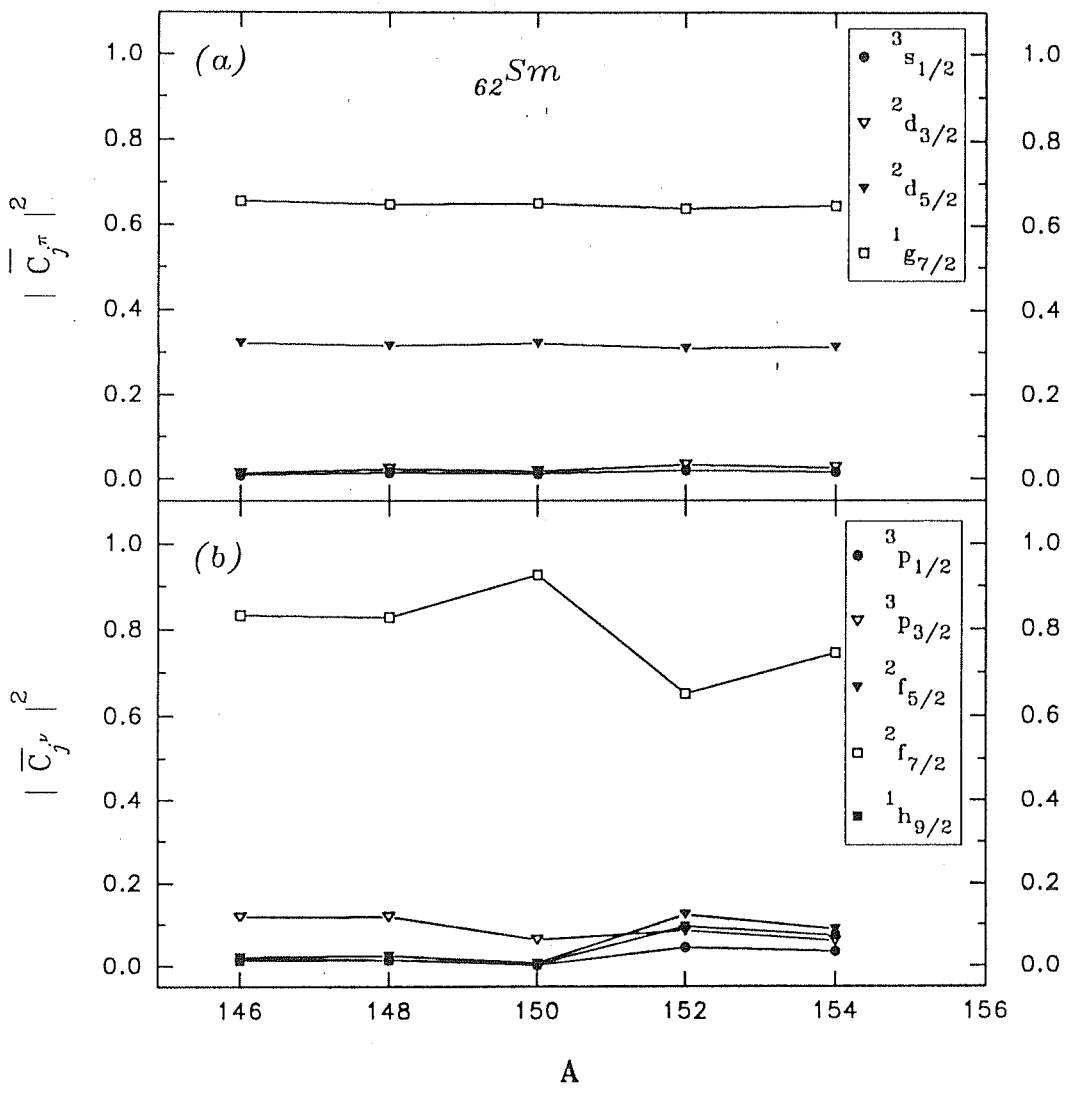

Figure 4.4: Effective occupancies $|\bar{C}_{j_i^\rho}|^2$ of s.p. (a) proton($\rho = \pi$) and (b) neutron ($\rho = \nu$) orbits from $|\rho; k = +\frac{1}{2}\rangle_{\text{eff}}$ orbits.

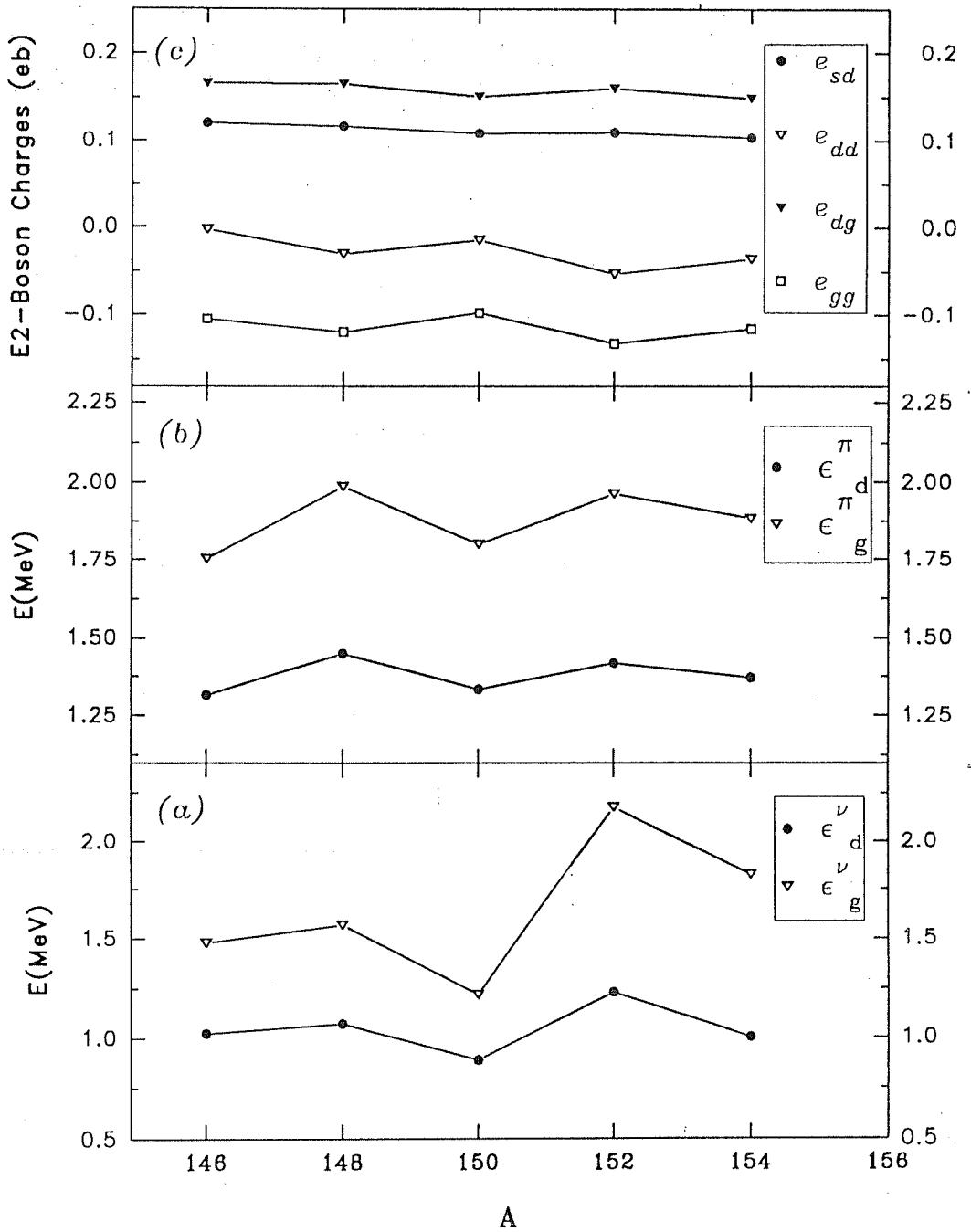

Figure 4.5: IBM-2 d- and g-boson energies ϵ_d^ρ and ϵ_g^ρ for (a) neutrons (ν) and (b) protons (π), and (c) the IBM-1 effective boson charges for $E2$-transitions.

noted by Scholten (1983).

The parameters $\mathcal{T}^{(E2)}_{\mathrm{IBM}-1}$ operator calculated with effective fermion charges $e^F_\nu = 0.5e$, $e^F_\pi = 1.3e$ are given in Fig. 4.5(c). All the parameters essentially remain constant through the chain. The relative phases also match with those of $\mathcal{T}^{(E2)}(SU(3))$ in eq. (4.8). However, the values of e_{dd} seem to be comparatively small. These values of our parameters compare well with the $\mathcal{T}^{(E2)}(SU(3))$ operator used by Devi and Kota (1991) in their study of $^{146-158}Sm$ isotopes, with the choice $e^B = 0.113eb$. The IBM-2 e^ν_{sd} and e^π_{sd} calculated to be $0.06eb$ and $0.14eb$ marginally differ from those of Otsuka (1984) (0.1 and 0.12 respectively).

The $J = 2^+_1, 4^+_1, 0^+_2$ and 2^+_2 levels of the spectra generated in our calculations are plotted in Fig. 4.6(a) alongwith the observed levels (Lederer and Shirley 1978). For comparison, we also present the results of Scholten (1983) alongwith the experimental levels in Fig. 4.6(b). The $J = 2^+_1$, 4^+_1 levels produced in our calculation are scaled up compared to the observed ones just like those of Scholten's IBM-2 calculations. The evidence of shape transition at $A = 150$ is clearly seen from the Yrast levels $J = 2^+_1$ and 4^+_1 plotted w.r.t. the ground state. As discussed by Scholten *et al.* (1978), the behavior of the 0^+_2 levels in the shape transition is the most interesting. It first drops linearly as a member of the 2-phonon multiplet of the spherical nucleus. But then as the transition to deformed shape occurs, it moves up again, to become the head of the β-band. This behavior is clearly seen in the 0^+_2 levels produced in our calculation. The 2^+_2 levels also go up as seen in the experimental curve of Fig. 4.6(a). However, in magnitude, our 0^+_2 and 2^+_2 levels for $^{152-154}Sm$ are much higher even compared to those of Scholten. As already mentioned earlier, the excess of pairing correlation supplied by a higher than realistic value of $A_{\nu\nu}$ and $A_{\pi\pi}$ may be playing a role in this scale-up. In addition, for our levels the mixing of F-spin mixed-symmetric states with those of F-spin symmetric ones may also be partly responsible. As Scholten's

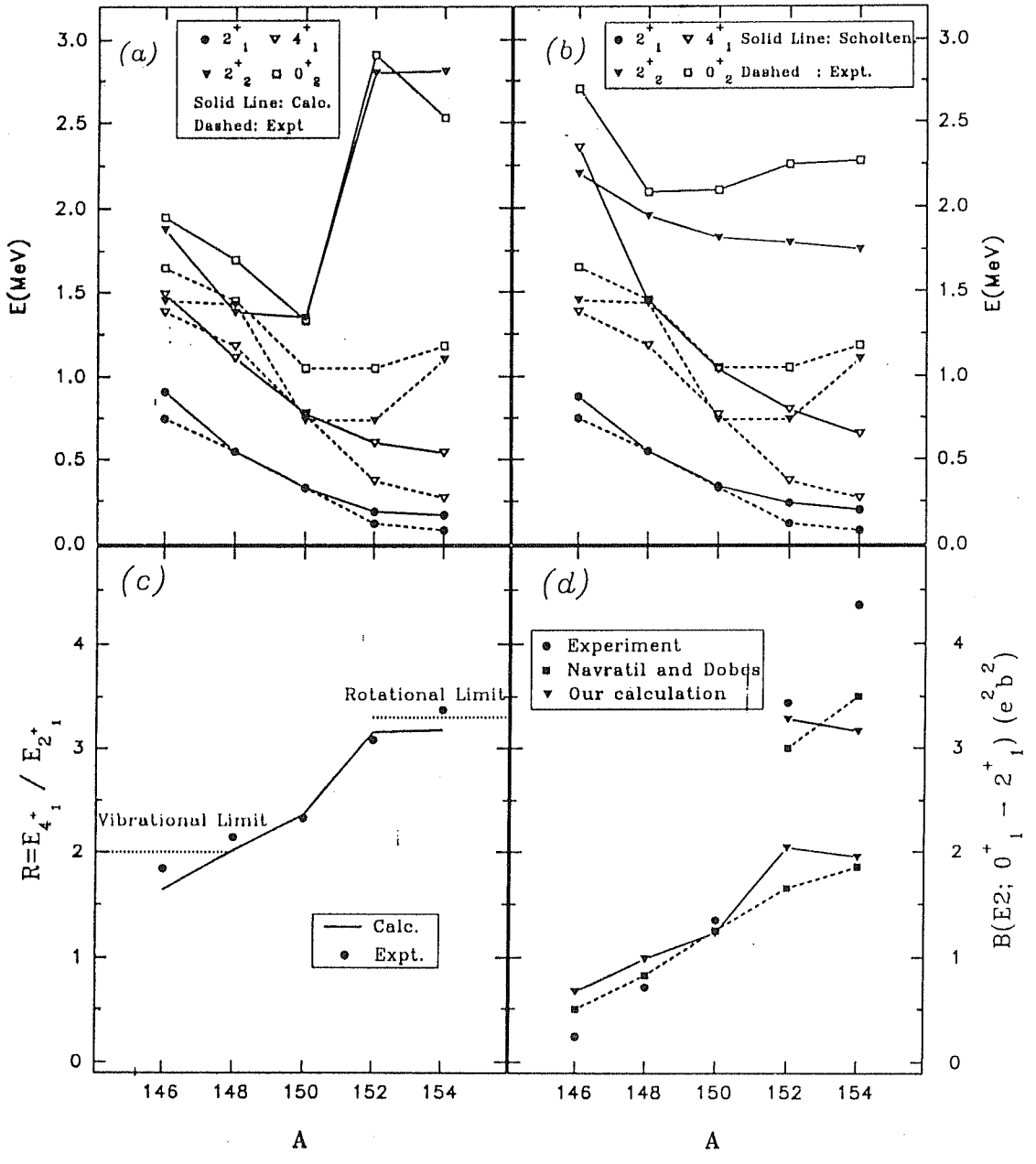

Figure 4.6: (a) Experimental (Expt.) and calculated (Calc.) spectra of Sm isotopes ; (b) Spectra produced in Scholten's (1983) calculation alongwith the Expt. levels; (c) Ratio of the energies of the $J = 4_1^+$ and the 2_1^+ levels and (d) The $B(E2)\uparrow$ in e^2b^2 units.

calculations are carried out in IBM-2 with a Majorana force which pushes the F-spin mixed symmetric levels up in energy, the $0_2^+, 2_2^+$ levels produced thereby should correspond closer to pure F-spin symmetric levels. Navrátil and Dobeš (1991) carried out their calculations by smoothly varying all the input fermion parameters (s.p.e.'s and the strength of the effective interactions) by an empirical function to reproduce the observed spectra. We have also carried out calculations for individual nuclei by varying only the strength parameters $A_{\nu\nu}$, $A_{\pi\pi}$ and $A_{\nu\pi}$ and we find that with a judicious choice of only these parameters one can reproduce the observed results to a very good extent. These results are discussed in the next section.

The ratios $R = E_{J_1^+}/E_{J_2^+}$ for each nucleus are plotted in Fig. 4.6(c). The transition at $A = 150$ is clearly observed. The $B(E2)\uparrow$ calculated in units of e^2b^2 are presented in Fig. 4.6(d) alongwith the experimentally (Raman *et al.* 1987) adopted values and those calculated by Navrátil and Dobeš (1990). With the fermion effective charges $e_\nu^F = 0.5e$ and $e_\pi^F = 1.3e$ chosen to reproduce the experimental value for ^{150}Sm, we observe a clear enhancement of the transition probability at A=150-152. However, it is also clear that the same set of e_ν^F and e_π^F is not able to produce enough enhancement as observed experimentally. A slightly different choice of these charges, *i.e.*, $0.7e$ and $1.6e$ respectively, yields the $B(E2)\uparrow$ value $3.28e^2b^2$ for ^{152}Sm, closer to the experimental value $3.44e^2b^2$. Navrátil and Dobeš also observed similar effects and chose two sets of charge parameters e_ν^F and e_π^F, *viz.*, $(0.7e, 1.3e)$ and $(1.0e, 1.7e)$ in order to produce values closer to the observed ones (see Fig. 4.6(d)). The $B(E2)$ value for ^{154}Sm seems to saturate very drastically for some reason in our calculation.

4.4.3 Discussion

It has long been known that while the short range pairing force produces sphericity, the long-range fields producing quadrupole force favors deformation. The interplay of

these two produces the spherical or deformed nuclei. Federman and Pittel (1977) first attempted to provide a unified microscopic description of the nuclear deformation. Analysing the shell model matrix elements of ^{20}Ne, they showed that it is the strong isospin-scalar $^3S_1$ nuclear force between the netrons and protons occupying the $d_{\frac{5}{2}}-d_{\frac{3}{2}}$ spin-orbit partner (SOP) orbits which is mainly responsible for the deformation in ^{20}Ne. They proposed a general thumb rule that the onset of nuclear deformation occurs in the region where valence neutrons and protons occupy spherical s.p. orbitals having a good overlap. Such a configuration enhances the neutron-proton interaction which is responsible for the deformation. It was shown by deShalit and Goldhaber (1953) that the overlap between the two orbitals $(n_\nu l_\nu j_\nu)$ and $(n_\pi l_\pi j_\pi)$ $(n, l, j$ are the s.p. SM quantum numbers) is maximum if $n_\nu = n_\pi$ and $l_\nu = l_\pi$. It is also very good for $n_\nu = n_\pi$ and $l_\nu = l_\pi \pm 1$ for large values of l_ν and l_π. With the thumb rule and the above observation of deShalit and Goldhaber, Federman and Pittel ascribed the onset of deformation in the Mo isotopes to the filling of $\pi-(g_{\frac{9}{2}})$ and $\nu-(g_{\frac{7}{2}})$ orbitals. Extending the same argument they also described the onset of deformation in the rare earth nuclei like Sm as a consequence of the occupation of intruder orbits $\pi-(^1h_{\frac{11}{2}})$ and $\nu-(^1h_{\frac{9}{2}})$. They also explicitly demonstrated (1978) this effect for Mo isotopes by carrying out HFB calculations. Khosa *et al.* (1982) reported that the deformation in the neutron-rich Mo and Zr isotopes is due to the occupation of intruder $(^1h_{\frac{11}{2}})$ orbit by the neutrons and not because of enhanced interaction by the occupied SOP $(\pi-(g_{\frac{9}{2}})\,\nu-(g_{\frac{7}{2}}))$ orbits.

In our HF calculations, as mentioned earlier, we find that neither in case of the Mo isotopes nor the Sm isotopes, the intruder s.p. orbits, (i.e. $^1h_{\frac{11}{2}}$ or $^1i_{\frac{13}{2}}$) are occupied. And yet, we clearly observe the onset of deformation in both the cases. This effect can still be explained by the thumb rule of Federman and Pittel. In case of Mo isotopes, the protons are in $\{g_{\frac{9}{2}}\}$ orbit. As seen in Fig. 4.2(a) and in Table 4.5, the occupation of $\nu-(g_{\frac{7}{2}})$ orbital increases at $A = 100$, 102 and is substantial at

Table 4.5: Occupancies of the neutron s.p. orbits in Mo isotopes.

A	$^3s_{\frac{1}{2}}$	$^2d_{\frac{3}{2}}$	$^2d_{\frac{5}{2}}$	$^1g_{\frac{7}{2}}$
96	0.3	0.17	3.39	0.13
98	0.24	0.13	5.52	0.11
100	1.04	0.54	5.96	0.47
102	1.99	1.20	5.99	0.81
104	2.00	2.85	6.00	1.15
106	2.00	3.64	6.00	2.36
108	2.00	4.00	6.00	4.00

$A = 108$. The neutron-proton interaction enhanced by this occupation is probably responsible for the onset of deformation.

In case of the Sm isotopes, as seen in Fig. 4.4(a) and (b) the most influential s.p. orbits are $(^2d_{\frac{5}{2}}\ ^1g_{\frac{7}{2}})$ for protons and $(^3p_{\frac{3}{2}}\ ^2f_{\frac{5}{2}}\ ^2f_{\frac{7}{2}}\ ^1h_{\frac{9}{2}})$ for neutrons. In Table (4.6), we have tabulated the occupancies of these orbits. Amongst the neutron orbits the $^2f_{\frac{7}{2}}$ orbit is getting filled upto $A = 150$. For $A = 152$, however, the occupancy of $^2f_{\frac{7}{2}}$ drops a little, and those of $^2f_{\frac{5}{2}}$ and $^1h_{\frac{9}{2}}$ increase drastically. All these neutron orbitals can be said to have good overlap with the influential proton orbitals by the $n_\nu = n_\pi$ and $l_\nu = l_\pi + 1$ rule. The combined effect of the neutron-proton interaction of all these orbitals may be responsible for the onset of deformation at $A = 152$. These observations are in variance with the predictions of Federman and Pittel (1977) who suggest that the deformation in the Sm isotopes should result from the interaction between the protons in $^1h_{\frac{11}{2}}$ and the neutrons in $^1h_{\frac{9}{2}}$ SOP orbits.

Table 4.6: Occupancies of the proton and neutron s.p. orbits in Sm isotopes.

A	Protons		Neutrons			
	$^2d_{\frac{5}{2}}$	$^1g_{\frac{7}{2}}$	$^3p_{\frac{3}{2}}$	$^2f_{\frac{5}{2}}$	$^2f_{\frac{7}{2}}$	$^1h_{\frac{9}{2}}$
146	3.87	7.86	0.24	0.04	1.66	0.02
148	3.80	7.76	0.48	0.10	3.31	0.05
150	3.86	7.79	0.38	0.04	5.56	0.02
152	3.71	7.66	0.68	0.99	5.21	0.76
154	3.76	7.75	0.60	0.88	7.44	0.73

4.5 Detailed Calculations

In this section, the results of the detailed calculations of energy levels and the $E2$-transition probability for ^{148}Sm, ^{150}Nd and ^{152}Sm are presented. The gross features of the observed vibrational collectivity of ^{148}Sm and rotational collectivity of ^{152}Sm were obtained in our calculation with one set of interaction parameters for the SDI and one set effective fermion charges. However, the spectrum of ^{152}Sm was scaled up (Fig. 4.6(a)). In this section, we show that by suitably choosing two interaction parameters, namely, $A_{\nu\nu}(= A_{\pi\pi})$ and $A_{\nu\pi}$ we can reproduce the spectrum of the ground band and a few levels of the higher bands to very good accuracy. Further, with a judicious choice of the fermion effective charges e_ν^F and e_π^F, we are able to reproduce the experimentally observed $B(E2)$ values quite well. Besides these two Sm isotopes, we also calculate with remarkable success the spectrum and the $B(E2)$ values for ^{150}Nd known to be a rotational nucleus.

The single particle energies of the model spaces are chosen to be the same as in the previous calculations (table 4.4). The rest of the fermion input parameters are

Table 4.7: Choice of the free fermion input parameters

parameter(unit)	^{148}Sm	^{150}Nd	^{152}Sm
$A_{\nu\nu}(MeV)$	0.33	0.15	0.10
$A_{\pi\pi}(MeV)$	0.33	0.15	0.10
$A_{\nu\pi}(MeV)$	0.12	0.12	0.17
$e_\nu^F(e)$	0.2	1.0	1.1
$e_\pi^F(e)$	1.2	1.9	2.1

chosen as presented in table 4.7.

4.5.1 ^{148}Sm

In Fig. 4.7 we present the spectrum of ^{148}Sm (labelled "Calc.") alongwith the experimental ("Ex") levels. The theoretical levels produced by the microscopic *sdg*IBM calculations of Navrátil and Dobeš (1991) ("ND") and phenomenological calculations of Devi and Kota (1992) ("DK") are also plotted for comparison. The exerimental levels are read off from Devi and Kota (1992). Apart from the good agreement of the ground state band ("Quasi-GS"), we also find fair agreement of the "Quasi-β" band. The "Quasi-γ" levels are however very poorly reproduced in our calculations. The same seems to be the case also with the microscopically calculated levels of ND.

As noted before, our assumption of complete F-spin symmetry of all IBM-2 states of the Hamiltonian is an approximation. This approximation may be badly broken for levels of higher bands farther from the ground state 0_1^+. In fact, Otsuka and Ginocchio (1985) have shown that the 2_3^+ level of ^{148}Sm is an F-spin vector state. Such factors may be responsible for the poor reproduction of the Quasi-γ band in our

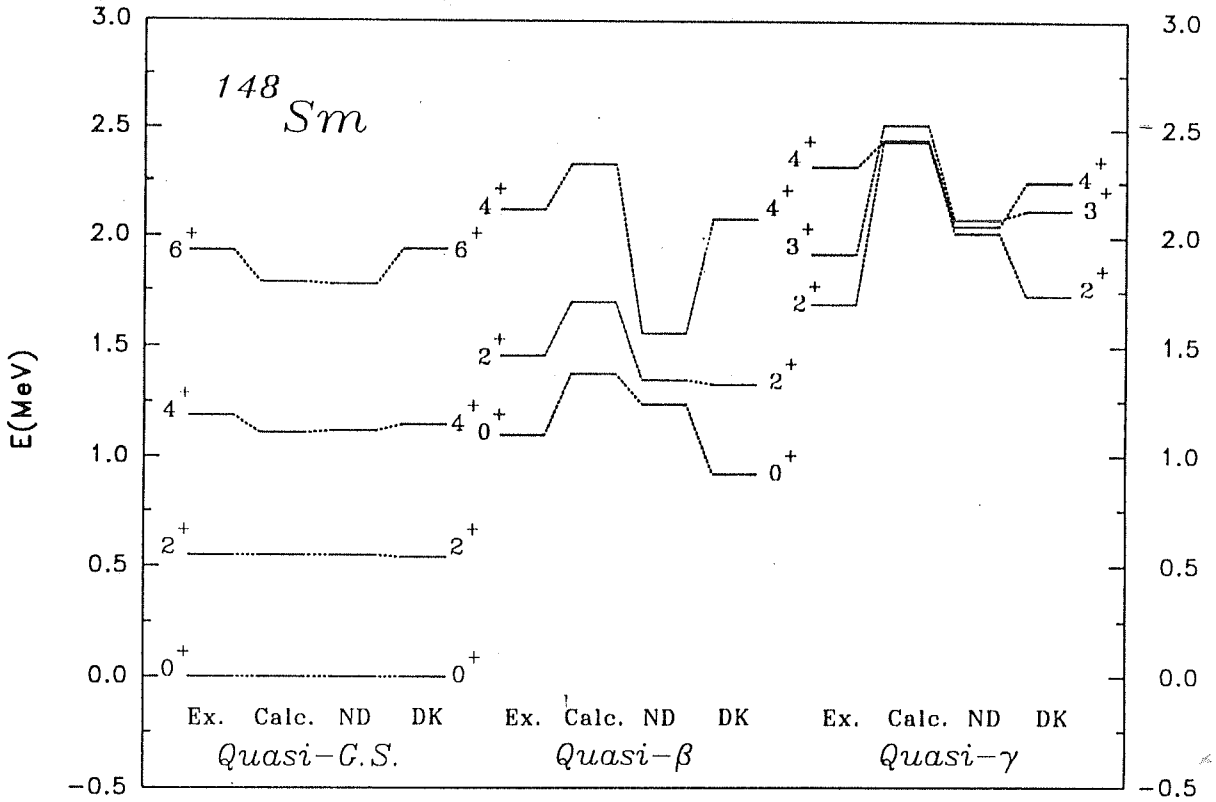

Figure 4.7: Spectrum of ^{148}Sm. Our calculated levels (Calc.) are plotted with the experimental levels (Ex.), the results of (*sdg*-) microscopic calculations of Navrátil and Dobeš (ND) (1991) and phenomenological calculations of Devi and Kota (DK) (1992).

Table 4.8: $B(E2)$ values in units of e^2b^2 for ^{148}Sm. The "Ex" and "ND" values are taken from Navrátil and Dobeš (1991). The static quadrupole moment $Q_{2_1^+}$ in barns (b) of the 2_1^+ level is also tabulated.

$J_i \rightarrow J_f$	Ex.	Calc.	ND
$2_1^+ \rightarrow 0_1^+$	0.151(10)	0.143	0.151
$4_1^+ \rightarrow 2_1^+$	0.25(7)	0.239	0.222
$2_\beta^+ \rightarrow 0_1^+$	0.0069(11)	0.010	0.042
$2_\beta^+ \rightarrow 2_1^+$	–	0.114	–
$0_\beta^+ \rightarrow 2_1^+$	–	0.146	–
$0_\beta^+ \rightarrow 2_\beta^+$	–	0.171	–
$Q_{2_1^+}(b)$	-0.97(27)	-0.631	-0.519

calculation.

The $E2$-transition probabilities from initial states J_i to final states J_f, $B(E2; J_i \rightarrow J_f)$ of a few of the low-lying levels are presented ("calc.") in table 4.8. The experimental values and those of ND (*sdg*- calculation) match well with ours for the Yrast levels. The static quadrupole moment $Q_{2_1^+}$ (in units of b) of the first 2^+ level produced in our calculation also matches fairly with the observed value.

4.5.2 ^{150}Nd

The spectra of ^{150}Nd are plotted in Fig. 4.8. The experimental levels are taken from de Mateosian (1986). The calculated (*sdg*)-spectrum of Navrátil and Dobeš (ND) are also plotted for comparison. The levels of the ground state (GS) band in our calculation ("Calc") match with the experimental levels remarkably well. The levels

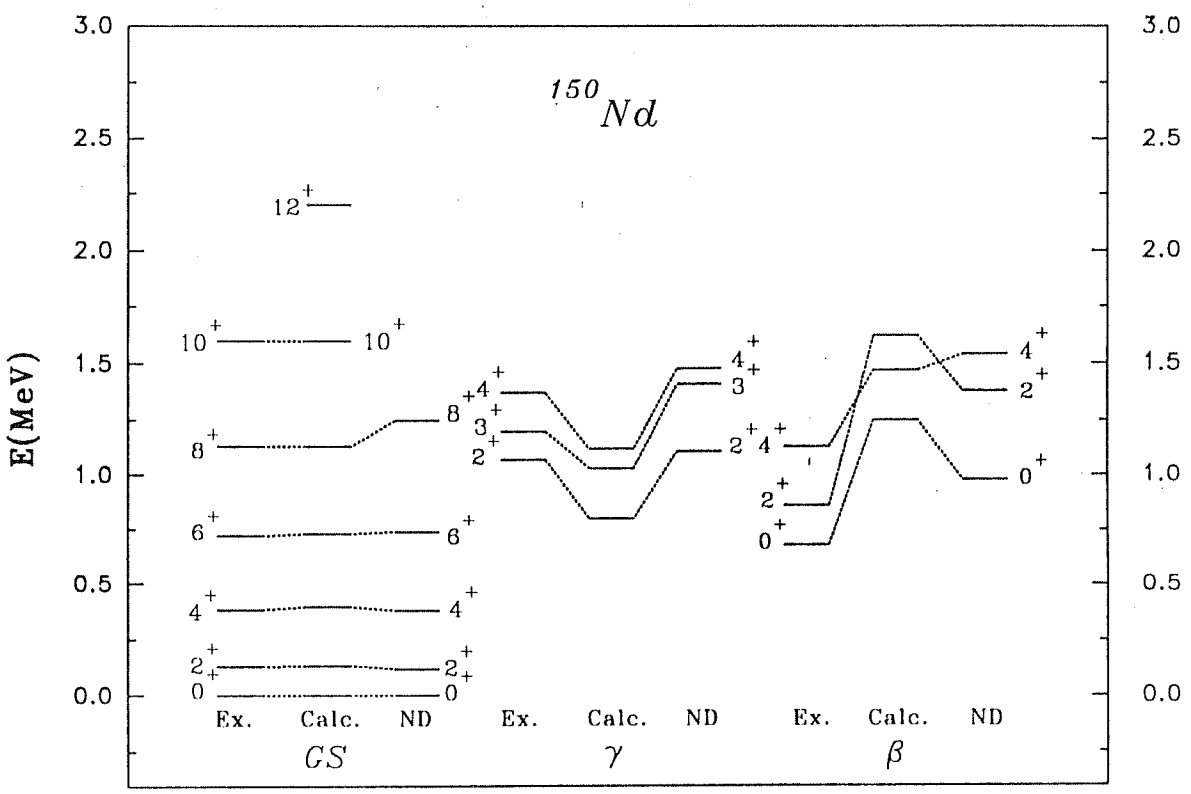

Figure 4.8: Spectrum of ^{150}Nd. The calculated levels (Calc.) are plotted alongwith the experimentally observed (Ex.) levels (de Mateosian (1986)) and the calculated *sdg*-spectrum of Navrátil and Dobeš(ND) (1991).

of the γ-band though clearly reproduced in our calculation are slightly pushed down. The reproduction of the β-band is poor. Besides being pushed up in our calculation, the 4^+ level of this band is pushed below the 2^+ level. As remarked earlier, such discrepancies in the higher levels may be because of substantial mixing of states with $F < F_{max}$ with F_{max} states.

In table 4.9, the $B(E2)$ values are listed. The values for the transition in the GS band are in close agreement with the experimental and ND values. Barring the case of $B(E2; 2^+_\gamma \rightarrow 2^+_1)$, the cross-band values produced in our calculation are small, as they are expected to be. The intraband transitions, especially in the γ-band are as prominent as they are in the GS band.

4.5.3 ^{152}Sm

The calculated spectrum (Calc.) of ^{152}Sm is plotted alongwith the experimental (Ex.) and phenomenologically calculated (Devi and Kota (DK) 1992) spectra in Fig.4.9. The "Ex." and "DK" numbers are read off from Devi and Kota (1992). The agreement of our calculated levels in the G.S. band even upto $J^\pi = 12^+$ is quite good. The $J = 2^+$ to 6^+ levels of γ-band are also produced to very good accuracy with the band head tallying with the experiment. Our β-band is, however, pushed high up and is poorly reproduced.

In Table 4.10, we present the $B(E2)$ values alongwith the experimental and calculated values from Kumar (1974). The E2- matrix elements $M_{ij}(E2)$ listed by Kumar are related to the $B(E2; J_i \rightarrow J_f)$ by the relation

$$B(E2; J_i \rightarrow J_f) = \frac{1}{(2J_i + 1)} M^2_{ij}(E2) \tag{4.9}$$

With the fermion effective charges $e^F_\nu = 1.2e$ and $e^F_\pi = 1.7e$ the $B(E2; 0^+_1 \rightarrow 2^+_1)$ is calculated to be 3.44 (e^2b^2), comparable with 3.37 (Expt.) and 3.25 (Kumar).

Table 4.9: $B(E2)$ values in units of e^2b^2 for ^{150}Nd. The experimental (Ex.) and ND (sdg)-values are from Navrátil and Dobeš (1991).

$J_i \rightarrow J_f$	Ex.	Calc.	ND
$2_1^+ \rightarrow 0_1^+$	0.563(2)	0.557	0.560
$4_1^+ \rightarrow 2_1^+$	0.819(28)	0.848	0.810
$6_1^+ \rightarrow 4_1^+$	0.980(90)	0.859	0.883
$8_1^+ \rightarrow 6_1^+$	1.207(118)	0.893	0.904
$2_\gamma^+ \rightarrow 3_\gamma^+$	–	0.686	–
$2_\gamma^+ \rightarrow 4_\gamma^+$	–	0.592	–
$3_\gamma^+ \rightarrow 4_\gamma^+$	–	0.370	–
$2_\beta^+ \rightarrow 0_\beta^+$	–	0.312	–
$2_\gamma^+ \rightarrow 2_1^+$	0.034(7)	0.155	0.037
$2_\gamma^+ \rightarrow 0_1^+$	0.0151(9)	0.017	0.012
$2_\gamma^+ \rightarrow 4_1^+$	–	0.006	–
$0_\beta^+ \rightarrow 2_1^+$	0.208(9)	0.039	0.0705
$2_\beta^+ \rightarrow 4_1^+$	0.095(28)	0.023	0.0326
$2_\beta^+ \rightarrow 2_1^+$	0.036(17)	0.002	0.004
$2_\beta^+ \rightarrow 0_1^+$	0.0024(5)	0.001	0.0117

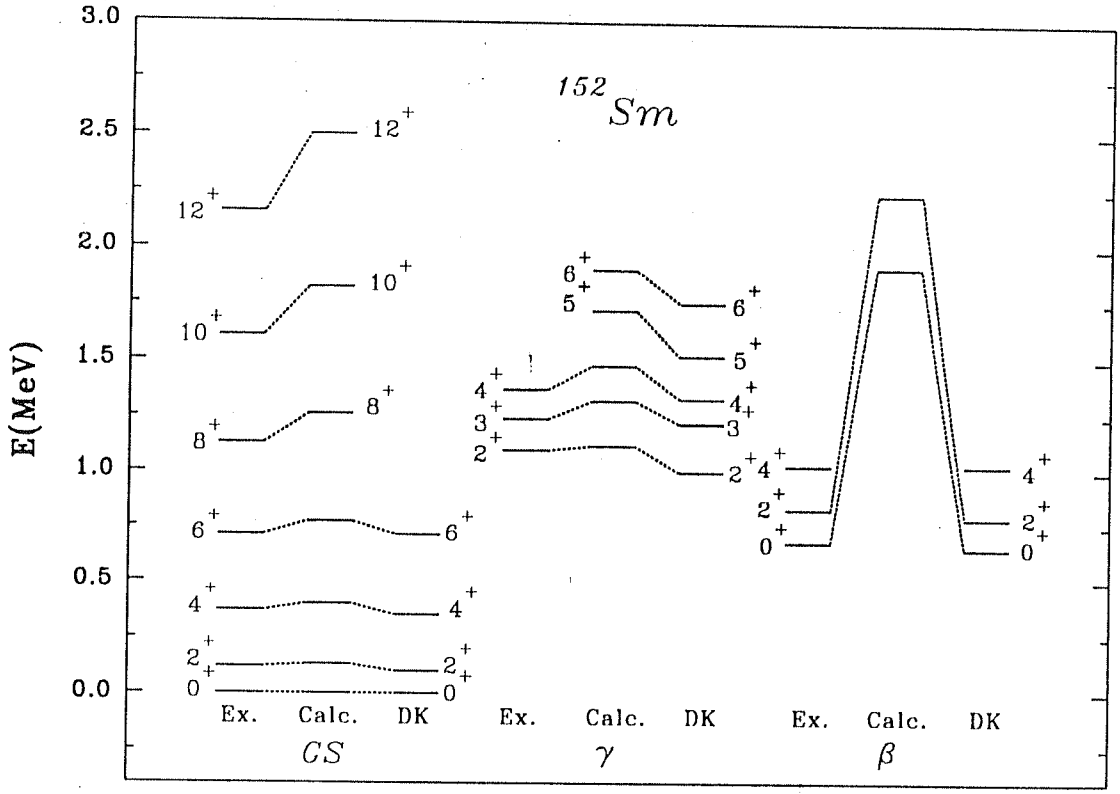

Figure 4.9: Spectrum of ^{152}Sm. The calculated spectrum is plotted alongwith the experimental (Ex.) and phenomenologically calculated spectrum of Devi and Kota (DK). Both the Ex. and DK values are read off from Devi and Kota (1992).

However, with this choice the other $B(E2)$'s are found to be consistently less than the experimental or calculated values of Kumar. A slightly different choice $e_\nu^F = 1.1e$, $e_\pi^F = 2.1e$ optimises the values. The $B(E2)$ values calculated with this choice are tabulated in Table 4.10. The enhanced intraband and suppressed cross-band E2 transition probabilities are clearly seen from this tabulation. However, it is not clear why large discrepancies occur between our values, the "Ex." and calculated values of Kumar.

4.6 Conclusion

We have applied our formulation developed and discussed in Chapter 2 to study the collective properties of vibrational and rotational nuclei. The observed transition from spherical to axially deformed shape in even-even $^{96-108}Mo$ and $^{146-154}Sm$ isotopes is clearly reproduced by the IBM Hamiltonian and $E2$-operators derived microscopically by our scheme. The detailed calculations performed on the spherical ^{148}Sm and deformed ^{150}Nd and ^{152}Sm reproduced the observed spectra and $B(E2)$ values in the (quasi-) G.S. bands very well. This verifies our claim (see Sec. 4.3)) that the assumption of complete F-symmetry in these levels is a good approximation.

However, there are a few unsavoury observations. First, we found it necessary to vary the fermion input parameters in order to be able to closely reproduce the observed spectra and $E2$-transition probabilities. To be specific, for satisfactory reproduction of the spectra we had to vary the two interaction strength parameters, i.e. $A_{\nu\nu}(= A_{\pi\pi})$ and $A_{\nu\pi}$. We also had to vary, less often though, the fermion effective charges e_ν^F and e_π^F to reproduce closely the observed $B(E2)$ values. In case of Sm isotopes, we demonstrated explicitly that if we keep these strength parameters fixed,

Table 4.10: $B(E2)$ values in e^2b^2 for ^{152}Sm. For comparison we have also tabulated the experimental (Ex.) and calculated values of Kumar (1974).

$J_i \rightarrow J_f$	Ex.	Calc.	Kumar
$0_1^+ \rightarrow 2_1^+$	3.37	4.41	3.25
$2_1^+ \rightarrow 4_1^+$	1.81	1.79	1.79
$4_1^+ \rightarrow 6_1^+$	1.71	1.27	1.71
$2_\gamma^+ \rightarrow 3_\gamma^+$	–	1.26	1.26
$2_\gamma^+ \rightarrow 4_\gamma^+$	–	0.70	0.65
$3_\gamma^+ \rightarrow 4_\gamma^+$	–	0.82	0.92
$3_\gamma^+ \rightarrow 5_\gamma^+$	–	0.90	0.94
$4_\gamma^+ \rightarrow 5_\gamma^+$	–	0.50	0.64
$4_\gamma^+ \rightarrow 6_\gamma^+$	–	0.81	1.12
$5_\gamma^+ \rightarrow 6_\gamma^+$	–	0.33	0.49
$0_\beta^+ \rightarrow 2_\beta^+$	–	2.74	3.72
$2_\gamma^+ \rightarrow 0_1^+$	0.02	0.02	0.02
$2_\gamma^+ \rightarrow 2_1^+$	0.05	0.11	0.05
$3_\gamma^+ \rightarrow 2_1^+$	–	0.02	0.03
$4_\gamma^+ \rightarrow 2_1^+$	0.004	0.0	0.008
$5_\gamma^+ \rightarrow 4_1^+$	–	0.01	0.03
$6_\gamma^+ \rightarrow 4_1^+$	–	0.0	0.005
$0_\beta^+ \rightarrow 2_1^+$	0.181	0.02	0.21
$2_\beta^+ \rightarrow 0_1^+$	0.005	0.001	0.003
$2_\gamma^+ \rightarrow 2_\beta^+$	0.001	0.08	0.001

then we get scaled up spectra for the heavier ($^{152-154}Sm$) isotopes (Fig. 4.6(a)). Besides the similar scaled up spectra produced in Scholten's work (Fig. 4.6(b)), Druce *et al.* (1987) have also reported similar effects in their microscopically calculated spectra of $^{194-202}Hg$ isotopes with the choice of parameters kept constant throughout the isotopic chain. By choosing them suitably, we could reproduce the observed spectra to very good accuracy (Figs. 4.7 to 4.9). Similar observations have also been made by Navrátil and Dobeš in their calculations for the Sm isotopic chain employing the similarity transformed Dyson mapping procedure.

In our calculations, we have kept the number of free parameters minimal – at 2. These are the effective interaction strength parameters. The s.p.e. of the model orbits are kept fixed. Navrátil and Dobeš vary all the input parameters including the s.p.e. by an empirical function with one empirically chosen parameter. It should be noted that the choice of s.p.e. in our calculation coincides exactly with the initial choice of Navrátil and Dobeš which they then vary smoothly in the above mentioned manner. And yet, our results and theirs are however very similar as seen in Figs. (4.7, 4.8). However, such a necessity to vary the fermion input parameters for the same isotopic chains shows that a complete understanding as well as capability to carry out fully microscopic IBM calculations is yet to be achieved.

Secondly, reproducibility of higher bands in our calculations is poor. The band next to the (quasi-)G.S. band (quasi-β for ^{148}Sm and γ for ^{150}Nd and ^{152}Sm) is comparatively much beter reproduced. The third band is very poorly produced in all the three detailed calculations. As pointed out earlier, a more than permissible mixing of F-mixed-symmetric states with the assumed completely F-symmetric IBM-2 states may be a strong factor. The other possible factor may be inherent to our approach in that our construct is based on only the lowest energy HF solution. There may occur, in many a case, close local minima on the energy hyper-surface. The higher bands

of the spectrum will naturally get affected if the solutions corresponding to these nearby minima are not taken into account. One may, in the spirit of HF band-mixing calculations, construct distinct correlated pairs $S, S'..$, $D, D'..$ etc., a set from each of the solutions and construct the expanded IBM scenario with the corresponding $s, s'..$, $d, d'..$ bosons. Such calculations are out of the scope of our present calculations. Thirdly, the approximations involved, namely, the absence of identical boson two-body interaction in $\mathcal{H}_{\text{IBM}-2}$ and the restrictions put on N_s and N_g, the s and g boson numbers, because of computational limitations may also be playing a non-negligible role in these higher bands.

4.7 References

1. Bayman B F and Lande A 1966 *Nucl. Phys.* **77** 1
2. Brussaard P J and Glaudemans P W M 1977 in *Shell Model Application in Nuclear Spectroscopy* (North Holland, Amsterdam)
3. Casten R F, Frank W and von Brentano P 1985 *Nucl. Phys.* **A444** 133
4. Cheifetz E, Jared R C, Thompson S G and Wilhelmy J B 1970 *Phys. Rev. Lett.* **25** 38
5. Chen Hsi-Tseng, Kiang L L, Yang C C, Chen L M, Chen T L and Jiang C W 1986 *J. Phys.* **G12** L217
6. de Shalit A and Goldhaber M 1953 *Phys. Rev.* **92** 1211
7. der Mateosian E 1986 *Nuclear Data Sheets* **48** 345
8. Devi Y D and Kota V K B 1990, FORTRAN PROGRAMMES FOR SPECTROSCOPIC CALCULATIONS IN (sdg)-BOSON SPACE: THE PACKAGE SSGIBM1 (Physical Research Laboratory, India, Technical Report, PRL-TN-90-68)
9. Devi Y D and Kota V K B 1992 *Phys. Rev.* **C45** 2238
10. Druce C H, Pittel S, Barrett B R and Duval P D 1987 *Ann. Phys.* **176** 114
11. Federman P and Pittel S 1977 *Phys. Lett.* **69B** 385
12. Federman P and Pittel S 1978 *Phys. Lett.* **77B** 29
13. Khosa S K, Tripathi P N and Sharma S K 1982 *Phys. Lett.* **119B** 257

14. Kota V K B, Van der Jeugt J, De Meyer H and Vander Berghe G 1987 *J. Math. Phys.* **28** 1644

15. Kota V K B 1991 Private Discussion

16. Kumar K 1974 *Nucl. Phys.* **A231** 189, and the refernces therein

17. Lederer C M and Shirley V S 1978 (Eds.) *Tables of Isotopes* (Seventh Ed.) (John Wiley & Sons, Inc.)

18. Liang M, Ohm H, De Sutter B, Sistemich K, Fazekas B and Molnár G 1991 *Z. Phys.* **A340** 223

19. Mach H, Wohn F K, Molnaŕ G, Sistemich K, Hill J C, Moszyński M, Gill R L, Krips W and Brenner D S 1991 *Nucl. Phys.* **A523** 197

20. Navrátil P and Dobeš J 1991 *Nucl. Phys.* **A533** 223

21. Otsuka T 1984 *Phys. Lett.* **138B** 1

22. Otsuka T and Ginocchio J N 1985 *Phys. Rev. Lett.* **54** 777

23. Otsuka T and Sugita M 1988 *Phys. Lett.* **215B** 205

24. Pannert W, Ring P and Gambhir Y K 1985 *Nucl. Phys.* **A443** 189

25. Pittel S and Dukelsky J 1983 *Phys. Lett.* **128B** 9

26. Pittel S, Duval P D and Barrett B R 1982 *Ann. Phys.* **144** 168

27. Raman S, Malarkey C H, Milner W T, Nestor C W and Stelson P H 1987 *At. Data Nucl. Data Tables* **36** 1

28. Raman S, Nestor C W, Kahane S and Bhatt K H 1989 *At. Data Nucl. Data Tables* **42** 1

29. Sambataro M and Molnaŕ G 1982 *Nucl. Phys.* **A376** 201

30. Scholten O 1980 Ph. D. Thesis, University of Groningen, The Netherlands.

31. Scholten O 1983 *Phys. Rev* **C28** 1783

32. Scholten O, Iachello F and Arima A 1978 *Ann. Phys.* (N.Y.) **115** 325

33. Wohn F K, Mach H, Moszyński M, Gill R L and Casten R F 1990 *Nucl. Phys.* **A507** 141c

34. Wu H C 1981 *Phys. Lett.* **110B** 1

Chapter 5

Summary and Conclusion

5.1 Summary

In this chapter, the objective of this work, its extent of success and the limitations are summarised. Further calculations to investigate the limitations are also proposed.

The objective was to construct the IBM operators in microscopic (fermion) basis in a dynamic way so that the same scheme is applicable to any even-even nucleus with valence neutrons and protons. Secondly, we aimed at applying this scheme to reproduce and study the collective spectroscopic properties of vibrational and rotational nuclei.

The IBM-2 Hamiltonian $\mathcal{H}_{\text{IBM}-2}$ and the $E2$-transition operator $\mathcal{T}^{(E2)}_{\text{IBM}-2}$ were constructed microscopically and dynamically by (a) constructing the correlated identical nucleon pairs from the deformed HF solutions for every nucleus considered and (b) evaluating the parameters of these operators through calculations of appropriate matrix elements of the fermion operators in the space of the correlated pairs. This

was achieved by establishing a Marumori mapping from the correlated pair space onto the boson space. In all calculations, the g-bosons (G-pairs) were explicitly taken into account. The approximation involved was that identical boson two-body interaction terms were ignored. Secondly, for constructing the correlated pairs, it was necessary to have prolate-deformed axially symmetric HF solutions. For the Mo and Sm isotopes to which we applied the scheme, these solutions were in fact found to be prolate solutions. Hence this requirement did not prove to be as restrictive as it might appear.

Applying this scheme, we carried out IBM-2 studies of a few simple nuclei, *viz.* ^{20}Ne, ^{44}Ti, ^{60}Zn and ^{94}Mo, chosen with the criterion that they have only one boson of each kind ($N_\nu = N_\pi = 1$) outside the core. The Yrast levels of these nuclei obtained by diagonalising the $\mathcal{H}_{\text{IBM}-2}$ showed good agreement with those of the experimental and shell model results. Non-Yrast levels of ^{94}Mo were also reproduced well whereas those of the three lighter nuclei were pushed up because of isospin mixing. It is to be noted that ^{20}Ne is a well known rotational nucleus. The other nuclei exhibit vibrational spectra in low-energy regions. It has been previously shown (Elliott *et al.* 1987) that for nuclei with valence neutrons and protons occupying the same single particle SM space, one ought to carry out IBM-3 studies in order to preserve the isospin symmetry. From our calculations for the three lighter nuclei, it seems, however, that in case of the Yrast levels, the IBM-2 calculations may still be sufficient.

The principal application of the scheme was to the study of shape transitions in even-A $^{96-108}Mo$ and $^{146-154}Sm$ isotopes. Due to the lack of an IBM-2 code incorporating g-bosons explicitly, we carried out these studies in IBM-1 regime by projecting from the IBM-2 operators. The shape transition from spherical to axial rotor with increasing neutron number which is chacterised by a transition from vibrational to rotational spectrum as well as the characteristic enhancement of $B(E2; 0_1^+ \rightarrow 2_1^+)$

for the rotational nuclei was clearly reproduced by our calculations. While similar calculations following other proposed schemes have been previously carried out for the Sm isotopes, we have reported here the first microscopic IBM calculations for the Mo isotopes.

Detailed calculations of spectra and $E2$-transition probabilities for the vibrational ^{148}Sm and rotational ^{150}Nd and ^{152}Sm nuclei were also carried out. The levels in the ground and first excited band were very well reproduced as were the intra- and inter-band $B(E2)$ values. The second excited band was however poorly produced in all three cases.

5.2 Further Investigations

In the study of shape transitions in both the isotopic chains, it was observed that the same set of fermion input parameters do not reproduce the experimental spectra of all the isotopes in the chain to the same degree of accuracy. It was necessary to vary the strength parameters of the fermion two-body interaction (SDI) and the fermion effective charges to reproduce the spectra and $B(E2)$ values close to the observations. The variation of the interaction strength parameters was more crucial. It could however be broadly said that the parameters remained essentially the same in the range of vibrational and, separately, in the range of rotational nuclei (Table (4.3)) and changed from one set of values to the other through the transitional region. It was also observed that the interaction strength parameter amongst the identical nucleons, namely, $A_{\nu\nu}$ and $A_{\pi\pi}$, which represent the pairing strength reduced drastically across the transitional region for the heavier (deformed) isotopes. It can be argued that such transitions in the strength parameters is a manifestation of the transition.

However, it remains a dissatisfactory fact that the whole scenario of shape transition could not be derived completely microscopically, with the same set of fermion parameters throughout the isotopic chain. This aspect calls for further investigation especially to explore if a systematic and analytical behavior of such a transition of fermion input parameters exists. At this juncture, this variation remains phenomenological. Navrátil and Dobeš (1991) also observed a similar necessity to vary the input parameters and carried out the variation using a smoothly varying function having one empirically chosen constant for every set of parameters, *viz.*, the single particle energies and the interaction strength. Such investigations could be carried out in our formulation too. The plausibility and origin of the empirical parameter and the function may also be investigated.

In carrying out these calculations, it should, however, be borne in mind that the two-body identical boson interaction terms in $\mathcal{H}_{\text{IBM}-2}$ are always ignored as an approximation.

The reason behind the poor reproduction of the higher excited bands, as discussed in Chapter 4, may be two-fold. For one, it may be due to the occurence of multiple local minima of the energy hyper-surface which was minimized in the HF procedure. By incorporating the effects of these minima in terms of a set of bosons of each type $(s, s', .., d, d', ..)$ corresponding to each local minimum it may be possible to generate the higher bands to a better accuracy. This necessitates a generalisation of the SDGIBM1 code.

The other possibility is that the eigenstates of $\mathcal{H}_{\text{IBM}-2}$ corresponding to the levels in the higher bands do not correspond to maximum F-spin. Contrary to our assumption in carrying out the IBM-2 $\rightarrow$ IBM-1 projection procedure, these states may be actually having substantial mixture of lower F-spin states. In order to ascertain the validity of this conjecture, it is desirable to carry out an F-spin analysis of

the $\mathcal{H}_{\text{IBM}-2}$ prior to the IBM-2 $\rightarrow$ IBM-1 projection. Following Pittel *et al.* (1982) one can decompose the $\mathcal{H}_{\text{IBM}-2}$ into a sum of the F-spin symmetric, antisymmetric and non-conserving pieces and then carry out the projection only on the F-spin symmetric part assuming that it is the most dominant piece in the full Hamiltonian.

Apart from the absence of the identical two-body boson terms in the IBM-2 Hamiltonian, we have one more approxiamtion. Due to limitations of available computational facilities, restrictions have been put on the number of s and g bosons, N_s and N_g respectively, in the boson configuration space in which the IBM-1 Hamiltonian matrix is finally constructed and diagonalised. These factors may also be playing a substantial role in the reproduction of the higher bands.

Besides, to further explore and establish the validity of the scheme presented here, it is desirable to carry out similar studies in actinide regions for example in $Os-Pt-Hg$ isotopes. The isotopes in this region are known to undergo γ-unstable to axial rotor shape transitions. These properties could be studied by the application of our procedure.

5.3 References

1. Elliott J P, Evans J A and Williams A P 1987 *Nucl. Phys.* **A469** 51

2. Navrátil P and Dobeš J 1991 *Nucl. Phys.* **A533** 233

3. Pittel S, Duval P D and Barrett B R 1982 *Ann. Phys.* (N.Y.) **114** 168

Appendix-A

Here we present the calculation of the matrix element (m.e.)

$$\langle(\rho; k_r l_r) J_r || (a^\dagger_{j\rho} \times \tilde{a}_{j'\rho})^J || (\rho; k_s l_s) J_s \rangle. \tag{A1}$$

We reduce this m.e. into two s.p. matrix elements by intermediate state expansion

$$\langle(\rho; k_r l_r) J_r || (a^\dagger_{j\rho} \times \tilde{a}_{j'\rho})^J || (\rho; k_s l_s) J_s \rangle =$$
$$(-1)^{J_r+J_s-J}[J]^{\frac{1}{2}} \sum_{j''\rho} \left\{ \begin{array}{ccc} J_r & j^\rho & j''^\rho \\ j'^\rho & J_s & J \end{array} \right\}$$
$$\langle(\rho; k_r l_r) J_r || a^\dagger_{j\rho} || j''^\rho \rangle \langle j''^\rho || \tilde{a}_{j'\rho} || (\rho; k_s l_s) J_s \rangle \tag{A2}$$

The two matrix elements on the r.h.s. of equation (A2) are in a general sense, the 1 to 2 particle c.f.p.'s. They are evaluated with the help of angular momentum recoupling rules and the fermion anticommutation relations.

For example, we take $\langle(\rho; k_r l_r) J_r || a^\dagger_{j\rho} || j''^\rho \rangle$. We recall the notation we introduced in equation (2.28), and write this m.e. in terms of the spherical tensors as a vacuum expectation value(v.e.v.) (following French *et al.* (1969), eqn(2.30) of the ref.)

$$\langle(\rho; k_r l_r) J_r || a^\dagger_{j\rho} || j''^\rho \rangle = (-1)^{J_r - j^\rho - j''^\rho} \zeta_{k_r l_r} \langle (((\tilde{a}_{j^\rho_{k_r}} \times \tilde{a}_{j^\rho_{l_r}})^{J_r} \times a^\dagger_{j\rho})^{j''} \times a^\dagger_{j''\rho})^0 \rangle_0 \tag{A3}$$

The quantity $\langle(...)^0\rangle_0$ on the r.h.s. of the above equation is the v.e.v. We, now, suppress the subscript ρ until needed, and proceed by first recoupling the operators

in the v.e.v. (French 1966)

$$\langle(((\tilde{a}_{j_{k_r}} \times \tilde{a}_{j_{l_r}})^{J_r} \times a_j^\dagger)^{j''} \times a_{j''}^\dagger)^0\rangle_0 =$$

$$\sum_\Lambda U(j_{k_r} j_{l_r} j'' j; J_r \Lambda)\langle((\tilde{a}_{j_{k_r}} \times (\tilde{a}_{j_{l_r}} \times a_j^\dagger)^\Lambda)^{j''} \times a_{j''}^\dagger)^0\rangle_0 \quad \text{(A4)}$$

The standard fermion anticommutation relation, transcribed to coupled tensor form is given by

$$[a_j^\dagger, \tilde{a}_{j'}]_+^\Gamma \equiv (a_j^\dagger \times \tilde{a}_{j'})^\Gamma + (-1)^{j+j'-\Gamma}(\tilde{a}_{j'} \times a_j^\dagger)^\Gamma = [j]^{\frac{1}{2}}\delta_{jj'}\delta_{\Gamma 0} \quad \text{(A5)}$$

Substituting for $(\tilde{a}_{j_{l_r}} \times a_j^\dagger)^\Lambda$ from this relation in eq. (A4) we proceed

$$\begin{aligned}
&\langle(((\tilde{a}_{j_{k_r}} \times \tilde{a}_{j_{l_r}})^{J_r} \times a_j^\dagger)^{j''} \times a_{j''}^\dagger)^0\rangle_0 \\
&= \sum_\Lambda U(j_{k_r} j_{l_r} j'' j; J_r \Lambda)\big(- (-1)^{j+j_{l_r}-\Lambda}\langle((\tilde{a}_{j_{k_r}} \times (a_j^\dagger \times \tilde{a}_{j_{l_r}})^\Lambda)^{j''} \times a_{j''}^\dagger)^0\rangle_0 \\
&\qquad + (-1)^{j+j_{l_r}-\Lambda}[j_{l_r}]^{\frac{1}{2}}\delta_{jj_{l_r}}\delta_{\Lambda 0}\langle(\tilde{a}_{j_{k_r}} \times a_{j''}^\dagger)^0\rangle_0\big) \\
&= -\sum_{\Lambda\Delta}(-1)^{j+j_{l_r}-\Lambda}U(j_{k_r} j_{l_r} j'' j; J_r \Lambda)U(j_{k_r} j j'' j_{l_r}; \Delta\Lambda) \\
&\qquad \langle((\tilde{a}_{j_{k_r}} \times a_j^\dagger)^\Delta \times (\tilde{a}_{j_{l_r}} \times a_{j''}^\dagger)^\Delta)^0\rangle_0 \\
&\quad + U(j_{k_r} j_{l_r} j'' j; J_r 0)(-1)^{j+j_{l_r}}[j_{l_r}]^{\frac{1}{2}}\langle(\tilde{a}_{j_{k_r}} \times a_{j''}^\dagger)^0\rangle_0
\end{aligned} \quad \text{(A6)}$$

In the first term of the above expression we have recoupled the operators and in the second we have carried out the summation over Δ. We, now, again apply the anti-commutation relation (A5), recalling that annihilation operator acts on the vacuum to give zero, *i.e.*, $\langle(a_j^\dagger \times \tilde{a}_{j'})^0\rangle_0 = 0$. In the first term anticommutation demands that $\Delta = 0$. Hence, we have after summation over Δ,

$$\begin{aligned}
&\langle(((\tilde{a}_{j_{k_r}} \times \tilde{a}_{j_{l_r}})^{J_r} \times a_j^\dagger)^{j''} \times a_{j''}^\dagger)^0\rangle_0 \\
&= -\sum_\Lambda(-1)^{j+j_{l_r}}(-1)^{-\Lambda}U(j_{k_r} j_{l_r} j'' j; J_r \Lambda)U(j_{k_r} j j'' j_{l_r}; 0\Lambda) \\
&\qquad (-1)^{j_{k_r}+j}[j_{k_r}]^{\frac{1}{2}}\delta_{j_{k_r} j}(-1)^{j_{l_r}+j''}[j_{l_r}]^{\frac{1}{2}}\delta_{j_{l_r} j''} \\
&\quad + U(j_{k_r} j_{l_r} j'' j; J_r 0)(-1)^{j+j_{l_r}}[j_{l_r}]^{\frac{1}{2}}\delta_{jj_{l_r}}(-1)^{j_{k_r}+j''}[j_{k_r}]^{\frac{1}{2}}\delta_{j_{k_r} j''}
\end{aligned} \quad \text{(A7)}$$

Recalling that in the long last, we will be summing over the j's and j''s, we replace them whereever encountered, on the r.h.s. of equation (A7) as prompted by the Kronecker delta's in the respective terms. This allows us to apply the following relations of U-coefficients compiled by French (1966) (equation (2.9) and (2.12) of the ref.)

$$\sum_{\Lambda}(-1)^{-\Lambda}U(j_{k_r}j_{l_r}j_{l_r}j_{k_r};J_r\Lambda)U(j_{k_r}j_{k_r}j_{l_r}j_{l_r};0\Lambda) = (-1)^{J_r-2j_{k_r}-2j_{l_r}}U(j_{k_r}j_{l_r}j_{k_r}j_{l_r};J_r0) \tag{A8}$$

and

$$U(j_{k_r}j_{l_r}j_{k_r}j_{l_r};J_r0) = (-1)^{j_{k_r}+j_{l_r}-J_r}\left[\frac{J_r}{j_{k_r}j_{l_r}}\right]^{\frac{1}{2}} \tag{A9}$$

We use these relations in equation (A7), remember that $2j = odd$ for all small j's, recall the subscript ρ and write the final expression for equation (A3)

$$\begin{aligned}\langle(\rho;k_rl_r)J_r||a^{\dagger}_{j^{\rho}}||j''^{\rho}\rangle &= [J_r]^{\frac{1}{2}}\zeta_{k_rl_r}(\delta_{j^{\rho}_{k_r}j''^{\rho}}\delta_{j^{\rho}_{l_r}j^{\rho}} - (-1)^{j^{\rho}_{k_r}+j^{\rho}_{l_r}-J_r}\delta_{j^{\rho}_{k_r}j^{\rho}}\delta_{j^{\rho}_{l_r}j''^{\rho}}) \\ &= -(-1)^{j^{\rho}_{k_r}+j^{\rho}_{l_r}-J_r}[J_r]^{\frac{1}{2}}\zeta_{k_rl_r}\mathcal{E}_{k_rl_rJ_r}\delta_{j^{\rho}_{k_r}j^{\rho}}\delta_{j^{\rho}_{l_r}j''^{\rho}}\end{aligned} \tag{A10}$$

where $\mathcal{E}_{klJ}$ is the exchange operator introduced by French (1966)(see equation A-1 of the ref.)

$$\mathcal{E}_{klJ}f(k,l,J) = f(k,l,J) - (-1)^{j_k+j_l-J}f(l,k,J) \tag{A11}$$

Proceeding along identical lines we evaluate

$$\langle j''^{\rho}||\tilde{a}_{j'^{\rho}}||(\rho;k_sl_s)J_s\rangle = [J_s]^{\frac{1}{2}}\zeta_{k_sl_s}\mathcal{E}_{k_sl_sJ_s}\delta_{j'^{\rho}j^{\rho}_{k_s}}\delta_{j''^{\rho}j^{\rho}_{l_s}} \tag{A12}$$

We now put the expressions derived in equations (A10) and (A12) in equation (A2) and sum over the intermediate states j''^{ρ} to write the expression

$$\begin{aligned}&\langle(\rho;k_rl_r)J_r||(a^{\dagger}_{j^{\rho}}\times\tilde{a}_{j'^{\rho}})^{J}||(\rho;k_sl_s)J_s\rangle \\ &= -(-1)^{j^{\rho}_{k_r}+j^{\rho}_{l_r}+J_s-J}[J_rJ_sJ]^{\frac{1}{2}}\zeta_{k_rl_r}\zeta_{k_sl_s} \\ &\qquad \begin{Bmatrix} J_r & j^{\rho} & j^{\rho}_{l_r} \\ j'^{\rho} & J_s & J \end{Bmatrix}\mathcal{E}_{k_rl_rJ_r}\mathcal{E}_{k_sl_sJ_s}\delta_{j^{\rho}_{k_r}j^{\rho}}\delta_{j'^{\rho}j^{\rho}_{k_s}}\delta_{j^{\rho}_{l_r}j^{\rho}_{l_s}}\end{aligned} \tag{A13}$$

Appendix-B

Derivation of the $\vec{T}^2$ operator

For a nucleus with n_1 valence neutrons and n_2 valence protons, the isospin operator $\vec{T}$ is defined as

$$\vec{T} = \sum_{i=1}^{n_1} \vec{t}_i^{\nu} + \sum_{j=1}^{n_2} \vec{t}_j^{\pi} \tag{B1}$$

where $\vec{t}_i^{\nu}$ ($\vec{t}_j^{\pi}$) is the single particle isospin operator with quantum numbers $(t_i^{\nu},\, t_{3_i}^{\nu}) = (\frac{1}{2},\, \frac{1}{2})$ and $(t_j^{\pi},\, t_{3_j}^{\pi}) = (\frac{1}{2},\, -\frac{1}{2})$ respectively. Squaring it we get

$$\vec{T}^2 = \sum_{i=1}^{n_1} \vec{t}_i^{\nu 2} + \sum_{j=1}^{n_2} \vec{t}_j^{\pi 2} + 2 \sum_{i<k=1}^{n_1} \vec{t}_i^{\nu} \cdot \vec{t}_k^{\nu} + 2 \sum_{j<l=1}^{n_2} \vec{t}_j^{\pi} \cdot \vec{t}_l^{\pi} + 2 \sum_{i=1}^{n_1} \sum_{j=1}^{n_2} \vec{t}_i^{\nu} \cdot \vec{t}_j^{\pi} \tag{B2}$$

The operators $\vec{t}_i^{\rho 2}$ and $\vec{t}_i^{\rho} \cdot \vec{t}_j^{\rho}$ act on the 2-particle coupled isospin states

$$|(t_i^{\rho} t_k^{\rho}) t t_3\rangle \equiv |(\frac{1}{2}\frac{1}{2}) 1 \pm 1\rangle \tag{B3}$$

following usual angular momentum algebra

$$\vec{t}_i^{\rho 2} |(t_i^{\rho} t_k^{\rho}) t t_3\rangle = \frac{3}{4} \tag{B4}$$

$$\vec{t}_i^{\rho} \cdot \vec{t}_k^{\rho} |(t_i^{\rho} t_k^{\rho}) t t_3\rangle = \frac{1}{2} \left(\vec{t}^{\rho 2} - \vec{t}_i^{\rho 2} - \vec{t}_k^{\rho 2} \right) |(t_i^{\rho} t_k^{\rho}) t t_3\rangle = \frac{1}{4} \tag{B5}$$

The term $2\vec{t}_i^{\nu} \cdot \vec{t}_j^{\pi}$ is related to the the neutron-proton exchange operator $\mathcal{P}_{\nu\pi}$ as

$$2\vec{t}_i^{\nu} \cdot \vec{t}_j^{\pi} = -\frac{1}{2} - \mathcal{P}_{\nu\pi} \tag{B6}$$

As the indices i and j go alongwith the ν and π respectively, we drop them on the r.h.s. of eq. (B6). Substituting from eqs. (B4–B6) in eq. (B2) and carrying out the summations, we have

$$\vec{T}^2 = \frac{3}{4}(n_1 + n_2) + \frac{1}{4}(n_1(n_1 - 1) + n_2(n_2 - 1)) - \frac{1}{2}n_1 n_2 - \sum_{\nu\pi} \mathcal{P}_{\nu\pi} \qquad \text{(B7)}$$

We now examine the action of $\mathcal{P}_{\nu\pi}$, on coupled 2-particle (fermion) states

$$\mathcal{P}_{\nu\pi}|(j^\nu j'^\pi)J\rangle \rightarrow |(j^\pi j'^\nu)J\rangle = (-1)^{j+j'-J}|(j'^\nu j^\pi)J\rangle \qquad \text{(B8)}$$

The phase factor in the above equality results by rearrangement of arguments in the Clebsch-Gordan coefficient of the coupled state $|(j^\nu j'^\pi)J\rangle$. It is to be carefully noted here, that the action of $\mathcal{P}_{\nu\pi}$ on $|(j^\nu j'^\pi)J\rangle$ will yield a vanishing result if the orbit j', which is a valence orbit for protons, is filled for the neutrons and the Pauli principle prohibits creation of a neutron in it. In other words, if there is an overlap between the model spaces of neutrons and protons, then and only then we get a non-zero contribution from the last term in eq. (B7). In the phase factor of eq. (B8), the superscipts ν and π on j and j' are omitted for the reason that in case of a non-zero result j and j' are common to both the model spaces.

Using the relationship given in eq. (B8), we can turn the particle summation over ν and π in the last term of eq. (B7) into a summation over the states j and j'. In second quantized representation, we have

$$\sum_{\nu\pi} \mathcal{P}_{\nu\pi} = \sum_{jj';J} [J]^{\frac{1}{2}} (-1)^{j+j'+J} \left((a^\dagger_{j^\nu} \times a^\dagger_{j'^\pi})^J \times (\tilde{a}_{j'^\nu} \times \tilde{a}_{j^\pi}) \right)^0 \qquad \text{(B9)}$$

By spherical tensor recoupling rules, eq. (B9) can be rewritten in multipole expansion form. With this and by rearranging the terms in eq. (B7), we get the final expression for the $\vec{T}^2$ operator

$$\begin{aligned} \vec{T}^2 \;=\; & \frac{1}{4}((n_1 - n_2)^2 + 2(n_1 + n_2)) \\ & - \sum_{jj';J'} (-1)^{j-j'+J'} \, [J']^{\frac{1}{2}} \, \left((a^\dagger_{j^\nu} \times \tilde{a}_{j'^\nu})^{J'} \times (a^\dagger_{j'^\pi} \times \tilde{a}_{j^\pi})^{J'} \right)^0 \end{aligned} \qquad \text{(B10)}$$